Copy number variations of the mitochondrial DNA as potential cause of mitochondrial diseases

Dissertation

zur

Erlangung des Doktorgrades (Dr. rer. nat.)

der

Mathematisch-Naturwissenschaftlichen Fakultät

der

Rheinischen Friedrich-Wilhelms-Universität Bonn

vorgelegt von

Miriam Baron

aus

Bonn-Bad Godesberg

Bonn, 2010

Angefertigt mit Genehmigung der Mathematisch-Naturwissenschaftlichen Fakultät
der Rheinischen Friedrich-Wilhelms-Universität Bonn

1. Gutachter Prof. Dr. Wolfram S. Kunz
2. Gutachter Prof. Dr. Thomas Magin
Tag der Promotion: 09.07.2010
Erscheinungsjahr: 2010

Table of contents

1. Abstract

Aim: The aim of this thesis was the analysis of copy number variations of the mitochondrial DNA (mtDNA) in several tissues and cell types with regard to different mitochondrial associated disorders.

Background: The mtDNA copy number can be reduced due to mutations in the nuclear encoded DNA polymerase γ (POLG) or damages caused by deleterious reactive oxygen species (ROS), which are created by the respiratory chain. This leads to the insufficient expression of mitochondrial encoded subunits of complexes of the oxidative phosphorylation system (OXPHOS). Consequently an impairment of the biochemical activity and integrity of the cells occurs.

Methods: The quantification of the mtDNA was performed by quantitative PCR (qPCR). Biochemical activities were determined by enzymatic assays such as direct measurement of the citrate synthase (CS) activity or comprehensive measurement of the respiratory activity.

Results: Mutations in the nuclear inherited gene *POLG* result in mtDNA depletion in mitochondrial disorders including a mild phenotype of progressive external ophthalmoplegia (PEO) with epilepsy/ataxia. A mtDNA depletion was detected in different tissues and cell types of Alpers-Huttenlocher patients with pathogenic nuclear mutations. The mtDNA copy number was reduced in specific hippocampal regions of temporal lobe epilepsy (TLE) patients with Ammons' horn sclerosis (AHS) accompanied by a decreased CS activity. An *in vitro* reduction of the mtDNA in fibroblasts results in an impaired respiratory activity.

Conclusions: The mtDNA content is proportional to the mitochondria content and the energy demand of the respective tissue or cell type under normal conditions. A cell type- and tissue-specific depletion of the mtDNA can be present in several inherited and somatic mitochondrial disorders *in vivo* or can be generated by an *in vitro* system. The mtDNA depletion diminishes the biochemical activity and integrity of the cells and can contribute to the disease phenotype.

2. Introduction

2.1 Roles of Mitochondria

Eukaryotic cells contain a number of organelles with specialized functions like the mitochondria. Mitochondria are broadly known as double-membrane-bounded organelles, which perform a number of indispensable functions for the life of most eukaryotic cells (Henze and Martin, 2003).

Their main function is the production of energy in the form of ATP via the citric acid cycle and the oxidative phosphorylation system (OXPHOS), but they are also involved in the biosynthesis of many metabolites like pyrimidines, amino acids or cellular iron sulphur cluster proteins (Attardi and Schatz, 1988; Bereiter-Hahn, 1990; Lill et al., 1999). A consequence of an OXPHOS dysfunction is a higher production of reactive oxygen species (ROS) (Camello-Almaraz et al., 2006). Mitochondria control the ability of the cell to generate and detoxificate ROS (Nicholls et al., 2003).

Beside their role as ATP generators, mitochondria have also the ability to remove Ca^{2+} ions out of the cytosol and accumulate them in their matrix (Vasington and Murphy, 1962).

The release of mitochondrial proapoptotic factors like cytochrome *c* into the cytoplasm can induce a signaling cascade, which plays a prominent role in apoptotic cell death (Hengartner, 2000).

2.2 Energy generation via mitochondria

The citric acid cycle, which takes place in the mitochondrial matrix, is a central metabolic pathway involved in the catabolic oxidation of substrates (figure 1; Krebs, 1970).

Acetyl-CoA, which is generated by the decomposition of nutrients such as glucose, transfers two carbon acetyl groups to oxaloacetate to generate citrate. The citrate is metabolized through a series of chemical transformations and releases two carboxyl groups as CO_2. The energy-rich electrons generated by the cycle are transferred to NAD^+/$NADP^+$ and FAD^+ to form NADH/NADPH and $FADH_2$. The citric acid cycle is regulated by several substances like NADH, ATP and Ca^{2+} (Krebs, 1970).

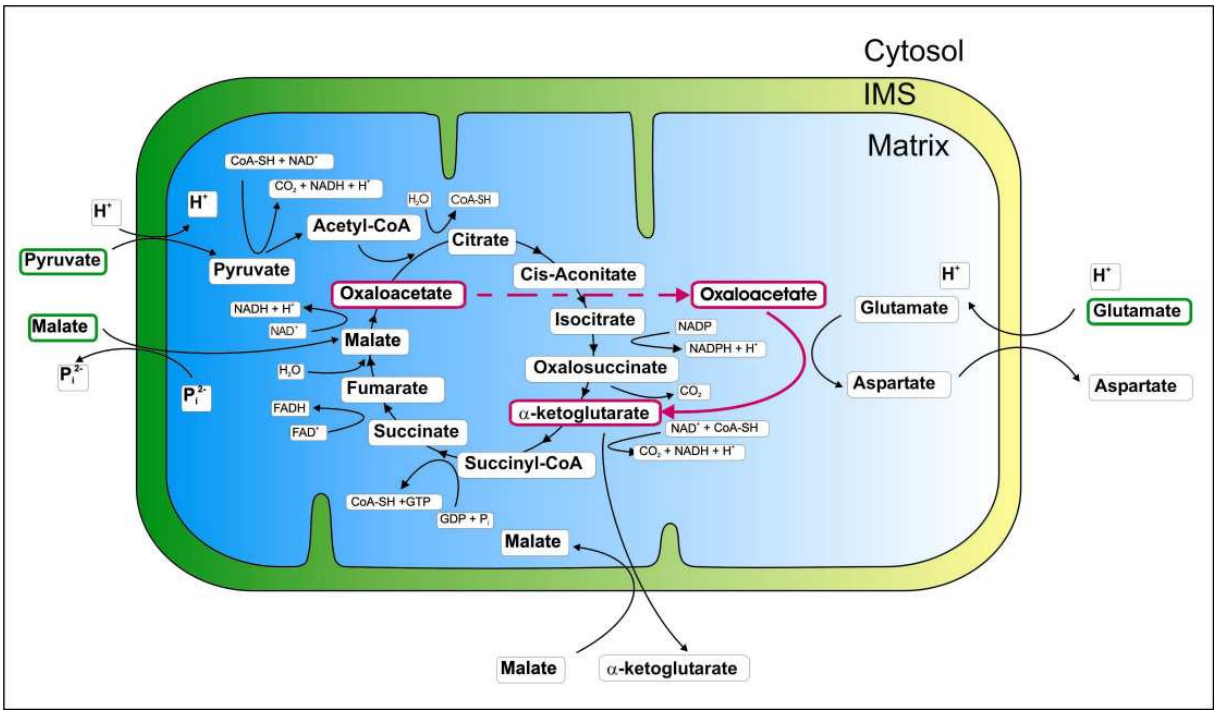

Figure 1. Citric acid cycle (modified from Munnich, 2008). IMS – intermembrane space.

The electrons generated via the citric acid cycle are afterwards transferred to the multisubunit enzyme complexes, also called oxidative phosphorylation system (OXPHOS), of the respiratory chain (Smeitink et al., 2001).

The OXPHOS is embedded in the inner mitochondrial membrane (IMM). Functionally, it is composed of the five enzyme complexes NADH:ubiquinone oxidoreductase (complex I), succinate:ubiquinone oxidoreductase (complex II, succinate dehydrogenase, SDH), cytochrome *c* oxidoreductase (complex III, cytochrome bc_1 complex), ubiquinol:ferricytochrome *c*:oxygen oxidoreductase (complex IV, COX) and F_1F_0-ATPase (complex V) as well as the two electron carriers coenzyme Q and cytochrome *c* (Chinnery and Schon, 2003; Hatefi, 1985; Saraste, 1999; Schapira and Cock, 1999).

The electrochemical gradient across the IMM transfers the energy of NADH/NADPH and $FADH_2$ for the synthesis of ATP according to the chemiosmotic hypothesis (Mitchell, 1961).

The electrons are transferred to oxygen to generate water at complex IV. The transport of electrons via the respiratory chain generates a proton gradient across the membrane (Smeitink et al., 2001), which is used to synthesize ATP by complex V (Saraste, 1999; Smeitink et al., 2001).

Superoxide anions are generated as side products of the OXPHOS mainly at complex I (Kudin et al., 2004; Murphy, 2009). A negligible amount is also produced at complex III (Kudin et al., 2004; Kudin et al., 2005; Murphy, 2009). The superoxide anions are released into the matrix by complex I and into the intermembrane space by complex III (figure 2; Kudin et al., 2004; Kudin et al., 2005).

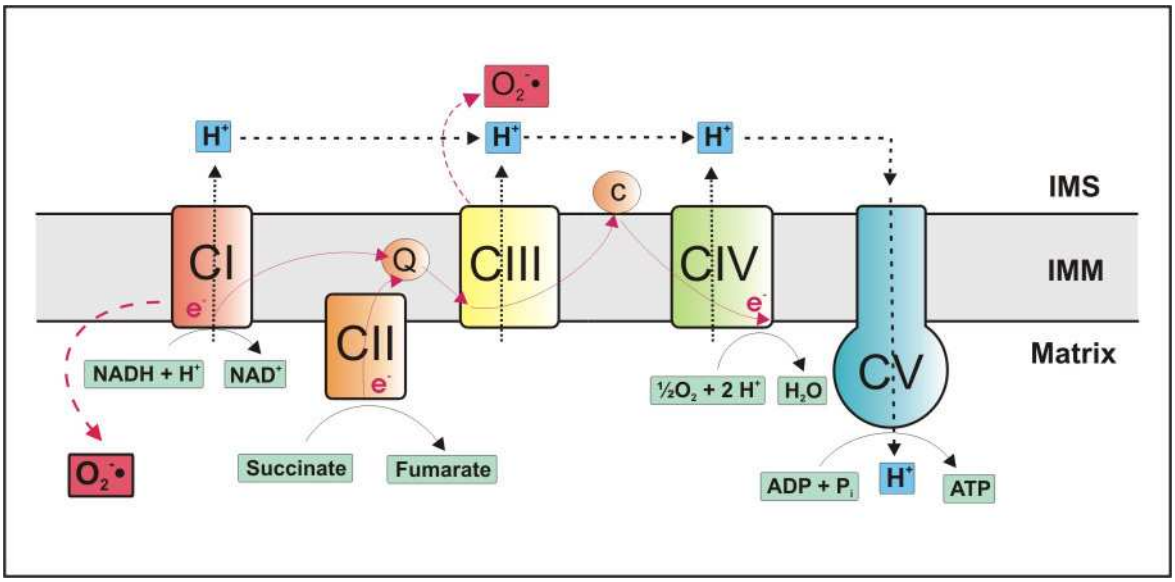

Figure 2. Generation of reactive oxygen species (ROS) at the oxidative phosphorylation system (OXPHOS) (modified from Kudin et al., 2005 and Smeitink et al., 2001). C – complex, IMS – intermembrane space, IMM - inner mitochondrial membrane, $O_2^{-}\bullet$ - superoxide anion.

The energy equivalent ATP is not only required in typical metabolic household reactions of the cells, but also in tissue- and celltype-specific reactions. A notable example in this issue are neuronal cells, where the main ATP consuming reaction is the Na^+/K^+-ATPase, which stabilizes the Na^+ electrochemical potential gradient across the neuronal plasma membrane (Nicholls et al., 2003).

2.3 Mitochondrial DNA (mtDNA) and the interaction of mitochondria with the nucleus

Mitochondria were originally independent prokaryotes, which were assimilated by other cells. This symbiosis (Schimper, 1883) led to the generation of eukaryotic cells (Margulis, 1981). Mitochondria transferred a part of their genome to the nucleus, but they still maintained genes, which are essential for their specific functions within the

cell (Margulis, 1981). They retained own metabolic functions and their own mitochondrial genome, though they also require proteins encoded by the nucleus and manufactured in the cytoplasm. In this context, the mitochondria evolved into semiautonomous organelles relying on the interaction with the nucleus (Thorsness and Weber, 1996).
Most multiprotein enzyme complexes of the respiratory chain are partly encoded by both the nuclear and the mitochondrial DNA (Smeitink et al., 2001). The only enzyme complex exclusively encoded by nuclear DNA and therefore independent of the mtDNA background is complex II (Smeitink et al., 2001).
It is assumed that different nuclear encoded isoforms could lead to tissue specific absences or defects in subunits thus preventing the correct synthesis of respiratory chain complexes (Johnson et al., 1983). This could result in a tissue specific or in a developmental dependent disease phenotype (Johnson et al., 1983). The conversion of a fetal to an adult form of the subunit can trigger the onset of such a disease (Johnson et al., 1983).

Each mitochondrion is estimated to contain from two to ten copies of mtDNA (Graziewicz et al., 2006; Shuster et al., 1988; Wiesner et al., 1992). The mtDNA is packed into protein-DNA complexes called nucleoids (Chen and Butow, 2005; Wang and Bogenhagen, 2006). Each mitochondrion holds between one and more than ten nucleoids (Satoh and Kuroiwa, 1991).
The nucleoids are suggested to occur in discrete membrane-spanning structures, the mitochondrial replisomes (Meeusen and Nunnari, 2003). These structures are proposed to provide a mechanism for linking mtDNA replication and transcription (Meeusen and Nunnari, 2003). Although the composition of the nucleoids is poorly understood, a high number of nuclear encoded proteins that control the mtDNA replication, the mtDNA transcription, the mitochondria fusion and the attachment of the nucleoids to the cytoskeleton have been detected (Chen and Butow, 2005; Wang and Bogenhagen, 2006).

The mitochondrial genome contains 37 genes from which 13 are encoding proteins involved in the electron transport or oxidative phosphorylation of the respiratory chain (Anderson et al., 1981). The remaining genes encode for 22 mitochondrial tRNAs and 2 mitochondrial rRNAs (Anderson et al., 1981). Despite the fact, that

mitochondria possess their own DNA, this DNA only encodes for a small number of proteins. The majority of nearly 1000-1500 proteins located in the mitochondria are encoded by the nucleus (Calvo et al., 2006; Lopez et al., 2000). These nuclear encoded proteins strongly influence the localization, proliferation and metabolism of mitochondria.

Nuclear encoded factors regulate the transcription and replication of the mtDNA. The essential protein for mtDNA replication is polymerase γ, the only nuclear encoded polymerase located within mitochondria (Graziewicz et al., 2006).

2.4 Replication of mtDNA molecules

Two types of mtDNA replication models exist, the asynchronous strand displacement model and a strand-coupled bidirectional replication model (figure 3). The two ways of mtDNA replication are both assumed to be present in eukaryotic cells.

The unidirectional, asynchronous mtDNA replication model describes the initiation of the replication at two replication origins (Clayton, 1982). Both mtDNA strands dissociate during the initiation of the replication at the first origin. The synthesis process is performed unidirectionally at one strand, while the other single strand is displaced until the second replication origin is exposed. Then the replication is initiated in the opposite direction (figure 3; Clayton, 1982; Krishnan et al., 2008; Schmitt and Clayton, 1993; Shadel and Clayton, 1997).

The bidirectional replication model describes an alternative strand-coupled mechanism. According to this model, the replication is initiated at one replication zone and proceeds symmetrically in both directions (figure 3; Bowmaker et al., 2003; Holt et al., 2000; Krishnan et al., 2008; Yao Yang et al., 2002).

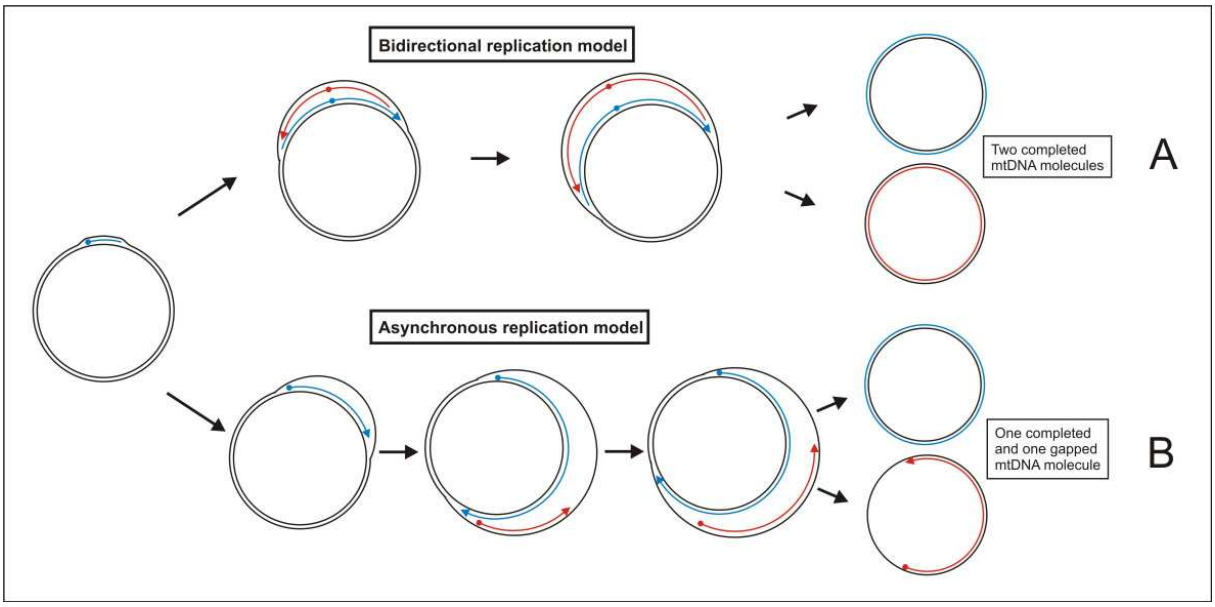

Figure 3. mtDNA replication mechanisms (according to Graziewicz et al., 2006). A – bidirectional replication model, B – asynchronous replication model.

A different balance between these replication mechanisms is assumed to influence the mtDNA copy number potentially in several physiological and developmental conditions (Holt et al., 2000). In cells increasing their mtDNA copy number, the bidirectional replication mechanism is predominantly observed. In contrast, in growing cells with lower mtDNA synthesis rate that mainly maintain a stable mtDNA copy number for the descendent daughter cells, the asynchronous mode of mtDNA replication occurs (Holt et al., 2000).

2.5 Mitochondrial distribution

The mitochondrial distribution is directly correlated with its cellular localization. An important aspect during the proliferation of cells is the allocation of mitochondria (Yaffe, 1999). It is assumed that a cellular machinery navigates the positioning and inheritance of mitochondria (Thorsness, 1992; Yaffe, 1999). Indicators for this process are the reticular morphology of mitochondria, their association with the cytoskeleton and moreover coordinated mitochondrial movements during cellular division and differentiation (Yaffe, 1999).

Mitochondria are morphologically and functionally heterogeneous and form distinct populations with differing biochemical and respiratory properties within the cell

(Battersby and Moyes, 1998; Collins et al., 2002; Frazier et al., 2006; Gauthier and Padykula, 1966; Kayar et al., 1988; Lombardi et al., 2000). For instance, they are found to accumulate around the nucleus. This specific localization can potentially generate a hypoxic environment and protect the nuclear DNA from ionizing radiation (Bereiter-Hahn, 1990; Jones and Aw, 1988). Another example for the characteristic positioning of mitochondria refers to mitochondria in skeletal muscle fibers. A predominant accumulation takes place at the outer region of the sarcomere units of muscle fibers, the I-band level, whereas mitochondria occur in a low amount in the subsarcolemmal space (Kelley et al., 2002; Ogata and Yamasaki, 1997).
This localization could be related to the demand for important molecules like oxygen diffusing over the outer mitochondrial membrane (OMM) (Jones and Aw, 1988). The morphological variations of mitochondria are intricately linked to many cellular processes, including development, cell cycle progression and apoptosis (Frazier et al., 2006).

The mitochondria also form a largely interconnected, dynamic network (Frazier et al., 2006; Rizzuto et al., 1998). Specialized cell types respond to their specific energy requirements with drastic changes of this mitochondrial network (Frazier et al., 2006; Minin et al., 2006). The localisation of mitochondria within this network can be altered by the transport of these organelles within the cell.
A prominent example for mitochondrial transport within the cell is the transport of mitochondria in neuronal cells along the length of the axon to ensure the supply of ATP and the regulation of Ca^{2+} (Hollenbeck and Saxton, 2005; Minin et al., 2006).
The observation that mitochondria feature heterogeneous populations within the cell, which communicate over a continuous network, has consequences for understanding the mechanisms that navigate the distribution of the mitochondrial DNA (mtDNA).

2.6 Variations in the mtDNA

The human mtDNA sequence with a length of 16,569 nucleotides was determined in 1981 (Anderson et al., 1981). The maternally inherited mtDNA plays an essential role for the mitochondrial functionality and consequently for the survival of the cells.
Deleterious changes in the mtDNA are known to contribute to several mitochondrial diseases. Prominent variations of the mtDNA are point mutations and deletions.

The correlation between the mtDNA and the disease phenotype exceeds the simplified picture of a cause-effect-relationship of sequence changes and the onset of a mitochondrial disorder. The genetics of mitochondria is unique from the Mendelian inheritance (Mendel, 1866) observed in the nucleus since cells have a variable number of mitochondria and each of these mitochondria contains several mtDNA molecules (Clay Montier et al., 2009).

The mtDNA molecules in a cell can exist in a heteroplasmic state, which refers to a mixture of wildtype and mutant mtDNA molecules (Bender et al., 2006; Sciacco et al., 1994; Taylor and Turnbull, 2005; Zsurka et al., 2005). The level of heteroplasmy can shift during transmission over generations (Chinnery et al., 2000) and also during tissue development (Chinnery et al., 1999; Nekhaeva et al., 2002).

The accumulation of a fraction of mtDNA molecules, which is called heteroplasmic drift, can finally influence the physiology of the cell (Coller et al., 2001; Nekhaeva et al., 2002). This process has been termed clonal expansion (Coller et al., 2002; Nekhaeva et al., 2002).

Different heteroplasmic levels of the cellular mtDNA content result in a mosaic pattern of a tissue with normal and deficient cells (Bender et al., 2006; Zsurka et al., 2004). It is assumed that the heteroplasmic level of wildtype and mutant molecules has to reach a certain threshold before the mitochondrial function is impaired and a biochemical phenotype occurs (Rossignol et al., 2003; Sciacco et al., 1994). A prevalent example for the dependence of a disease phenotype on the heteroplasmic level are the syndromes neuropathy, ataxia and retinitis pigmentosa (NARP) and the maternally-inherited Leigh syndrome (MILS), which are both associated with the T8993G mtDNA mutation (Alexeyev et al., 2008; Mäkelä-Bengs et al., 1995). Patients with a heteroplasmic level of less than 60 % are generally asymptomatic. By contrast, patients with 60-90 % heteroplasmy are affected by NARP, whereas MILS is associated with a level of more than 90 % heteroplasmy (Alexeyev et al., 2008; Mäkelä-Bengs et al., 1995).

Pathogenic single-nucleotide changes in the mitochondrial genome were firstly described in 1988 (Wallace et al., 1988) as a cause of the maternally inherited, neurological disorder Leber's hereditary optic neuropathy (LHON). Since this time, several point mutations in the mtDNA have been identified and associated with a number of mitochondrial disorders like mitochondrial encephalomyopathy, lactic

acidosis and stroke-like episodes (MELAS) or myoclonic epilepsy and ragged red fibers (MERRF) (Chinnery and Schon, 2003; von Kleist-Retzow et al., 2003; Wallace, 1992). The threshold value is often specific for the respective mtDNA point mutation and features a value of around 90 % (Rossignol et al., 2003).

The presence of deletions of the mitochondrial genome in patients with mitochondrial myopathies was first reported in 1988 (Holt et al., 1988). Large-scale deletions of the mtDNA are found in specimen of about 40 % of adult patients affected by several mitochondrial myopathies, prevalently in chronic progressive external ophthalmopegia (PEO), Kearns-Sayre syndrome (KSS) and Pearson's syndrome (Harding and Hammans, 1992; Holt et al., 1988; Holt et al., 1989a; Holt et al., 1989b; Porteous et al., 1998). The heteroplasmy level shows a range of 20-90 % of total mtDNA (Holt et al., 1988; Holt et al., 1989a). Defects of the respiratory chain occur at a threshold of 50-60 % heteroplasmy (Hayashi et al., 1991; Porteous et al., 1998).

The deletions can be divided into two classes (Mita et al., 1990). Class I deletions are flanked by short nucleotide direct repeats (Holt et al., 1989b; Mita et al., 1990; Schon et al., 1989), whereas class II deletions possess no repeat elements (Mita et al., 1990).
The underlying mechanism causing mtDNA deletions is controversely discussed. The mtDNA deletions may arise from intramolecular recombination events mediated by enzymes that recognize short homologies (Holt et al., 1989b; Mita et al., 1990; Schon et al., 1989; Zsurka et al., 2005). On the other hand, they can potentially result from cleavage at topoisomerase sites (Blok et al., 1995; Nelson et al., 1989) or also generated as a result of slippage during replication (Holt et al., 1989b; Mita et al., 1990; Shoffner et al., 1989).

The importance of the presence of a sufficient amount of wildtype molecules is reflected in a number of literature reports that point out the relationship between depletion of the mtDNA and the occurrence of a mitochondrial disease phenotype (Clay Montier et al., 2009; Durham et al., 2005).
A severe reduction of the mtDNA copy number in tissues of clinically heterogeneous patients with mitochondrial encephalomyopathies was initially described by Moraes et al., 1991. The mtDNA depletion is a prominent hallmark of Alpers-Huttenlocher

syndrome (Naviaux et al., 1999) and accompanies several other mitochondrial disorders like mitochondrial neurogastrointestinal encephalomyopathy (MNGIE) (Nishino et al., 1999; Papadimitriou et al., 1998).
The degree of mtDNA depletion correlates with the severity of tissue involvement and the presence of biochemical defects (Treem and Sokol, 1998). The affected patients show an impaired respiratory chain activity due to a decrease of mtDNA encoded proteins (Moraes et al., 1991).

2.7 Diseases associated with mitochondrial defects

A wide range of diseases affecting various organs and cell types of the human body are associated with mitochondrial defects. This clinically, histologically, biochemically and genetically heterogeneous group of disorders (Chinnery and Schon, 2003) is correlated with deleterious variations of nuclear and mitochondrial genes (von Kleist-Retzow et al., 2003).

The mitochondrial disorders, which are based on a primary mtDNA defect, i.e. they result from specific changes of the mitochondrial DNA, include mitochondrial encephalopathy lactic acidosis with stroke-like episodes (MELAS), myoclonic epilepsy with ragged red fibers (MERRF), neuropathy, ataxia, and retinitis pigmentosa (NARP) or Kearns Sayre syndrome.

In contrast, other mitochondrial diseases are related to a secondary mtDNA defect. These diseases result from defects in nuclear encoded genes, which have an impact on the mitochondrial genome. They include a range of disorders with Alpers-Huttenlocher syndrome and progressive external ophthalmoplegia (PEO) as the most prominent examples.

The clinical features and the neuropathology of the Alpers-Huttenlocher syndrome were initially described by Alpers (1931). The onset of the Alpers-Huttenlocher syndrome usually occurs during childhood (Harding et al., 1995).
The syndrome is inherited in an autosomal recessive way (Huttenlocher et al., 1976; Sandbank and Lerman, 1972). It is a mtDNA depletion disorder, which is characterized by deficiency in mtDNA polymerase γ (POLG) resulting from specific

mutations in the nuclear gene *POLG* (Naviaux et al., 1999). Beside the high number of publications, where a mtDNA depletion was associated with Alpers-Huttenlocher syndrome, only few reports on mtDNA point mutations (Zsurka et al., 2008) or deletions (Ashley et al., 2008; Zsurka et al., 2008) exist.
Hallmarks of this disease are a loss of neuronal cells, gliosis and demyelinization in the cerebral cortex and epileptic seizures in the brain (Alpers, 1931), paired with a decreased liver function (Huttenlocher et al., 1976). The impaired liver function is accompanied by hepatic lesions consisting of cirrhosis or of subacute hepatitis (Huttenlocher et al., 1976). Furthermore, elevated levels of glutamic oxaloacetate transaminase and lactic dehydrogenase are detected in liver serum (Huttenlocher et al., 1976). Biochemical characteristics are a deficiency of the partial mitochondrial encoded respiratory chain complexes I and IV in liver (Gauthier-Villars et al., 2001) and complexes I, III and IV in muscle (Naviaux et al., 1999).
It has been reported that the metabolic defect underlying the Alpers-Huttenlocher syndrome predisposes to drug related hepatotoxicity, notably to sodium valproate, promoting hepatic failure (Gauthier-Villars et al., 2001; McFarland et al., 2008; Schwabe et al., 1997).

Another mitochondrial disorder, which results from mutations in nuclear encoded proteins is progressive external ophthalmoplegia (PEO) (Graziewicz et al., 2006). PEO is characterized by ptosis, external ophthalmoplegia, cardiomyopathy and slowly progressive weakness of the skeletal muscle tissue (Bohlega et al., 1996; Copeland, 2008; Van Goethem et al., 2001; Zeviani et al., 1989). The autosomal dominant form of PEO (adPEO) is mainly associated with mutations in the nuclear genes *POLG, Twinkle* and *adenine nucleotide translocator 1 (ANT1)* (Spinazzola and Zeviani, 2005). A high number of mutations, which are correlated with PEO, have been detected in *POLG* (Chan and Copeland, 2009; Graziewicz et al., 2006). These mutations are also related to autosomal recessive PEO (arPEO) and sporadic PEO (Spinazzola and Zeviani, 2005). Genetic hallmarks of PEO are multiple deletions and the accumulation of point mutations (Cardaioli et al., 2007; Spinazzola and Zeviani, 2005; Zeviani et al., 1989). Biochemical characteristics are ragged red muscle fibers with abnormal mitochondria combined with a lowered respiratory activity (Copeland, 2008; Graziewicz et al., 2006).

Mitochondrial defects are also involved in neurodegenerative disorders. The neurodegenerative diseases with mitochondrial impairment include morbus Parkinson (MP) (Jenner, 2003; Moore et al., 2005), Friedreich's ataxia (FRDA) (Huang et al., 2006), Alzheimer's disease (Blass and Gibson, 1991; Hirai et al., 2001; Maurer et al., 2000; Swerdlow et al., 1997), amyotrophic lateral sclerosis (ALS) (Bowling et al., 1993; Sasaki and Iwata, 1996; Wong et al., 1995) or temporal lobe epilepsy (TLE) with Ammon's horn sclerosis (AHS) (Kunz, 2002; Kunz et al., 2000). The cause-effect-relationship between the disease phenotype and deleterious changes in mitochondria and their mtDNA remains to be elucidated (Kunz, 2002).

The mesial temporal lobe epilepsy (TLE) is the best known and most intensively studied form of epilepsy (Sloviter, 2005). The hippocampal sclerosis or Ammon's horn sclerosis (AHS) occurs as the prevalent pathological abnormality in brain specimen from patients with TLE (Liu et al., 1995; Sommer,1880).
The hippocampus has the form of a curved tube, which can be divided into the subfield area dentata (AD) and the cornu ammonis (CA) sections one to four (figure 4; Liu et al., 1995; Lopes da Silva and Arnolds, 1978). The AD contains a thick layer of small granule cells (Amaral and Lavenex, 2007; Liu et al., 1995; Lopes da Silva and Arnolds, 1978), whereas the CA regions are densely packed with pyramidal neurons (Amaral and Lavenex, 2007; Liu et al., 1995; Lopes da Silva and Arnolds, 1978). The major pathway, where a signal flow is transmitted from the region AD to cornu ammonis 3 (CA3) and subsequently to cornu ammonis 1 (CA1), is named the trisynaptic circuit (Andersen et al., 1971)

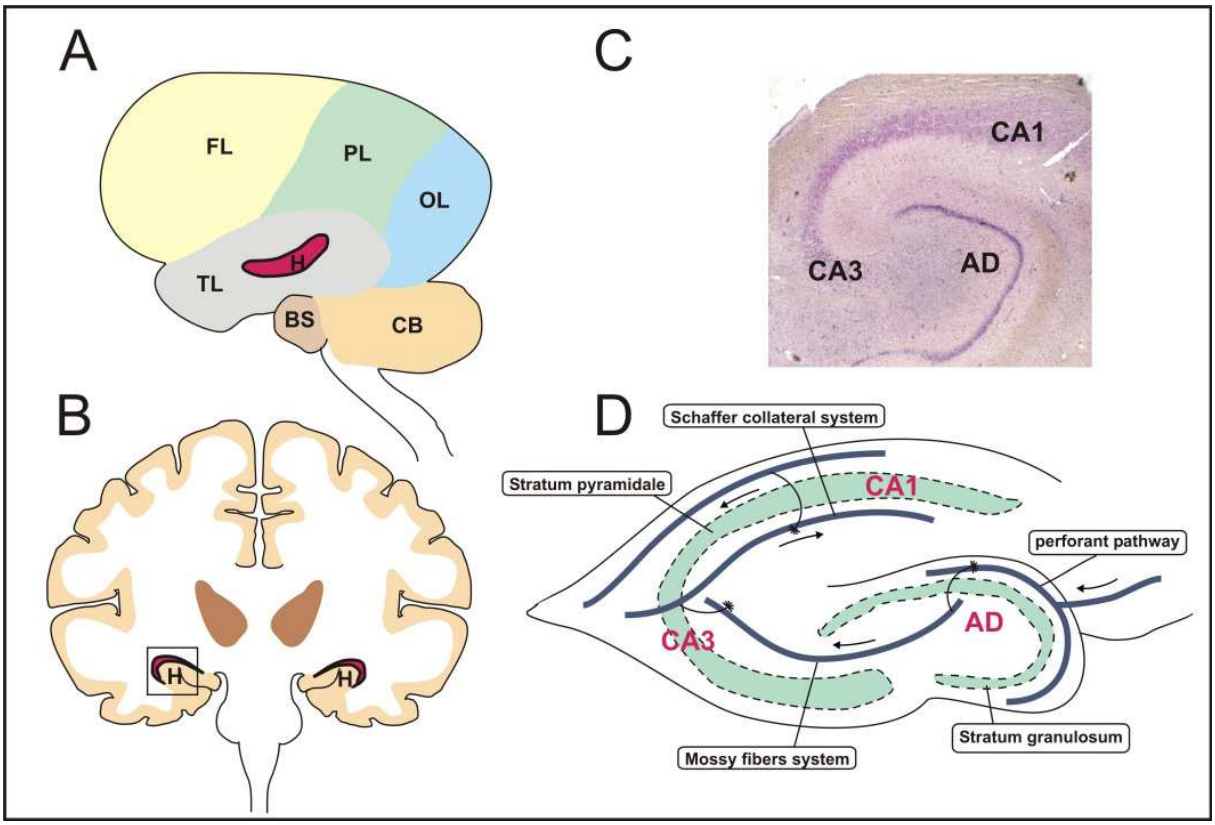

Figure 4. Structure of the hippocampus (modified from Amaral and Lavenex, 2007; Chang and Lowenstein, 2003; Kudin et al., 2009; Lopes da Silva and Arnolds, 1978). A – cross-section scheme of the human brain; B – frontal section scheme of the human brain; C – Nissle stained slice of the hippocampus of a patient with parahippocampal lesion; D – graphical overview of the hippocampus structure. AD – area dentata; BS – brain stem; CA1 – cornu ammonis 1; CA3 – cornu ammonis 3; CB – cerebellum; FL – frontal lobe; H – hippocampus; OL – occipital lobe; PL – parietal lobe; TL – temporal lobe.

In hippocampal sclerosis, a selective loss of pyramidal neurons in the regions CA1 and CA3 occurs (Baron et al., 2007; Ben-Ari et al., 1980; Kunz et al., 2000; Liu et al., 1994; Liu et al., 1995; Nadler, 1981). The accumulation of glia cells, which accompanies the neuronal cell loss, causes a shrinkage and hardening of the tissue named sclerosis (Chang and Lowenstein, 2003).

The mechanisms causing the selective neuronal degeneration remain unclear (Baron et al., 2007). One of the factors could be an increased level of ROS, which has already been observed in various epilepsy models (Kovacs et al., 2001; Liang et al., 2000). An increased ROS production is a hallmark of impaired mitochondria with an inhibited complex I activity (Han et al., 2001; Kudin et al., 2004). ROS can activate a vicious cycle, which results in mitochondrial degeneration and neuronal cell death (Kudin et al., 2004).

2.8 Polymerase γ (POLG) and *POLG* mutations

The enzyme polymerase γ was primarily identified as an RNA-dependent DNA polymerase (Fridlender et al., 1972) and is among overall 16 mammalian polymerases the only polymerase detected in mammalian mitochondria (Bolden et al., 1977; Graziewicz et al., 2006). POLG is responsible for the replication and repair of the mtDNA (Graziewicz et al., 2006).

The enzyme is a heterotrimer consisting of a catalytic and a dimeric accessory subunit (Carrodeguas et al., 2001).

The gene *POLG*, which is localized on chromosome 15 with a length of 18.5 kbp and 23 exons, encodes the catalytic subunit of POLG (figure 5; Ropp and Copeland, 1996). This catalytic subunit is a 140 kDa enzyme with DNA-polymerase, 3'-5'-exonuclease and 5'-deoxyribose phosphate (dRP) lyase activities (Longley et al., 1998a; Longley et al., 1998b; Ropp and Copeland, 1996). It contains a mitochondrial targeting sequence, an exonuclease domain with three Exo motifs (I-III) and a polymerase domain with three Pol motifs (A-C) (figure 5). These domains are connected by a linker region, which harbors four conserved blocks γ1-γ4 (figure 5; Chan and Copeland, 2009; Luoma et al., 2005; Ropp and Copeland, 1996). Another two conserved sequence elements (γ5 and γ6) are located in the polymerase domain (figure 5; Graziewicz et al., 2006).

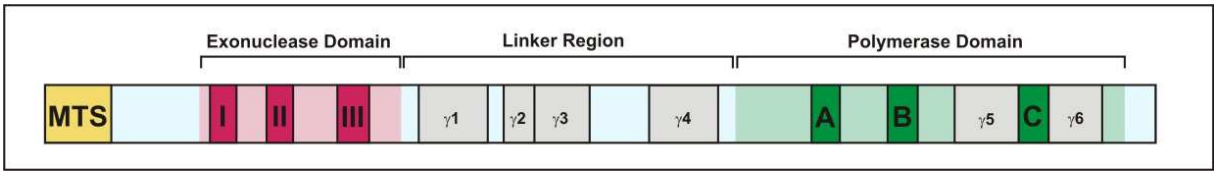

Figure 5. Catalytic subunit of POLG (modified from Chan and Copeland, 2009 and Graziewicz et al., 2006). MTS – mitochondrial targeting sequence, I-III – Exo motifs, A-C – Pol motifs, γ1-γ6 – conserved sequence elements.

The accessory subunit, encoded by the gene *POLG2*, is a 55 kDa protein, which is characterized as a processivity factor for DNA (Johnson et al., 2000; Lim et al., 1999). Upon interaction with the catalytic subunit, p55 promotes tighter DNA binding to increase the polymerization rate (Johnson et al., 2000; Lim et al., 1999).

The first pathogenic *POLG* and *POLG2* mutations were identified in 2001 and 2006, respectively (Longley et al., 2006; Van Goethem et al., 2001).

A total of approximately 150 pathogenic mutations in *POLG* have been reported currently, which underlines the importance of *POLG* as a major locus for mitochondrial diseases (Chan and Copeland, 2009). These mutations can be localized in all regions of *POLG* (Chan and Copeland, 2009).

Beside the broad number of known pathogenic mutations in *POLG*, plenty of neutral polymorphisms in this gene may influence moderately the variable genetic foundations and potentially even the susceptibility to mitochondrial defects within the human population.

3. Goals of this study

Mitochondria are semiautonomous organelles with essential importance for the energy production of the cell. They contain their own mitochondrial DNA (mtDNA). Mitochondrial disorders can result from mtDNA mutations, which are intensively studied in a number of systemic mitochondrial diseases, as well as from rarely examined variations in the mtDNA content.

Aim of this study was the analysis of molecularbiological variations in the mtDNA copy number in different human tissues and cell types.

Firstly, it was planned to determine the total mtDNA copy number values of several tissues and cell types of healthy control patients.
Subsequently, these values have to be compared with the mtDNA content of patients with the mitochondrial disorders Alpers-Huttenlocher syndrome and progressive external ophthalmoplegia (PEO) with epilepsy/ataxia.

These disorders can be related to mutations in the nuclear gene *POLG*, which encodes for the catalytic subunit of polymerase γ (POLG). POLG, known as the only DNA polymerase present in mammalian mitochondria, is essential for the replication and repair of the mtDNA. The cause and consequences of the mtDNA depletion due to these disorders is of special interest.
In this context, it was intended to examine the correlation between *POLG* and the mitochondrial phenotype. Relevant aspects of this correlation were the communication between the nucleus and the mitochondria as well as the effect of the inheritance of nuclear-encoded mutations on the onset of a mitochondrial disorder.

Diseases with mitochondrial involvement like temporal lobe epilepsy (TLE) with Ammons' horn sclerosis (AHS) can be expected to be associated with the occurrence of a mtDNA depletion. AHS is hallmarked by the selective loss of neuronal cells. The neuronal cell death is accompanied by the production of reactive oxygen species (ROS). An increased ROS production suggests mitochondrial degeneration. The cause and effect of mitochondrial changes during AHS still remains to be elucidated.

Therefore, it was interesting if mtDNA depletion specifically occurs in areas of selective loss of neuronal cells.

In patients affected by a mild phenotype of PEO with epilepsy/ataxia, the accumulation of mtDNA deletions has been reported. The Alpers-Huttenlocher syndrome is regarded as mitochondrial depletion disorder. Only few reports about a low degree of mtDNA deletions in Alpers-Huttenlocher syndrome are available.
It has to be evaluated if either the reduction of the mtDNA content or the amount of deleted molecules have a higher relevance for the onset of these disorders.

The mtDNA depletion can lead to an impairment of the cellular metabolism. This includes that the dynamics of a decrease of the mtDNA content and the biochemical activity could be compared. It was of special interest to investigate if the reduction of the mtDNA and a possible decrease of the biochemical activity of the cells would be correlated in a linear relation or if a threshold value would exist.
One possibility to determine the influence of the depletion on the respiratory skills is an *in vitro* assay. The advantages of this system are a short examination time and the opportunity to vary the favored parameters.

4. Materials and Methods

4.1 Materials

4.1.1 Synthetic oligodeoxynucleotides

The following synthetic oligodeoxynucleotides for the mitochondrial genome (Anderson et al., 1981), the nuclear single copy gene *Kir4.1* (GenBank accession no. U52155), and the nuclear low copy gene *β-actin* (GenBank accession no. NM_001101), purchased from the companies Thermo Fisher Scientific Inc. (Waltham, USA) and Eurofins MWG GmbH (Martinsried, Germany), were utilized in polymerase chain reactions:

Table 1. Synthetic oligodeoxynucleotides for nuclear DNA as well as mitochondrial DNA (mtDNA).

Locus	Designation	Region	Direction	Sequence
Kir4.1; nuclear	KIR835F	835-853	forward	5'-GCGCAAAAGCCTCCTCATT-3'
	KIR857TM	857-883	forward	5'-FAM-TGCCAGGTGACAGGAAAACTGCTTCAG-TAMRA-3'
	KIR903R	903-885	reverse	5'-CCTTCCTTGGTTTGGTGGG-3'
β-Actin; nuclear	BA341F	341-363	forward	5'-GGCACCACACCTTCTACAATGAG-3'
	BA392TM	392-411	forward	5'-FAM-TGCTGCTGACCGAGGCCCCC-TAMRA-3'
	BA444R	444-425	reverse	5'-GGTCATCTTCTCGCGGTTGG-3'
mtDNA; mitochondrial	MT16520F	16520-16543	forward	5'-CATAAAGCCTAAATAGCCCACACG-3'
	MT16557TM	16557-12	forward	5'-FAM-AGACATCACGATGGATCACAGGTCT-TAMRA-3'
	MT35R	35-12	reverse	5'-CCGTGAGTGGTTAATAGGGTGATA-3'

4.1.2 Enzymes, chemicals and solutions

The following enzymes, chemicals and solutions were used:

Table 2. Enzymes.

Enzyme	Company	Registered Office
acetyl coenzyme A	Sigma-Aldrich	St. Louis, USA
catalase	Serva Electrophoresis GmbH	Heidelberg, Germany
JumpStart *Taq* polymerase	Sigma-Aldrich	St. Louis, USA
proteinase K	QIAGEN N.V.	Venlo, Netherlands
restriction endonucleases and corresponding buffers	New England Biolabs	Ipswich, United Kingdom
trypsin	PAA Laboratories GmbH	Pasching, Austria

Table 3. Chemicals.

Chemical	Company	Registered Office
acetic acid	Sigma-Aldrich	St. Louis, USA
ADP	Sigma-Aldrich	St. Louis, USA
agarose	Sigma-Aldrich	St. Louis, USA
boric acid	Sigma-Aldrich	St. Louis, USA
bromophenol blue	Sigma-Aldrich	St. Louis, USA
cytochrome *c*	Sigma-Aldrich	St. Louis, USA
DAB	Sigma-Aldrich	St. Louis, USA
2', 3'-dideoxycytidine	Sigma-Aldrich	St. Louis, USA
digitonin	Serva Electrophoresis GmbH	Heidelberg, Germany
disodium EDTA	Sigma-Aldrich	St. Louis, USA
DMEM	PAA Laboratories GmbH	Pasching, Austria
DMSO	Merck	Darmstadt, Germany
dNTPs	Sigma-Aldrich	St. Louis, USA
double distilled water	Sigma-Aldrich	St. Louis, USA
DTNB	Sigma-Aldrich	St. Louis, USA
EDTA	Sigma-Aldrich	St. Louis, USA
ethidium bromide	Sigma-Aldrich	St. Louis, USA
FBS	Invitrogen Corporation	Carlsbad, USA
glutamic acid	Sigma-Aldrich	St. Louis, USA
glycerol	Sigma-Aldrich	St. Louis, USA
HCl	Merck	Darmstadt, Germany
JumpStart buffer	Sigma-Aldrich	St. Louis, USA

KCl	Sigma-Aldrich	St. Louis, USA
$KHCO_3$	Sigma-Aldrich	St. Louis, USA
KH_2PO_4	Sigma-Aldrich	St. Louis, USA
K_2HPO_4	Sigma-Aldrich	St. Louis, USA
malate	Sigma-Aldrich	St. Louis, USA
mannitol	Sigma-Aldrich	St. Louis, USA
marker for DNA; 1 kb Ladder	Sigma-Aldrich	St. Louis, USA
$MgCl_2$	Sigma-Aldrich	St. Louis, USA
NaCl	Sigma-Aldrich	St. Louis, USA
Na_2HPO_4	Sigma-Aldrich	St. Louis, USA
NBT	Serva Electrophoresis GmbH	Heidelberg, Germany
NH_4Cl	Sigma-Aldrich	St. Louis, USA
oxaloacetic acid	Sigma-Aldrich	St. Louis, USA
penicillin	Invitrogen Corporation	Carlsbad, USA
pyruvic acid	Sigma-Aldrich	St. Louis, USA
rotenone	Sigma-Aldrich	St. Louis, USA
Rox reference dye	Invitrogen Corporation	Carlsbad, USA
SDS	Sigma-Aldrich	St. Louis, USA
streptomycin	Invitrogen Corporation	Carlsbad, USA
succinate	Sigma-Aldrich	St. Louis, USA
sucrose	AppliChem GmbH	Darmstadt, Germany
triethanolamine	Sigma-Aldrich	St. Louis, USA
tris	Sigma-Aldrich	St. Louis, USA
Triton X-100	Sigma-Aldrich	St. Louis, USA
TTFB	The uncoupler TTFB was a kind gift from Prof. Dr. B. Beechey.	Institute for biological sciences, University of Wales, Aberystwyth, United Kingdom
Tween 20	Sigma-Aldrich	St. Louis, USA
uridine	Sigma-Aldrich	St. Louis, USA
xylene cyanol	Merck	Darmstadt, Germany

Table 4. Solutions.

Solutions	Ingredients
brain media	110 mM mannitol, 60 mM tris, 60 mM KCl, 10 mM KH_2PO_4, 0.5 mM NaEDTA, pH 7.4
cell freezing media	90 % [v/v] FBS, 10 % [v/v] DMSO
fibroblast media	DMEM (4.5 g/l glucose, GlutaMAX™, 1 mM sodium pyruvate), 10 % [v/v] FBS, uridine (0.005 g/l), penicillin (100,000 U/l), streptomycin (0.1 g/l)
laser dissection buffer	1x JumpStart buffer, 0.1x TE buffer, 0.005 % [v/v] Tween 20
loading dye	1x TBE buffer, 30 % [v/v] glycerol, 0.04 % [w/v] bromphenol blue, 0.04 % [w/v] xylene cyanole
lysis buffer A	155 mM NH_4Cl, 10 mM $KHCO_3$, 0.1 mM EDTA, pH 7.4
lysis buffer B	0.5 % [w/v] SDS, 10 mM EDTA, pH 7.4
PBS	137 mM NaCl, 2.68 mM KCl, 7.48 mM $Na_2HPO_4 \cdot 12\ H_2O$, 1.37 mM K_2HPO_4, pH 7.4
SE buffer	75 mM NaCl, 25 mM EDTA, pH 8
staining solution for cytochrome *c* oxidase (COX)	219 mM sucrose, 50 mM $Na_2HPO_4 \cdot 12\ H_2O$, 2.52 mM DAB·4 HCl·2 H_2O, 161.5 µM cytochrome *c*, 16.67 µM catalase (≙ 2,600 U), pH 7.4
staining solution for succinate dehydrogenase (SDH)	50 mM succinate, 12.5 mM tris-HCl, 2.5 mM $MgCl_2 \cdot 6\ H_2O$, 61.15 µM NBT, pH 7.4
TAE buffer (10x)	400 mM tris-acetate, 10 mM EDTA, pH 8.0
TBE buffer (10x)	890 mM tris-borate, 20 mM EDTA, pH 8.3
TE buffer	10 mM tris-HCl, 1 mM EDTA, pH 7.4
trypsin solution	2.5 mg/ml trypsin in 1x PBS, pH 7-7.5

4.1.3 Kits

The following kits were utilized:

Table 5. Kits.

Kit	Company	Registered Office
QIAamp DNA Mini Kit	QIAGEN N.V.	Venlo, Netherlands
QIAquick Gel Extraction Kit	QIAGEN N.V.	Venlo, Netherlands
QIAquick PCR Purification Kit	QIAGEN N.V.	Venlo, Netherlands
Total Protein Kit, Micro Lowry, Peterson's Modification	Sigma-Aldrich	St. Louis, USA

4.1.4 Equipment

The following electronic equipment was used in the experiments:

Table 6. Measurement equipment.

Electronic equipment	Model	Company	Registered Office
oxygraph	OROBOROS Oxygraph-2k	OROBOS® INSTRUMENTS GmbH	Innsbruck, Austria
quantitative real time PCR (qPCR) thermocycler	iCycler Thermal Cycler	Bio-Rad	Hercules, USA
spectrophotometer	Cary 50 scan	Varian, Inc.	Palo Alto, USA

Table 7. Other equipment.

Electronic equipment	Model	Company	Registered Office
analytical balance	TE214S	sartorius	Elk Grove, USA
camera	3 CCD Color Video Camera, Model DXC-9100P	Sony Corporation	Minato, Japan
epi-fluorescence microscope	Eclipse E800	Nikon	Tokyo, Japan
gel electrophoresis chamber	Sub-cell GT System	Bio-Rad	Hercules, USA
haemocytometer	BLAUBRAND®, Neubauer, IVD	BRAND GMBH + CO KG	Wertheim, Germany
homogenizer	ultraturrax homogenizer	IKA	Staufen, Germany
PCR thermocycler	GeneAmp® PCR system 9700	Applied Biosystems	Carlsbad, USA
PCR thermocycler	MJ Research PTC-100	GMI, Inc.	Ramsey, USA
phase contrast microscope	Axiovert 40 C	Carl Zeiss AG	Jena, Germany
pH meter	InoLab pH 720	WTW	Weilheim, Germany
power supply	PowerPac 300	Bio-Rad	Hercules, USA
sonicator	ultrasonic processor	GENEC	Montreal, Canada
UV illuminator	Geldoc™ XR	Bio-Rad	Hercules, USA

For the analysis of the experiments the following software was utilized:

Table 8. Measurement software.

Application area	Software	Company	Registered Office
qPCR	MyiQ™ Single-Color Real-Time PCR Detection System	Bio-Rad	Hercules, USA
respirometry	OROBOROS DatLab	OROBOS® INSTRUMENTS GmbH	Innsbruck, Austria
spectrophotometry	CaryWinUV	Varian, Inc.	Palo Alto, USA

Table 9. Other software.

Application area	Software	Company	Registered Office
formula derivation	Maple	Waterloo Maple Inc.	Waterloo, Canada
laser dissectioning	PalmWin 2.2.2A	Carl Zeiss AG	Jena, Germany
microscope image capturing	Lucia 32 G / Magic	Nikon	Tokyo, Japan
plotting and data analysis	SigmaPlot 2001	Systat Software Inc.	San José, USA
raster graphics editor	Adobe Photoshop	Adobe Systems	San José, USA
statistical analysis	GraphPad Prism 5	GraphPad Software, Inc.	San Diego, USA
vector graphics editor	CorelDraw	Corel Corporation	Ottawa, Canada

4.2 Patients and human material

4.2.1 Patient ascertainment

The study was performed according to the guidelines of the University Ethical Commission. All patients or their respective guardians gave consent to the scientific use of their anonymized data. The clinical data of the patients were provided by the Departments of Epileptology and Neurology, University Bonn.

4.2.2 Human samples

The control DNA samples were obtained from routine skeletal muscle biopsies without signs of mitochondrial disease, from brain surgery samples of patients with

temporal lobe epilepsy, from post mortem liver as well as from blood samples, buccal mucosa and skin fibroblasts of patients not suspect of mitochondrial disorder.

4.2.3 Cell lines

HeLa cells were applied as a control tumor cell line. The HeLa TG wildtype cell line and the according HeLa EB8 ρ^0 cell line (Hayashi et al., 1991; Hayashi et al., 1994) were kind gifts from Prof. Dr. Rudolf Wiesner from the Institute of Vegetative Physiology, University Cologne.

4.3 Cell culture

4.3.1 Thawing cells

The fibroblasts were stored in liquid nitrogen at –195 °C. For cultivation, they were quickly thawed to 37 °C and transferred to a tissue culture flask with desired size and required amount of fibroblast media (table 4). The cells were maintained in a cell incubator at 37 °C and 5 % CO_2.

4.3.2 Passaging cells

For passaging of the cells, the fibroblast media of the flask was aspirated and discarded. The cells were washed with 1x PBS and then detached by incubation in 2.5 mg/ml trypsin solution (table 2; table 4) at 37 °C. Trypsin cleaves the cell adhesion proteins. The trypsinised state of the cells was controlled under the microscope. After resuspending the cells in the required amount of fibroblast media, they were transferred to new tissue culture flasks.

4.3.3 Cell counting

Firstly, the fibroblasts were removed from the bottom of the culture dish with trypsin (paragraph 4.3.2) and resuspended in fibroblast media. 20 µl of this solution were transferred to a Neubauer haemocytometer and inspected using a microscope. For determination of the cell count, results from eight type A squares of the Neubauer

haemocytometer with a volume of 1 mm^3 each were averaged. On the basis of these data the total cell amount was calculated.

4.3.4 Depletion treatment

For depletion of mitochondrial DNA (mtDNA), cells were cultivated in fibroblast media containing 1mM pyruvate, 0.005 g/l uridine and either 0.13 µM ethidium bromide (EtBr) or 20 µM 2', 3'-dideoxycytidine (ddC).

4.3.5 Freezing cells

Trypsinised cells were resuspended in the desired amount of fibroblast media and centrifuged at 1,000 g for 5 min. After discarding the supernatant, the cells were resuspended in the required amount of cold cell freezing media (table 4). The cells were aliquoted in cryo reaction tubes and cooled down for 1 h at – 20 °C, then for 24 h at – 80 °C and finally in liquid nitrogen. By this slow cooling, the cells were protected from mechanical destruction by ice crystal formation.

4.4 DNA analysis

4.4.1 DNA isolation from blood by salting out

Lysis of red blood cells was carried out by adding 30 ml cooled lysis buffer A (table 4) to 10 ml EDTA-anticoagulated blood. After incubation for 30 min on ice, the sample was centrifuged at 1,000 g and 4 °C for 10 min. The supernatant was removed afterwards. The sample was carefully swayed in 10 ml of lysis buffer A and centrifuged again as before. Subsequently, the supernatant was removed, the pellet was rinsed with 10 ml of 0.15 M KCl and centrifuged at 1,000 g and 4 °C for 10 min. The pellet was mixed in 5 ml SE buffer (table 4) containing 0.9 % SDS [w/v] and 0.045 mg/ml proteinase K. After incubation at 55 °C for 1 h, the pellet was shaked vigorously in 1.7 ml 5 M NaCl and centifuged for 15 min and 5,000 g at room temperature. The supernatant was transferred to a new reaction tube. The DNA was precipitated as a thread by adding 2 volumes of pure ethanol and carefully swaying. The DNA thread was transferred to a new reaction tube, dried, dissolved in the desired amount of TE buffer (table 4) and stored at 4 °C.

4.4.2 DNA isolation from fibroblasts by salting out

Lysis of fibroblasts was performed by addition of lysis buffer B (table 4) containing 0.2 mg/ml proteinase K and incubation with shaking at 37 °C overnight. The DNA was precipitated by adding 0.3 volumes of 5 M NaCl and mixing vigorously for 15 s. The sample was centifuged at 5,000 g for 15 min at room temperature. The supernatant and 2 volumes of pure ethanol were inverted for 1 min. The DNA was centrifuged at 5,000 g for 10 min. The pellet was washed with 1 ml 70 % ethanol [v/v] and dried. The DNA was solved in the desired amount of TE buffer and stored at 4 °C.

4.4.3 DNA isolation with the QIAamp DNA Mini Kit

The DNA isolation was performed as specified in the manual of the QIAamp DNA Mini Kit (QIAGEN N.V., Venlo, Netherlands).

4.4.4 DNA isolation from liver slices

Cytochrome *c* oxidase (COX)-positive and COX-negative regions (paragraph 4.5.4) of 10 µm thick liver tissue slices were cut out on a phase contrast microscope with laser dissection. A region of approximately 50 cells was cut out. Cells were lysed in laser dissection buffer containing 1.67 mg/ml proteinase K.

4.4.5 Photometric quantitation of the nucleic acid concentration

The determination of the nucleic acid concentration occured by measurement of the optical density with a spectral photometer. Double-stranded DNA showed an absorption maximum at the wavelength λ = 260 nm, whereas proteins possessed an absorption maximum at the wavelength λ = 280 nm. 1 OD_{260nm} unit corresponded to 50 µg/ml for double-stranded DNA and accordingly 40 µg/ml for single-stranded DNA and RNA. The ratio OD_{260nm} /OD_{280nm} provided an estimate of the degree of purity of the nucleic acid. The quality of the DNA was considered suitable if it featured a ratio between 1.8 and 2.0.

4.4.6 DNA mutation analysis

DNA mutation analysis using restriction fragment length polymorphism (RFLP) analysis of PCR fragments were performed in the Department of Epileptology, University Bonn. The application of RFLP analysis involved cutting the DNA using restriction endonucleases to distinguish between wildtype and mutated molecules. The size of the resulting DNA fragments was analysed on polyacrylamide gels and, when required, further examined by sequencing.

4.4.7 Quantitative PCR (qPCR)

With the PCR method, an exponential amplification of DNA fragments of variable size is possible due to a heat resistant *Taq* polymerase (Mullis and Faloona, 1987). As a result of heat denaturation, single-stranded templates are formed, allowing an annealing of primers at a lower temperature. In this way, complementary copies can be elongated along the templates.

qPCR is a modification of this method allowing the monitoring of the DNA amplification in real time. The most prominent techniques for the time being are using either SYBR® Green I or specific probes. SYBR® Green I intercalates between the strands of the DNA and therefore stains DNA in an unspecific way. Specific probes such as TaqMan® probes contain, based on the effect of fluorescence resonance energy transfer (FRET; Förster, 1946), a fluorophore and a quencher molecule. The TaqMan® probe binds to a specific sequence during the annealing phase and is degenerated by the *Taq* polymerase as the template is elongated. The fluorescence signal of the fluorophore is no longer quenched after spatial separation of both molecules. This results in the fluorescence signal detectable in real time of the PCR.

Table 10. qPCR reaction mix.

Component	Volume [µl]	Final concentration
double distilled water	6.36	
$MgCl_2$ (25 mM)	2.5	2.5 mM
10x JumpStart buffer containing 1.5 % Triton X-100	2.5	1x
DMSO	0.38	1.5 %
dNTPs (25 mM each)	0.2	200 µM each
50x Rox reference dye	0.13	0.26x
JumpStart *Taq* polymerase (2.5 U/µl)	0.13	0.31 U
primer forward (12.5 pmol/µl)	0.3	150 nM
primer reverse (12.5 pmol/µl)	0.3	150 nM
TaqMan® probe (12.5 pmol/µl)	0.2	100 nM
DNA sample	12	
total volume	25	

Table 11. qPCR amplification protocol. * Cycles recorded by the camera of the qPCR thermocycler (table 6 and 8).

Step	Temperature [°C]	Time [s]	Cycles
denaturation	95	180	1
denaturation	95	15	45*
annealing/elongation	60	60	
denaturation	95	60	1
infinite hold	16	∞	1

Several analysis methods for determination of the cycle number (C_T-value) are existing. They are generally divided into the fit points method (Freeman et al., 1999; Pfaffl, 2001; Wittwer and Kusukawa, 2004; Wittwer et al., 1997), the second derivative maximum method (Tichopad et al., 2002; Zhao and Fernald, 2005) and the sigmoidal curve fit method (Liu and Saint, 2002; Rutledge, 2004).

Applying the fit points method, a threshold line is adjusted parallel to the x-axis. The x-axis is defining the strength of the fluorescence signal, the y-axis is related to the cycle number. The C_T-values are thus acquired in the region of the fluorescence curve measured by qPCR, where all reactions are in the exponential phase.

However, choosing the threshold line depends on subjective judgement of the user (Zhao and Fernald, 2005).
With the second derivative maximum method and the sigmoidal curve fit method, the second derivative of the curve is calculated. The C_T-value is determined by taking either the maximum of the second derivative using the second derivative maximum method or the zero value that is the inflection point using the sigmoidal curve fit method. The maximum of the second derivative curve corresponds to the beginning and the inflection point to the center of the linear phase of the fluorescence curve. It was shown by mathematical modeling of individual amplification reactions that a four-parametric sigmoidal curve-fitting shows remarkable accuracy and reliability (Rutledge, 2004).

For this reason, the C_T-value was calculated using the sigmoidal curve fit method on the basis of the inflection point of the regression equation (SigmaPlot 2001; table 9). The data collected by qPCR were fitted with a sigmoidal regression curve, namely Chapman curve, with four parameters provided by the software with the equation:

$$y = y_0 + a(1 - e^{-bx})^c$$

The four parameters y_0, a, b and c determined the shape of the curve and the degree of the exponential function.

For determination of the inflection point, this equation was differentiated using the mathematical software maple.
The first derivative was:

$$f'(x) = \frac{a(1 - e^{-bx})^c c\, b\, \mathrm{e}^{-bx}}{1 - e^{-bx}}$$

The second derivative was:

$$f''(x) = \frac{a(1 - \mathrm{e}^{-bx})^c c^2 b^2 (e^{-bx})^2}{(1 - e^{-bx})^2} - \frac{a(1 - \mathrm{e}^{-bx})^c c\, b^2 e^{-bx}}{1 - e^{-bx}} - \frac{a(1 - \mathrm{e}^{-bx})^c c\, b^2 (e^{-bx})^2}{(1 - e^{-bx})^2}$$

The inflection point can be calculated setting the second derivative to zero:

$$f''(0)=\frac{\ln(c)}{b}$$

The C_T-value equales to the *x* coordinate of the inflection point of the fluorescence curve. For each value, three dilutions were performed each in triplicate experiments. Furthermore, the arithmetic mean and the standard deviation of each triplicate were calculated.

The mtDNA copy number was deduced on the basis of the proportion of a single copy nuclear gene to the mtDNA content.
The cycle number difference (*D*) was calculated from the mean cycle number values of the reference gene (*cR*) and the gene of interest (*cI*):

$$D = cR - cI$$

From this, the absolute copy number (*CN*) of the gene of interest was derived:

$$CN = 2^D$$

The relation between a diploid single copy nuclear gene and a mitochondrial sequence is hence calculated as following:

$$CN = 2^D \cdot 2$$

To determine the efficiency of the reaction, a serial dilution of the measured C_T-values of DNA samples was plotted against their initial concentration in a semilogarithmic scale. Every dilution series contained three dilutions each in triplicates.
Statistically viewed, the total amount of DNA is duplicated in each reaction cycle according to an efficiency of 100 %. In this case, the negative correlation between

slope and intercept would have a value of –1. The slope *s* and the efficiency *E* were related to each other as following:

$$E = (\frac{1}{s}) \cdot (-100)$$

4.5 Enzymatic assays

4.5.1 Protein content determination

The determination of the protein content of cells was performed by using the Total Protein Kit, Micro Lowry, Peterson's Modification from Sigma-Aldrich (St. Louis, USA) according to Bensadoun and Weinstein (1976), Lowry et al. (1951), and Peterson (1977).

4.5.2 Citrate synthase (CS) assay

Tissue specimen or cells were pre-treated to release CS from the mitochondrial matrix. Frozen muscle or brain samples were homogenized in 0.1 M phosphate buffer (pH 7.4) with a homogenizer three times for 15 s at 24,000 rpm. The homogenate was centrifuged for 10 min, 4 °C at 20,000 g. For CS measurement, the supernatant was used. The homogenized tissue supernatant or cells diluted in 1x PBS were sonificated three times for 15 s with a sonicator.

The CS measurement was carried out in a modified way according to Bergmeyer (1970). CS was used as a marker of the mitochondrial matrix. CS catalyzed the following reaction:

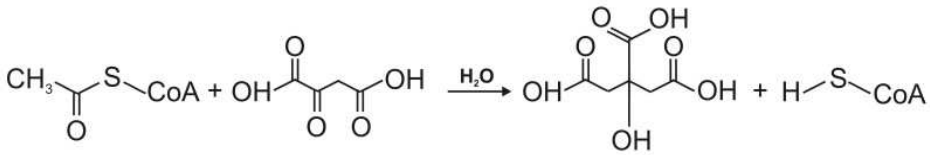

Figure 6. Reaction of acetyl coenzyme A (Acetyl-CoA) and oxaloacetic acid to citric acid and CoA-SH.

The thiolgroup of the product CoA-SH can be detected using 5, 5'-dithiobis-(2-nitrobenzoic acid) (DTNB):

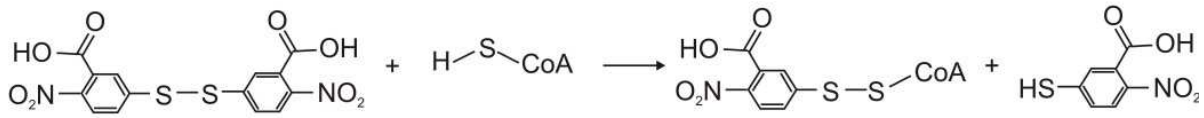

Figure 7. Reaction of 5, 5'-dithiobis-(2-nitrobenzoic acid) (DTNB) and CoA-SH to 5-Thio-2-nitrobenzoic acid (TNB) and CoA-S-S-TNB.

The yellow coloured TNB was detected spectrophotometrically by measuring the absorption maximum at the wavelength λ = 412 nm.

Table 12. CS reaction mix.

Component	Volume [ml]	Final concentration in the reaction
double distilled water	0.81	
DTNB (1mM, in 1 M tris-HCl, pH 8.1)	0.1	0.1 mM in 100 mM tris-HCl
oxalacetic acid (50 mM, in 500 mM triethanolamine, 5 mM NaEDTA)	0.05	2.5 mM in 25 mM triethanolamine, 0.25 mM NaEDTA
acetyl-CoA (12 mM)	0.03	0.36 mM
homogenate	0.01	
total volume	1	

Firstly, the background signal was measured, then the colorimetric reaction was started by adding 0.01 ml of the homogenate.

The activity of the photometric measured CS was calculated with the following formula:

$$CS\ activity = \frac{\frac{\Delta E_{412}}{min} \cdot V \cdot dil}{\varepsilon_{mM} \cdot L \cdot V_{enz}}$$

ΔE_{412} refers to the absorption difference measured at the wavelength λ = 412 nm. ε_{mM} specifies the particular extinction coefficient. The extinction coefficient of TNB at λ = 412 nm has a value of 13.6 $mM^{-1} \cdot cm^{-1}$. *L* and *V* are determining the length and

volume of the cuvette. V_{enz} exhibits the volume of the sample. The formula contains additionally the dilution factor *dil* when indicated.

4.5.3 Determination of the oxygen consumption

Examinations of the oxygen consumption were performed with an oxygraph (table 6; table 8) at 30 °C. To determine the respiratory activity of cells dependent on NADH dehydrogenase (complex I), 2 ml brain media (table 4) containing additionally 10 mM pyruvate, 5 mM malate and 3.33 mM $MgCl_2$ were filled into the oxygraph chamber. After closing the oxygraph chamber, the background changes in oxygen concentration, referring to the error of the electrode, were measured. The basic respiration of cells was detected after adding 100 µl cells diluted in brain media. The cells were permeabilized with 6.67 µM digitonin. By adding 2 mM ADP, the activity of mitochondria was stimulated. Apart from the addition of the substrates pyruvate and malate, 10 mM glutamate, another substrate of complex I, was injected to exclude an influence of pyruvate dehydrogenase on the reaction. To enhance respiration of cells further, an amount of 200 nM uncoupler TTFB was added three times to the oxygraph chamber.

The succinate dehydrogenase (complex II) dependent respiration was measured in the following way: 2 ml brain media containing additionally 3.33 mM $MgCl_2$ and 1 µm rotenone were filled into the oxygraph chamber. Rotenone inhibits complex I by blocking its ubiquinone binding site. Firstly, the background was measured. Afterwards, 100 µl cell solution and then 10 mM succinate, the substrate for complex II, were injected. The cells were permeabilized by adding 6.67 µM digitonin. By injection of 2 mM ADP the activity of mitochondria was stimulated. The respiration of cells was further enhanced by adding three times 200 nM TTFB.

4.5.4 Immunohistochemistry

Cryostat sections of liver slices (6 µm) were double-stained for cytochrome *c* oxidase (COX) and succinate dehydrogenase (SDH) as described by Dubowitz (1985) and Seligman et al. (1968). COX (complex IV) is encoded both by nuclear and mitochondrial genes. From the presence of the COX staining signal, the mtDNA

integrity can be deduced. SDH, the complex II of the respiratory chain, is encoded only by nuclear genes. SDH therefore indicates the occurrence of mitochondria independently from their mtDNA background. For a COX-SDH double-staining, tissue slices were incubated in COX staining solution (table 4) for 60 min and subsequently in SDH staining solution (table 4) for 90 min. The slices were then fixed in 4 % formalin for 5 min. All staining and fixation steps were followed by washing the respective slice three times in 1x PBS. The staining of slices was performed in the Department of Neurology, University Bonn.

4.6 Statistical analyses

For statistical analyses, the software programs Microsoft Office Excel and Graph Pad Prism 5 were utilized (table 9).

The difference of two empirical determined mean values belonging to two normally distributed sample populations was analysed using the student's t-test. The zero hypothesis indicates that the difference between those mean values is generated accidentally and that the mean values are identical. The probability of the occurence of a positive zero hypothesis was examined with the student's t-test. Level of significance was scaled to at least $p < 0.05$. Generally, a two-sided t-test for independent sample populations was applied.

A number of greater than two normally distributed sample populations was statistically analyzed using an one-way analysis of variance (ANOVA). In this regard the hypothesis, if the variance between the examined groups is bigger than the variance within these groups, was tested. The result of the ANOVA was further specified using a Dunnett test (Dunnett, 1955; Dunnett, 1964) comparing the variance of each sample population to the variance of the control population. The level of significance was scaled to at least $p < 0.05$.

5. Results

5.1 Validation of the quantitative PCR (qPCR) method

In this study, the copy number data were obtained utilizing a qPCR method. Cycle number differences between primers for the nuclear single copy gene *Kir4.1* and the mitochondrial DNA (mtDNA) were measured in qPCR reactions and subsequently analysed. A typical qPCR reaction for mtDNA determination is illustrated in figure 8. Triplicates of three different DNA concentrations for each primer were used. Assuming a comparable qPCR run, a difference of one cycle between the two different primers is equivalent to a twofold difference in copy number between the two compared genes.

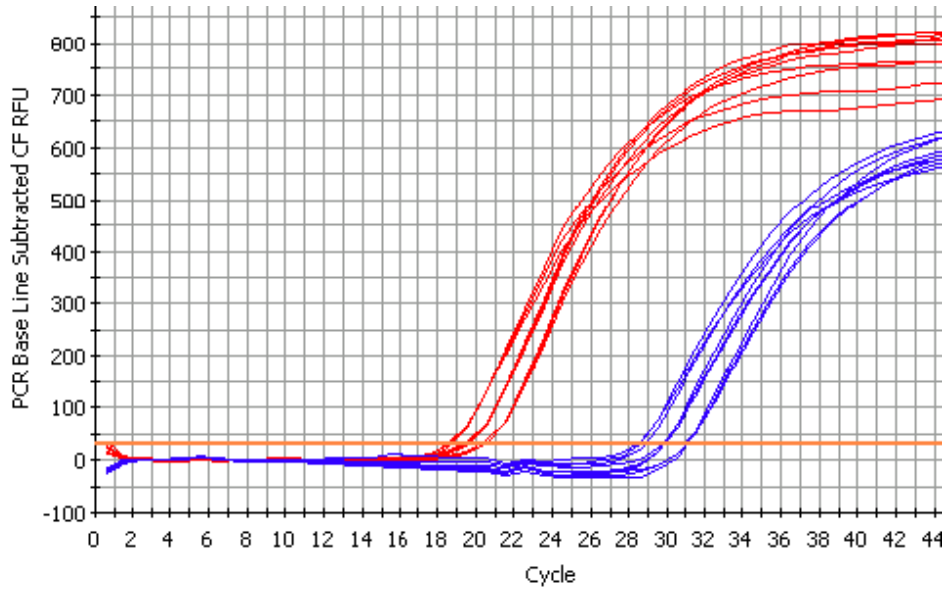

Figure 8. qPCR measurement for determination of the mtDNA copy number. Red – amplification with mtDNA primers, blue – amplification with nuclear primers, orange – threshold value provided by the qPCR thermocycler (table 6; table 8; paragraph 4.4.7). Three different DNA concentrations for each primer were used.

The appropriateness of the qPCR method was verified with several controls. The detected cycle number difference can be influenced by several disturbing factors like a reduced primer quality. A suboptimal qPCR reaction could lead to an accordingly less efficient amplification of molecules and finally to an inaccurate copy number difference value. Therefore, the accuracy of the measured cycle difference of molecules amplified by the primers for the mtDNA and the nuclear single copy gene

Kir4.1 was measured indirectly by using a comparison between the single copy gene *Kir4.1* and the low copy gene *β-actin* with already known copy number by database research. Performing an NCBI BLAST search, 13 hits for the *β-actin* region between the applied primers were found for the human genome (table 13). This fitted approximately to the measured *β-actin* copy number values of 11.53 ± 4.33 (n = 13) and 12.07 ± 2.21 (n = 6) copies in skeletal muscle and liver samples, respectively. In summary, one can say that the measured copy number difference between *β-actin* and *Kir4.1* was similar to the copy number data for *β-actin* obtained by database research indicating the reliability of the qPCR method.

Table 13. Hits from NCBI BLAST search for pseudogenes of gene-sequences from primer-amplified regions.

Gene	Reference hits for the amplified region
Kir4.1	1 hit
β-Actin	13 hits

A reaction efficiency of 100 % corresponds to optimal qPCR conditions, which results in a doubling of DNA molecules in each cycle. Variations of this value are indicators of a suboptimal reaction. The efficiency of the reaction was determined in each reaction according to paragraph 4.4.7. Since all primers exhibited a nearly 100 % efficiency (table 14), they were qualified for use in qPCR.

Table 14. Primer-dependent efficiency of qPCR reactions.

Gene	Primer-dependent efficiency [%]
Kir4.1	103 ± 14
β-Actin	104 ± 10
mtDNA	96 ± 10

Furthermore, the influence of the DNA isolation method (paragraph 4.4.1-4.4.4) on the relation between the detectable single copy gene *Kir4.1* and the mtDNA was examined. The comparison of different isolation techniques resulted in comparable values for the mtDNA copy number of wildtype fibroblasts (table 15) with 910 ± 209 mtDNA copies for DNA isolation by salting out and 999 ± 213 mtDNA copies for DNA isolation by the QIAamp DNA Mini Kit. A student's t-test (paragraph 4.6) revealed no

significant difference between the two DNA isolation methods. This led to the conclusion that the type of DNA isolation method had no effect on the ratio between mitochondrial and nuclear DNA.

Table 15. Comparison of the influence of different DNA isolation methods on the mtDNA copy number using cultivated wildtype fibroblasts.

Isolation method	Number of samples	mtDNA copy number
DNA isolation by salting out	10	910 ± 209
DNA isolation by the QIAamp DNA Mini Kit	10	999 ± 213

To estimate the linearity of the qPCR reaction, a dilution of a PCR fragment with a known concentration was performed. The measured cycle number was correlated to the PCR fragment copy number (figure 9). The leftmost and the rightmost points are corresponding to 1,000 and 16,284,000 PCR fragment molecules, respectively. A twofold higher concentration of the initial amount of DNA molecules resulted in an earlier qPCR signal, which was shifted by approximately one cycle. This indicates that the number of amplified molecules was doubled in each cycle underlining the linearity of this method.

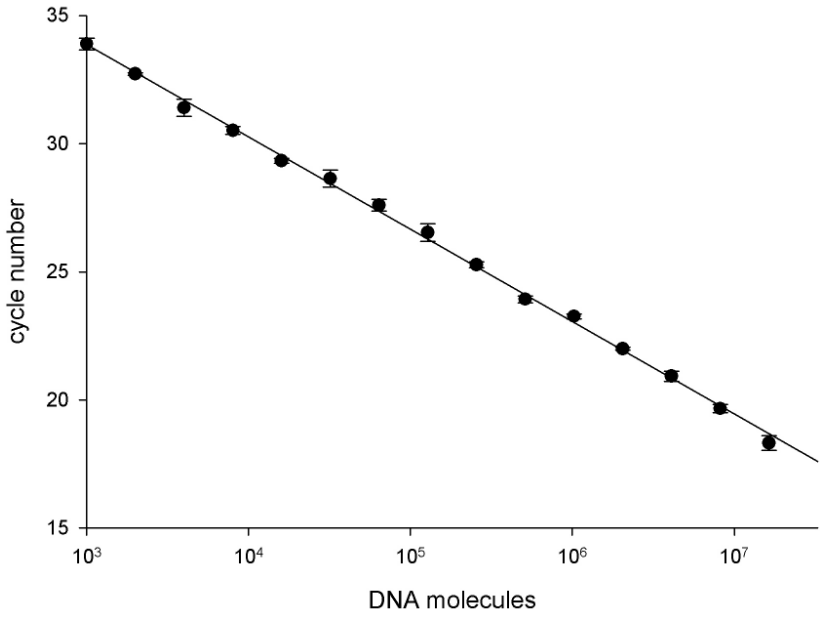

Figure 9. Illustration of the qPCR reaction in a linear regression curve. The initial amount of DNA molecules and the according cycle number data obtained by qPCR are correlated. The values are plotted in a semilogarithmic scale and represented with arithmetic mean and standard deviation.

The reliability of the qPCR measurement was further tested by comparing qPCR determinations of the mtDNA copy number in different mixtures of two cell lines exhibiting a different mtDNA copy number (figure 10). The selected cell lines were HeLa wildtype cells with a high mtDNA copy number and HeLa ρ^0 cells containing mitochondria without mtDNA molecules in their matrix. The leftmost and the rightmost data points represent exclusively HeLa ρ^0 and HeLa wildtype cells, respectively. HeLa ρ^0 cells exhibited a measured copy number of 0.81 ± 0.12 mtDNA copies per nucleus. This error could either be caused by inaccuracy of the qPCR reaction, by a detected single copy nuclear pseudogene or by the background of unspecifically amplified products. The mtDNA copy number increased with ascending amount of HeLa wildtype cells up to $1{,}161 \pm 228$ mtDNA copies for pure HeLa wildtype cells. These data suggested a linearity of the correlation between measured cycle number difference and calculated mtDNA copy number values.

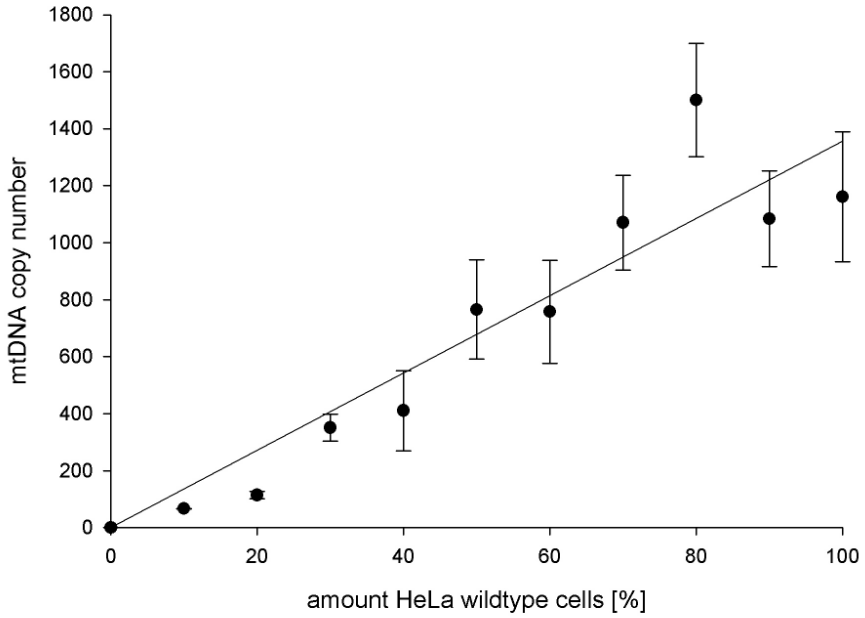

Figure 10. mtDNA copy number of HeLa wildtype and HeLa ρ^0 cells. Values are shown with arithmetic mean and standard deviation.

5.2 Tissue-specifity of the mtDNA content

The mtDNA copy number values in different tissues and species had already been examined by several groups. However, the mtDNA content of several human tissues has not been compared in detail within one study. One scope of this study was the determination of the mtDNA copy number in several human tissues and cell types. These mtDNA copy number data should be subsequently compared with according mtDNA copy number values of patients affected by diseases related to mitochondrial defects.

Therefore, data on the mtDNA copy number from several human tissues and cell types available for our group like skeletal muscle, brain specimen, liver, buccal mucosa, fibroblasts and blood were collected (paragraph 4.2.1; paragraph 4.2.2). Beside human tissues and cell types with ordinary occurrence and growth behaviour, the epithelial tumor HeLa cell line was used (paragraph 4.2.3).

The mtDNA copy number was determined for control patients (figure 11; table 16) using the quantitative PCR (qPCR) method (paragraph 4.4.7). Patients suffering from mitochondrial diseases like mitochondrial encephalomyopathy, lactic acidosis and stroke-like episodes (MELAS) or myoclonic epilepsy with ragged red fibers (MERRF) (paragraph 2.6; paragraph 2.7) were not included. Material from children under three years was also not included since especially in blood specimen very young patients showed a high variation of the mtDNA copy number. For each control patient, at least triplicate experiments were performed each in three dilutions.

Table 16. Content of mtDNA copies in human tissue samples. The values are represented with arithmetic mean and standard deviation, N – number of patients.

Tissue	Absolute mtDNA copy number	Age at sample delivery [years]	Number [N]
skeletal muscle	16,864 ± 8,843	21 ± 9	10
brain	7,145 ± 4,086	34 ± 14	43
liver	2,774 ± 1,153	47 ± 15	6
buccal mucosa	1,294 ± 756	35 ± 13	16
fibroblasts	961 ± 242	27 ± 16	8
blood	283 ± 99	25 ± 17	22
HeLa	1,161 ± 228	31	1

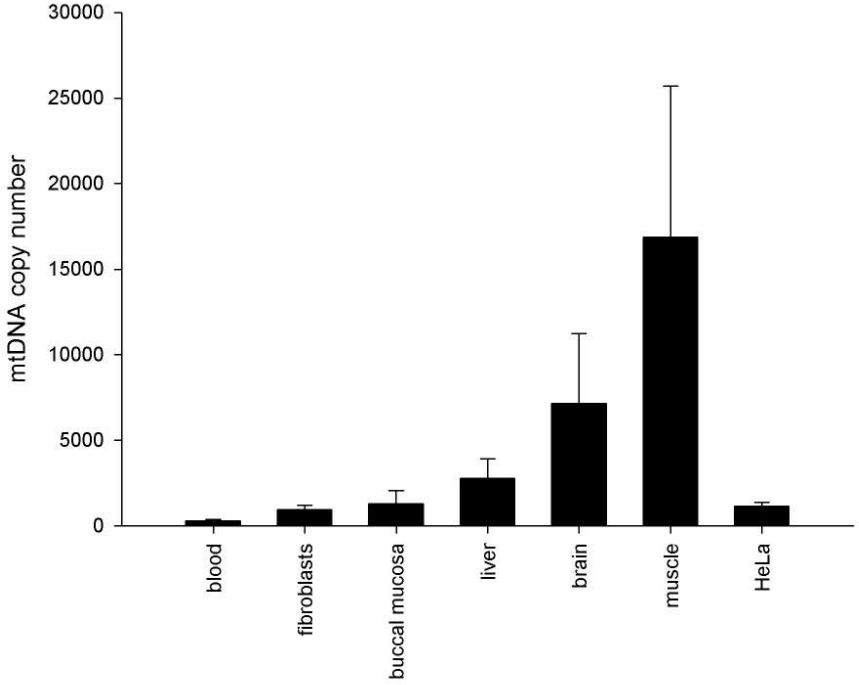

Figure 11. Comparison of the absolute mtDNA copy number in different tissues of control patients. Values are indicated with arithmetic mean and standard deviation.

The obtained mtDNA copy numbers are tissue- and celltype-specific.

5.3 Correlation between citrate synthase (CS) activity and mtDNA copy number in several tissues

A couple of literature reports state on the one hand a tissue- and celltype-specific varying mitochondria content, which is ranging from about 100,000 mitochondria per oocyte (Ankel-Simons and Cummins, 1996; Chen et al., 1995) to four mitochondria per platelet (Shuster et al., 1988). Beside the strongly varying mitochondria content, the mtDNA content is reported to be between two and ten mtDNA molecules per mitochondrion (Graziewicz et al., 2006; Shuster et al., 1988; Wiesner et al., 1992).

The mitochondria content and the mtDNA copy number were compared with each other in order to examine the stability of the ratio between the mitochondria and their DNA in different tissues. As a marker for the mitochondria content, CS is commonly used since it is regarded as a stably expressed enzyme located in the mitochondrial matrix (Figueiredo et al., 2008; Sarnat and Marín-García, 2005).

Both the mtDNA copy number and the CS activity [µmol/(g·min)] were measured and subsequently compared (table 17). The citrate synthase (CS) assay procedure of

brain and muscle tissue specimen was performed by Alexey Kudin, PhD, from our group and Karin Kappes-Horn, Department of Neurology, University Bonn.
The determination of the CS activity was performed in triplicates for each patient. The CS activity was normalised to the protein content referring to equal amounts of cell mass. Since the protein content in muscle tissue was firstly determined in g wet weight, the unit g wet weight was afterwards transformed to g protein with the factor 0.08 [g protein / g wet weight] for muscle tissue (Maia et al., 2005).
The CS activity was ranging from 32 ± 10 µmol/(g·min) in buccal mucosa to 195 ± 30 µmol/(g·min) in brain specimen. The mtDNA depleted HeLa ρ^0 cells had a marginally higher CS activity than HeLa wildtype cells with a high mtDNA content. The difference in the CS activity can possibly be related to a compensatory effect. This led to the conclusion that the mitochondrial content in HeLa cells was not severely affected by the amount of mtDNA.

The measured CS values resembled to available data in literature (Barthélémy et al., 2001; Gellerich et al., 2002; Kudin et al., 2002; Sarnat and Marín-García, 2005).
The ratio of the mtDNA content to the CS activity obtained values, which range from 14 to 35 for most examined tissues and cell types. In contrast to these similar ratio values, HeLa ρ^0 cells, containing only 0.81 ± 0.12 mtDNA copies, exhibited a low ratio of 0.01. This ratio resulted from the fact that HeLa ρ^0 cells contain mitochondria depleted of their DNA. On the contrary, in skeletal muscle fibers a high ratio of 109 was detected. This unexpected high value could be caused by a high accumulation of mtDNA molecules in mitochondria compared to the mitochondrial volume. Possible reasons for this peculiarity could lie in the muscle specific mitochondrial morphology or tasks.

Table 17. Correlation between mtDNA content and CS activity. The values are represented with arithmetic mean and standard deviation, N – number of patients.

Tissue/cell type	CS activity [µmol/(g·min)]	Absolute mtDNA copy number	Age at sample delivery [years]	Number [N]	mtDNA copy number/CS activity
skeletal muscle	166 ± 36	17,999 ± 9,296	19 ± 10	8	**109**
brain	195 ± 30	6,728 ± 3,991	21 ± 12	10	**35**
buccal mucosa	32 ± 10	954 ± 353	36 ± 7	10	**30**
fibroblasts	68 ± 7	961 ± 242	27 ± 16	8	**14**
HeLa wildtype	64 ± 2	1,161 ± 228	31	1	**18**
HeLa ρ^0	92 ± 1	0.81 ± 0.12	31	1	**0.01**

5.4 mtDNA depletion in blood specimen of patients with a mild phenotype of PEO with epilepsy/ataxia

Mutations in the nuclear encoded polymerase γ gene *POLG* are known to cause a variety of mitochondrial disease phenotypes including progressive external ophthalmoplegia (PEO) (Graziewicz et al., 2006). PEO is characterized by multiple deletions and mutations in the mitochondrial genome (Cardaioli et al., 2007; Spinazzola and Zeviani, 2005; Zeviani et al., 1989). It still remains to be elucidated how the nuclear *POLG* genotype influences the corresponding mitochondrial phenotype. We were especially interested if a reduction of mtDNA molecules within the mitochondria has, beside the existing deleted mtDNA molecules, an influence on the appearance of the disease. A family with hereditary pathogenic mutations provided us the opportunity to examine this correlation.

The total DNA content of blood specimen from a family with three daughters, two of them affected by several neurological symptoms like epilepsy, ataxia and neuropathy as well as a mild phenotype of PEO, was analysed for frequent mutations in the polymerase γ gene *POLG* (paragraph 2.7; paragraph 2.8; Paus et al., 2008). The DNA mutation analysis of this family was performed using restriction fragment length polymorphism (RFLP) analysis of PCR fragments by Gábor Zsurka, MD, PhD and Ulrike Strube, Departments of Epileptology and Neurology, University Bonn.

The healthy father harboured the heterozygous A467T *POLG* mutation, the healthy mother the heterozygous *POLG* mutation W748S in *cis* with the polymorphism E1143G (figure 12). Daughter two possessed the same *POLG* variations like the

mother and showed no symptoms characteristic for a mitochondrial disease. However, the daughters one and three featured the combination of the three DNA variations W748S and E1143G compound heterozygous with A467T (figure 12). These daughters developed the described symptoms of a mitochondrial disease (Paus et al., 2008). Since the mutation W748S and the polymorphism E1143G were generally found together (Chan et al., 2006; Hakonen et al., 2005; Nguyen et al., 2005; Van Goethem et al., 2004), this suggests that both rearrangements segregate together on the same allele.

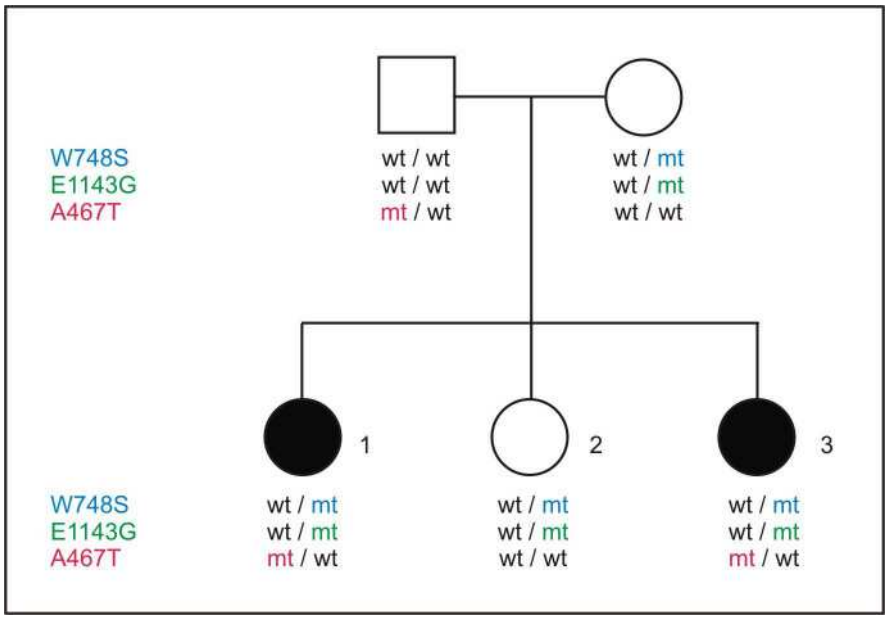

Figure 12. *POLG* genotyping of a family with members affected by a mild phenotype of PEO with epilepsy/ataxia. wt = wildtype, mt = mutant.

The mtDNA copy number values of blood samples from this family were compared to blood samples from age-matched controls (figure 13; table 18). The healthy father and the healthy daughter two exhibited mtDNA copy number values being within the range of the population of control blood samples. However, the mtDNA copy numbers in blood samples of both daughters, which were affected by the mild phenotype of PEO with epilepsy/ataxia, as well as the healthy mother are significantly decreased in a student's t-test with $p < 0.001$ in comparison to the controls. In particular, the mtDNA copy number content decreased to 69 % for the mother, to 50 % for daughter one and to 38 % for daughter three.

Table 18. Nuclear and mitochondrial features of patients with a mild phenotype of PEO with epilepsy/ataxia (modified from Paus et al., 2008). N – number of patients, n - number of experiments. Values are indicated with arithmetic mean and standard deviation, *** $p < 0.001$.

Relation	Control	Mother	Father	Daughter 1	Daughter 2	Daughter 3
pathogenic *POLG* mutations	—	E1143G + W748S	A467T	E1143G + W748S / A467T	E1143G + W748S	E1143G + W748S / A467T
	N	n	n	n	n	n
number	22	36	27	36	27	36
mtDNA copy number	283 ± 99	194 ± 35***	289 ± 53	141 ± 22***	245 ± 63	108 ± 41***
mtDNA content variation referring to control population [%]		69	102	50	87	38
age at sample delivery [years]	25 ± 17	64	64	37	38	39

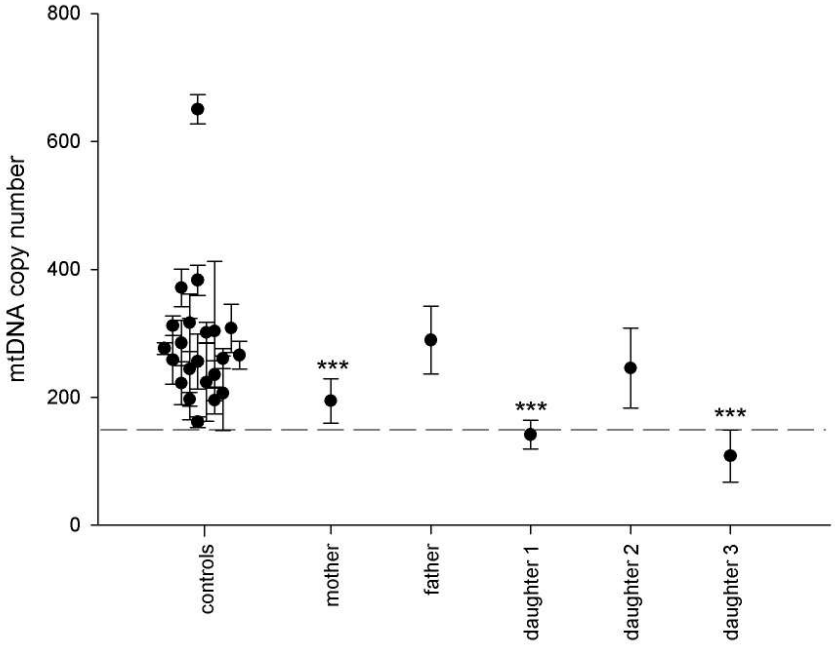

Figure 13. Comparison of the mtDNA copy number in blood specimen of controls and a family with members affected by a mild phenotype of PEO with epilepsy/ataxia (daughter one and three). Values are indicated with arithmetic mean and standard deviation, *** $p < 0.001$.

Concluding, we found a combined occurrence of a specific nuclear *POLG* genotype and a depletion of mtDNA in blood specimen of family members affected by a mild

phenotype of PEO with epilepsy/ataxia. Additionally, PEO is accompanied by the occurrence of large deletions within the mitochondrial genome. Multiple deletions were in fact detected previously by DNA mutation analysis in muscle tissue samples of both affected daughters (Paus et al., 2008). The heteroplasmic ratio of wildtype and deleted mtDNA molecules in the tissues of the affected patients might additionally enhance the severity of the clinical phenotype.

5.5 mtDNA depletion in patients with Alpers-Huttenlocher syndrome

Another well-known mitochondrial disease due to a mutation in the *POLG* gene is the Alpers-Huttenlocher syndrome. Patients with this syndrome show myoclonic epilepsy and several other symptoms such as seizures, psychomotor regression and valproate induced liver failure (paragraph 2.7). The Alpers-Huttenlocher syndrome is apart from severe mtDNA depletion accompanied by alterations of the mitochondrial genome like multiple deletions and certain point mutations (Ashley et al., 2008; Naviaux et al., 1999; Zsurka et al., 2008). The opportunity to examine to which extend several tissues exhibit a mtDNA copy number reduction was given. Furthermore, the importance of the mtDNA copy number reduction in comparison to mtDNA deletions was investigated.

The clinical features of five paediatric patients were examined (table 19; Zsurka et al., 2008). However, two patients showed no liver failure supposably due to the early diagnosis of the mitochondrial disease phenotype associated with the corresponding pathogenic *POLG* mutations.

The DNA mutation analysis of the five patients was performed using restriction fragment length polymorphism (RFLP) analysis of PCR fragments by Gábor Zsurka, MD, PhD and Ulrike Strube, Departments of Epileptology and Neurology, University Bonn. In these patients, several well-known *POLG* mutations have been detected with some of them occurring in a compound heterozygous way (table 19). Additionally to these well-known exonic *POLG* changes, several intronic variations as well as variations in the polyglutamine repeat of exon two were detected. These variations were so far not correlated to any known mitochondrial disease phenotype. Aside from the examination of nuclear changes on *POLG*, the patients were tested

for deletions within the mitochondrial DNA. They exhibited only a very low amount of deleted molecules (Zsurka et al., 2008).

Table 19. Genetic background and phenotype of patients with Alpers-Huttenlocher syndrome (according to Zsurka et al., 2008). p – patient. Single nucleotide polymorphisms (SNPs) marked in italic - coding region mutations numbered by amino acid positions. Non-marked SNPs – intronic mutations (accession no. NC_000015.8, region 87660554-87679030).

Patient	**Age at sample delivery [years]**	**Clinical phenotype**	**Pathogenic *POLG* mutations**	***POLG* SNPs**
p1	8; 17	epilepsia partialis continua; valproate induced liver failure († at 17 years)	A467T/A467T	del11751CGCGTGCG/ del11751CGCGTGCG
p2	16	epilepsia partialis continua; valproate induced liver failure	A467T/F749S	*del43QQQ*/wt; C9078T/wt; del11751CGCGTGCG/del11751CGC GTGCG; ins13710GTAG/wt; C13769T/wt; del15681GT/wt; T17677G/wt
p3	4	prolonged status epilepticus; elevated lactate and protein in cerebrospinal fluid	A467T/G848S	del11751CGCGTGCG/wt
p4	7	complex partial seizures; migraine; valproate induced liver failure († at 10 years)	W748S+E1143G/ L752P	C11741T/wt
p5	4	epilepsia partialis continua	W748S+E1143G/ G848S	*ins53Q*/wt; G1791T/wt; T10873C/wt; T11073C/wt; C11741T/wt; ins13710GTAG/wt; A15661G/wt;T15686C/wt; T17241G/wt; G17600A/wt;T17677G/wt

The mtDNA copy number in several tissues of these patients was measured. For each control, at least triplicate experiments were performed each in three dilutions.

The particular number of experiments performed for the respective Alpers-Huttenlocher patients are listed in table 20.

For patient one, samples from biopsies at the age of eight and 17 years (post mortem) were available. All examined patient tissues exhibited lowered mtDNA copy numbers compared to the controls (figure 14; table 19; table 20; Zsurka et al., 2008). In all five patients affected by Alpers-Huttenlocher syndrome, the reduction of the mtDNA copy number compared to the controls was significant in a student's t-test ($p < 0.05 – p < 0.001$).

At the age of eight years, the mtDNA copy number of patient one was reduced to values of 52 % and 37 % of the corresponding control values in skeletal muscle and blood, respectively. At the age of 17 years, the copy number in skeletal muscle was lowered further to 15 % of the according control value. In the other examined post mortem tissues, a reduction of the mtDNA copy number to 75 % for brain and 11 % for liver compared to the controls was measured. Patient two showed a lowered mtDNA copy number of 25 % and 45 % in skeletal muscle and blood, respectively. The mtDNA copy number values of patients three and four in blood were reduced similarly to 33 % and 34 %, respectively (table 20). Patient five suffering from a milder manifestation of the disease (table 19), exhibited likewise a lowered mtDNA copy number, which was only slightly decreased with mtDNA copy number values of 51 % in skeletal muscle and 54 % in blood (table 20).

The findings of a mtDNA copy number reduction in all examined tissues of the Alpers-Huttenlocher patients matched well to depletion data from the literature regarding this disease (Ashley et al., 2008; Naviaux et al., 1999).

Additionally to the decreased mtDNA copy number values in all patients exhibiting the biochemical and clinical phenotype, deleted mtDNA molecules were detected (Zsurka et al., 2008). However, since the amount of the deleted molecules was very low, a significant contribution to the disease phenotype is very unlikely.

Table 20. Depletion in various tissues of patients with Alpers-Huttenlocher syndrome (modified from Zsurka et al., 2008). N – number of patients, n - number of experiments, p - patient; Values are represented with arithmetic mean and standard deviation, * $p < 0.05$, ** $p < 0.01$, *** $p < 0.001$.

Patient	Age at sample delivery [years]	Skeletal muscle	Brain	Liver	Blood
controls	for age of controls refer to table 16	16,864 ± 8,843 (N = 10)	7,145 ± 4,086 (N = 43)	2,774 ± 1,153 (N = 6)	283 ± 99 (N = 22)
p 1	8	8,799 ± 1,760* (n = 36)	---	---	105 ± 13*** (n = 27)
p 1	17	2,564 ± 654*** (n = 54)	5,349 ± 671** (n = 27)	317 ± 111** (n = 45)	---
p 2	16	4,208 ± 809** (n = 54)	---	---	126 ± 16*** (n = 3)
p 3	4	---	---	---	92 ± 22*** (n = 27)
p 4	7	---	---	---	96 ± 22*** (n = 12)
p 5	4	8,606 ± 940* (n = 9)	---	---	153 ± 33*** (n = 36)

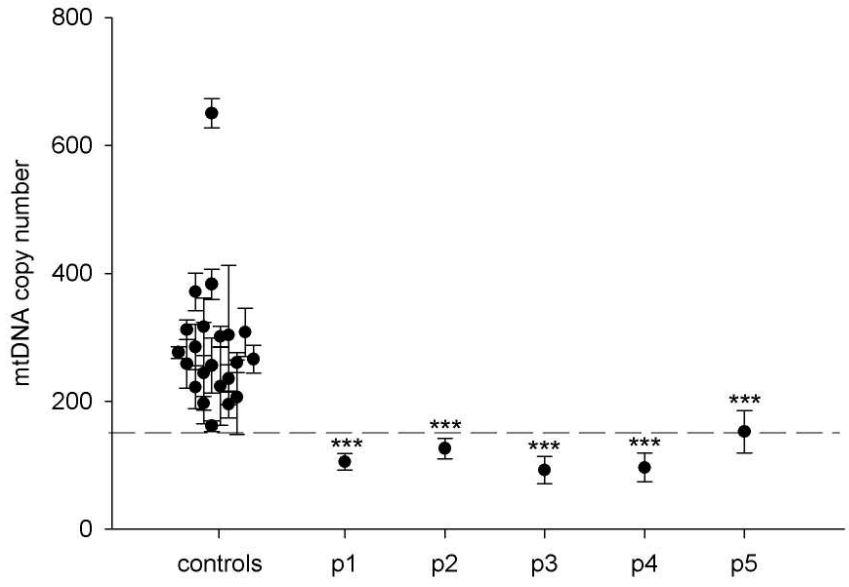

Figure 14. Depletion in blood samples of patients with Alpers-Huttenlocher syndrome (modified from Zsurka et al., 2008). p – patient. Values are indicated with arithmetic mean and standard deviation, *** $p < 0.001$.

The liver tissue of patient one, who died from valproate induced liver failure, was also examined histochemically. Tissue slices of post mortem liver were double stained for cytochrome *c* oxidase (COX, red staining) and succinate dehydrogenase (SDH, blue staining) activity (figure 15; paragraph 4.5.4). The COX and SDH activity staining of the slices was performed by Karin Kappes-Horn, Department of Neurology, University Bonn. A pattern of large COX negative (COX-) and small COX positive (COX+) areas was visualised indicating a pattern of regions with different mtDNA background resulting in intact and defect mitochondria.

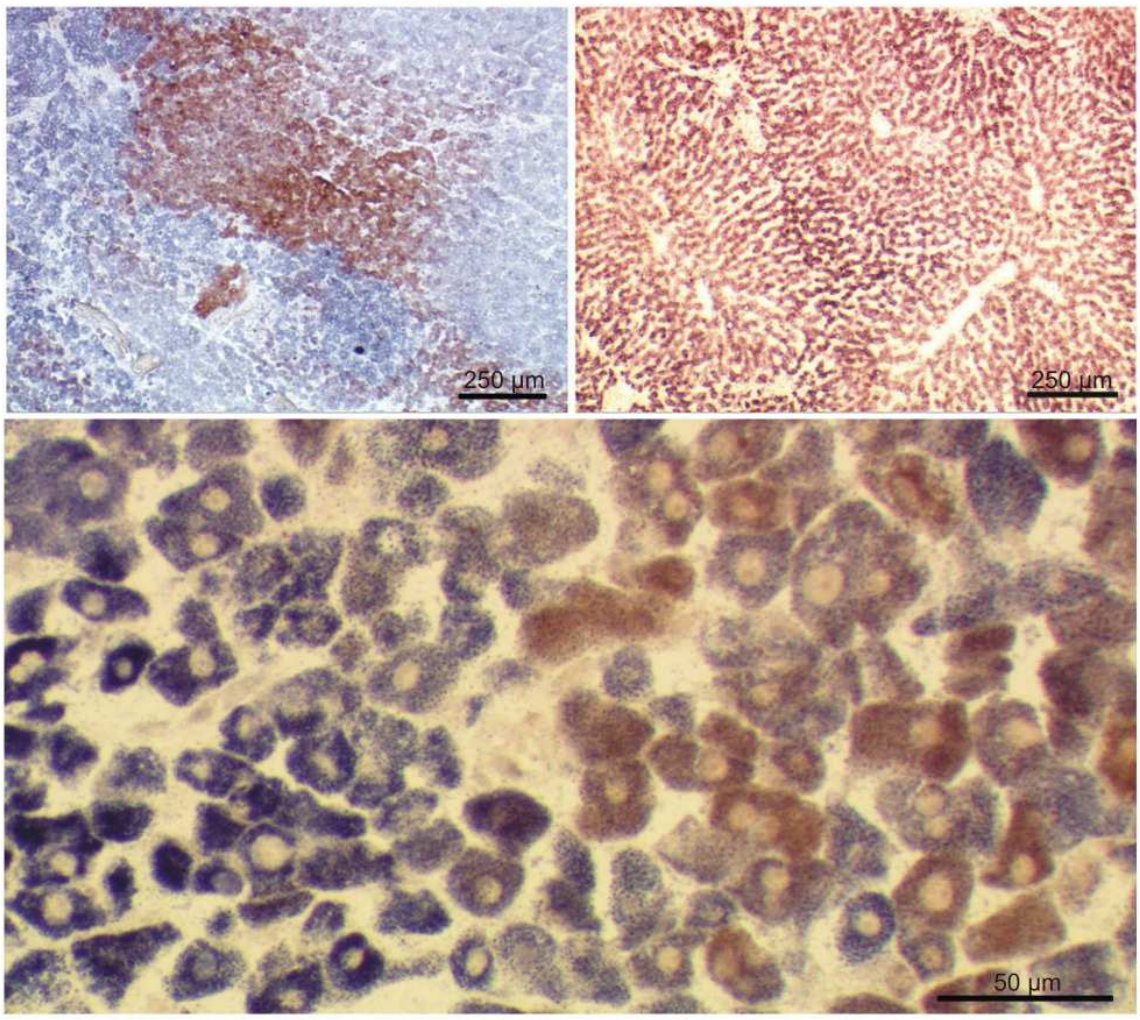

Figure 15. COX-SDH double staining of liver slices (modified from Zsurka et al., 2008). Red areas – COX+, blue areas – COX-. Left – COX+ and COX- areas of patient one featuring Alpers-Huttenlocher syndrome, right – control patient, low – higher magnification of a section of patient one liver.

The stained liver slices were microdissected to get cells from areas with different COX background. The obtained cells were examined for their mtDNA content

(paragraph 4.4.4). The mtDNA copy number in patient one was significantly ($p < 0.01$) higher in COX+ regions possessing an almost fivefold higher mtDNA content with 716 ± 247 mtDNA copies compared to COX- regions exhibiting 155 ± 59 mtDNA copies (figure 16; table 21). These mtDNA copy number values correspond to the COX staining differences observable in histological liver slices.

Table 21. mtDNA copy number distribution in liver regions of patient one (p1). Values are indicated with arithmetic mean and standard deviation, n – number of experiments.

Tissue area	mtDNA copy number
total	317 ± 111 (n = 45)
COX+	716 ± 247 (n = 6)
COX-	155 ± 59 (n = 11)

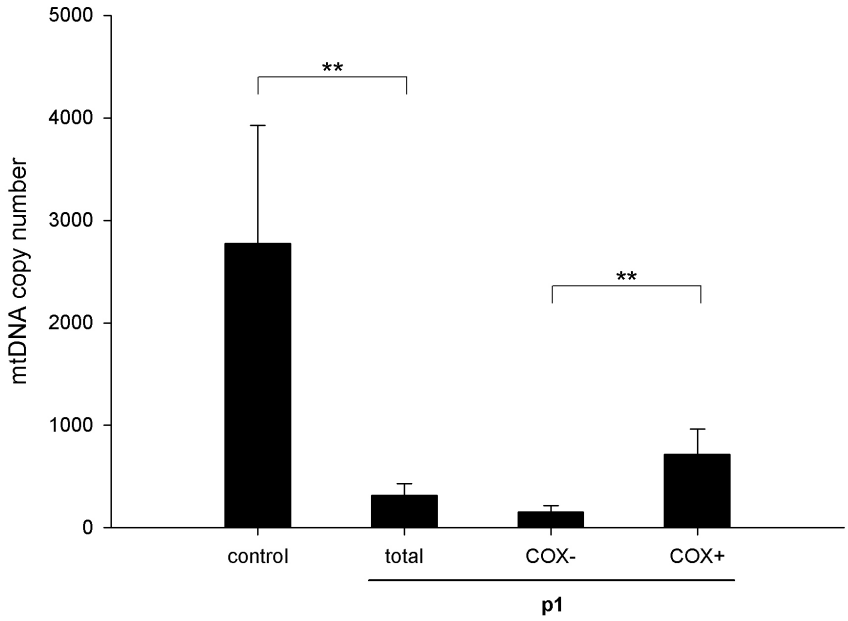

Figure 16. Mitochondrial dysfunction in COX+ and COX- regions of postmortem liver of patient one (p1) featuring Alpers-Huttenlocher syndrome (modified from Zsurka et al., 2008). Values are represented with arithmetic mean and standard deviation, ** $p < 0.01$.

5.6 Reduction of the mtDNA copy number in specific brain regions from Ammon's horn sclerosis (AHS) patients

The neurological disease temporal lobe epilepsy (TLE) with Ammon's horn sclerosis (AHS) is accompanied by the occurrence of status epilepticus, which is known to activate neuronal cell death mechanisms occurring mainly in the hippocampal cornu

ammonis 1 (CA1) and cornu ammonis 3 (CA3) neurons (Baron et al., 2007; Ben-Ari et al., 1980; Kunz et al., 2000; Liu et al., 1994; Liu et al., 1995; Nadler, 1981). An elevated level of reactive oxygen species (ROS) can be detected during status epilepticus (Kovacs et al., 2001; Liang et al., 2000). It is an important question, how changes in the function of mitochondria and the mtDNA level can affect this disease. Several areas of hippocampal brain specimen from control patients with lesion as well as patients affected by TLE with AHS were examined with regard to their mtDNA content (figure 17; table 22; Baron et al., 2007). The control patients exhibited only a lesional damage of the brain tissue close to the hippocampus (e. g. parahippocampal tumor), which is not causing neuronal cell death in the hippocampus. For each patient, at least triplicate experiments were performed each in three dilutions. The different hippocampal regions of patients with lesions or AHS are compared with a two-sided paired t-test.

The mtDNA copy number of AHS patients in the areas area dentata (AD) and parahippocampus (PH) was, in comparison to the lesion patients, only mildly reduced to 92 % and 94 % in AD and PH, respectively. However, this difference was not significant.

The other examined regions of the hippocampus, namely CA1 and CA3, showed a significant reduction to 47 % ($p < 0.01$) and 56 % ($p < 0.05$) of the control value, respectively. The reduction of the mtDNA content is in accordance to depletion data reported for CA1 and CA3 in rat hippocampus (Kudin et al., 2002). Furthermore, changes in these hippocampal regions are accompanied by both an impaired respiratory chain (Kudin et al., 2002; Kunz et al., 2000) and a reduction of the mitochondrial marker enzyme citrate synthase (CS) (Baron et al., 2007). These combined findings indicate an influence of the mtDNA copy number on the mitochondrial activity in CA1 and CA3 neurons.

Table 22. mtDNA copy number in hippocampal subfields of patients afflicted by temporal lobe epilepsy (TLE). Values are indicated with arithmetic mean and standard error, N – number of patients, * $p < 0.05$, ** $p < 0.01$. AHS – Ammon's horn sclerosis, CA1 – cornu ammonis 1, CA3 – cornu ammonis 3, AD – area dentata, PH – parahippocampus.

Subfield	CA1	AD	CA3	PH
lesion (N = 11)	8,758 ± 1,266	7,062 ± 975	6,001 ± 1,067	6,601 ± 1,149
AHS (N = 22)	4,131 ± 656**	6,474 ± 1,214	3,361 ± 380*	6,173 ± 773

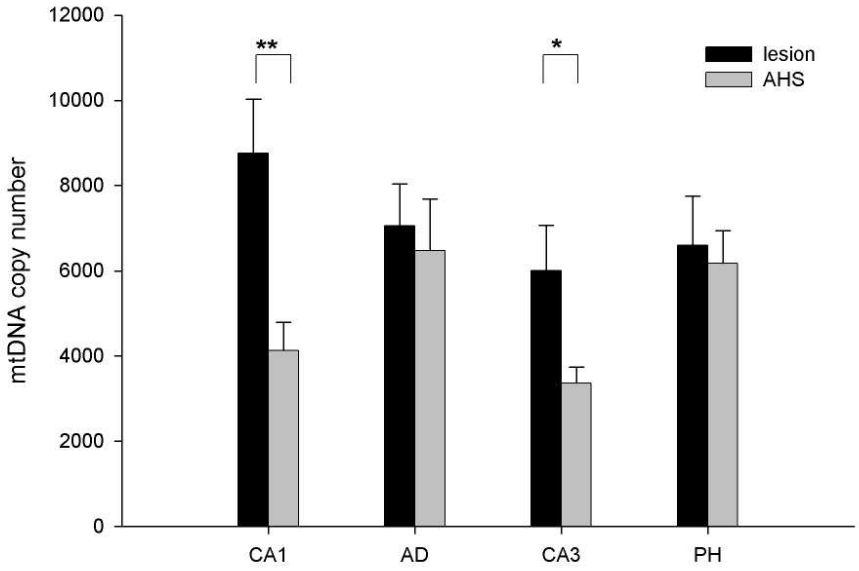

Figure 17. mtDNA copy number in hippocampal subfields of patients affected by temporal lobe epilepsy (TLE) (modified from Baron et al., 2007). AHS – Ammon's horn sclerosis, CA1 – cornu ammonis 1, CA3 – cornu ammonis 3, AD – area dentata, PH – parahippocampus. Values are indicated with arithmetic mean and standard error, * $p < 0.05$, ** $p < 0.01$, N (lesion) = 11, N (AHS) = 22.

5.7 Influence of the mtDNA content on the mitochondrial respiration activity

In several mitochondrial diseases, a threshold linked to bioenergetic defects and accordingly the clinical phenotype is postulated. This threshold refers to the heteroplasmic state of the cell and is specific for the respective mtDNA mutation (Rossignol et al., 2003). The bioenergetical context, in which this threshold occurs, has not been elucidated completely.

The described effect was examined in fibroblasts using an *in vitro* assay, in which cells were treated with 2', 3'-dideoxycytidine (ddC) or ethidium bromide (EtBr) to deplete their mtDNA. Depletion studies using ddC or EtBr have already been performed by other groups (Brown and Clayton, 2002; Chen and Cheng, 1989; Diaz et al., 2002; King and Attardi, 1989; Maniura-Weber et al., 2004; Martin et al., 1994; Miller et al., 1996; Pan-Zhou et al., 2000; Piechota et al., 2006a; Trounce et al., 1994; Zimmermann et al., 1980). EtBr intercalates between the bases of the DNA and hence inhibits the replication leading to a depletion. ddC is integrated into the DNA causing termination of strand elongation and therefore inhibits the replication as well.

Cultured skin fibroblasts of a 38 year old control patient were treated with EtBr or ddC for 25 days (paragraph 4.3.4). The treatment with these substances resulted each in a decrease of the mtDNA copy number (figure 18). In comparison to the wildtype cells with 563 ± 277 mtDNA copies, the number decreased to 1.74 ± 0.34 mtDNA copies (0.31 %) and 32 ± 4 mtDNA copies (5.65 %) in ddC- (figure 18A) and EtBr-treated cells (figure 18B), respectively. To proof the significance of the mtDNA reduction, a univariate variance analysis (ANOVA) was performed. The first significant difference, specified further in a following Dunnett test, appeared at day three of ddC-treatment and at day six of EtBr-treatment (figure 18). The significance strengthened during the further course of treatment. For each specific timepoint three measurements of independent samples were performed (n = 3).

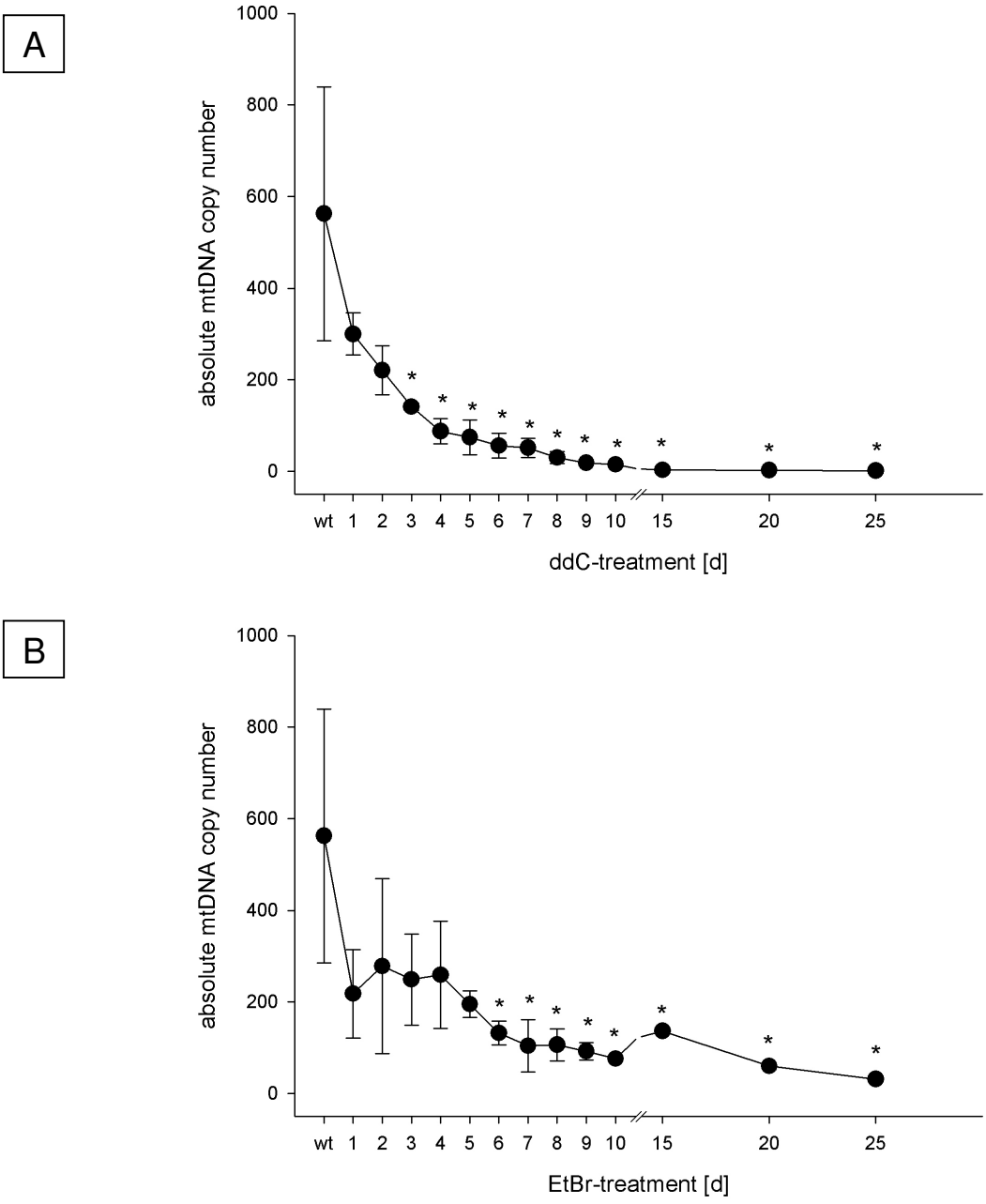

Figure 18. mtDNA depletion in ddC- and EtBr-treated fibroblasts. Measurement of mtDNA copy number changes in ddC- (A) and EtBr-treated (B) skin fibroblasts. Values are represented with arithmetic mean (n = number of experiments, = 3) and standard deviation, * $p < 0.05$.

Additionally to the mtDNA copy number, the citrate synthase (CS) activity was measured to correlate the mtDNA copy number to the mitochondrial content (figure 19). The CS activity was normalised to the protein content referring to equal amounts of cell mass. Wildtype fibroblasts showed a CS activity of 55 ± 4 µmol/(g·min). After 25 days of treatment, the cells featured a CS activity of 65 ± 5 µmol/(g·min) for ddC (figure 19A) and 63 ± 16 µmol/(g·min) for EtBr, respectively (figure 19B). The

enzymatic activity of wildtype and treated cells showed no significant difference in an one-way ANOVA followed by Dunnett test. For each specific timepoint, three measurements were performed in triplicates (n = 3). In spite of the depletion treatment, the mitochondria content of the cells stayed stable. This indicated that there was no loss of mitochondria but only of their mtDNA.

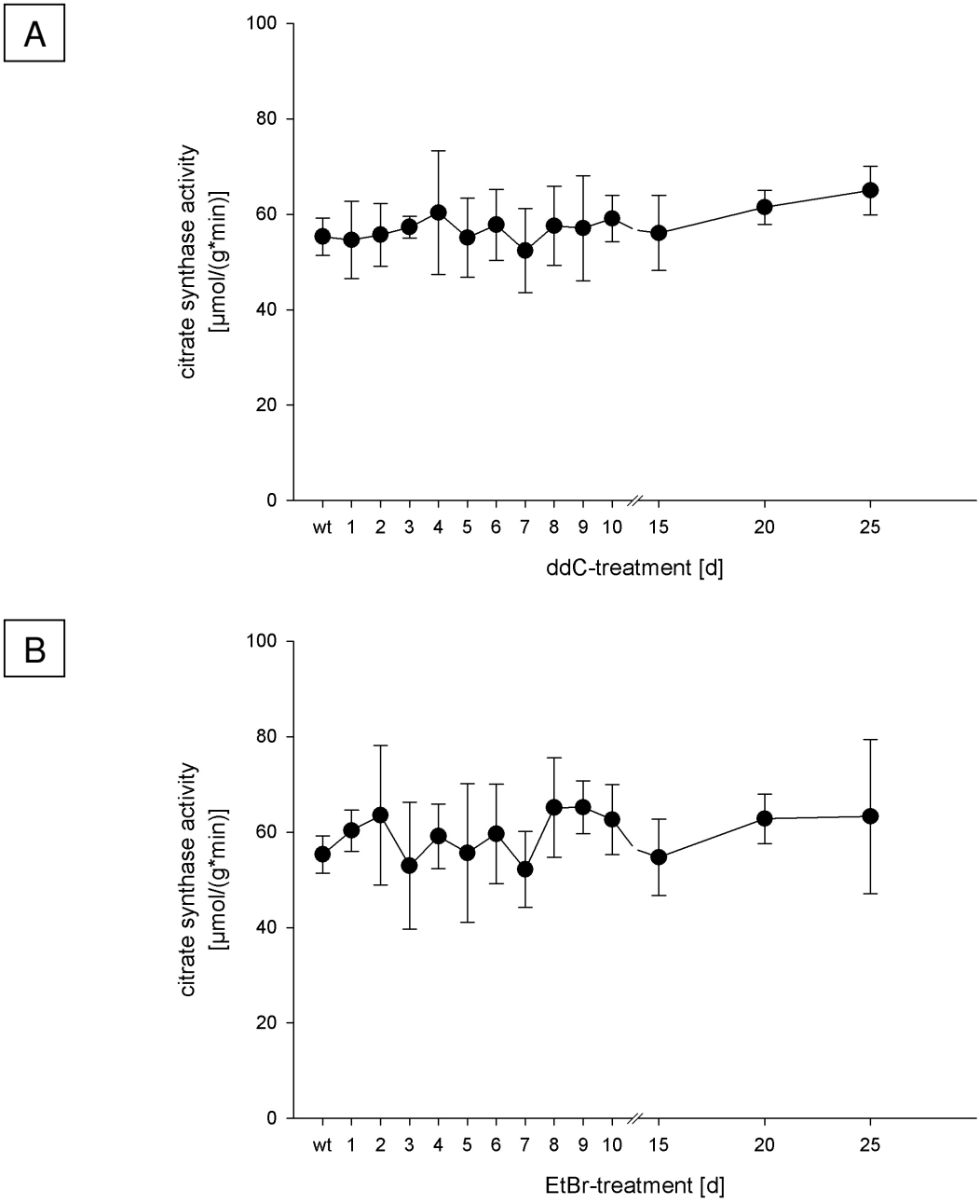

Figure 19. Detection of CS activity in ddC- (A) and EtBr-treated (B) fibroblasts. Values are indicated with arithmetic mean (n = number of experiments, = 3) and standard deviation.

During the depletion treatment the respiratory activity of the fibroblasts was measured using an oxygraph (figure 20; figure 21; table 6; table 8; paragraph 4.5.3).

The respiratory activity was measured in order to examine both if the depletion had an influence on the bioenergetic state of the cells and how the correlation between mtDNA depletion and the onset and severity of the bioenergetic impairment would be.

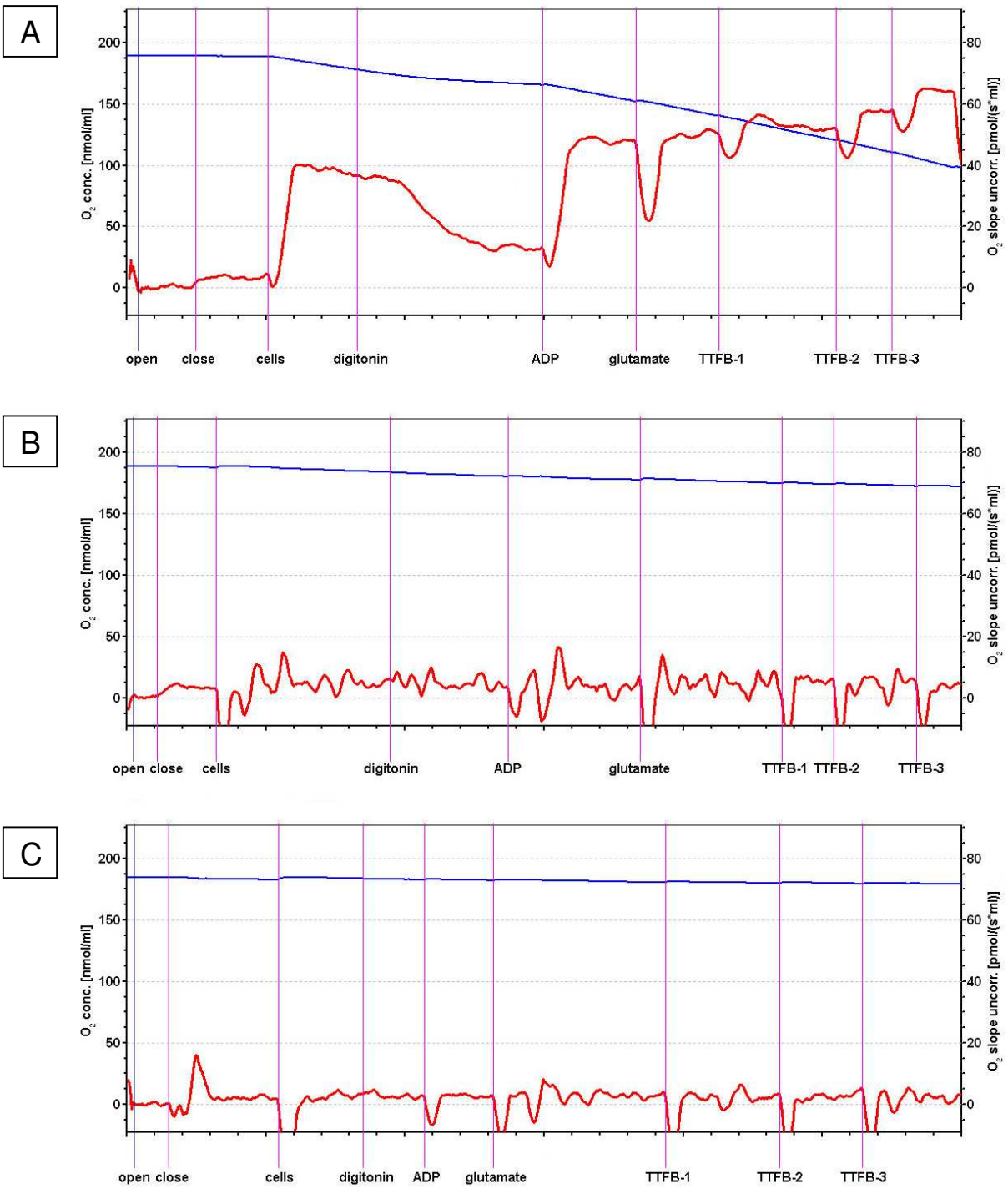

Figure 20. Complex I-dependent respiration of fibroblasts. Blue – oxygen concentration [nmol/ml], red – first derivative [pmol/(s·ml)]. A – wildtype fibroblasts, B – 25 days treatment with 2', 3'-dideoxycytidine (ddC), C – 25 days treatment with ethidium bromide (EtBr). Cells – addition of

fibroblasts to the chamber, digitonin – permeabilization with digitonin, ADP – stimulation with ADP, glutamate – substrate for complex I, TTFB-1 up to TTFB-3 – stepwise addition of the toxic uncoupler TTFB for stimulation of the respiratory chain.

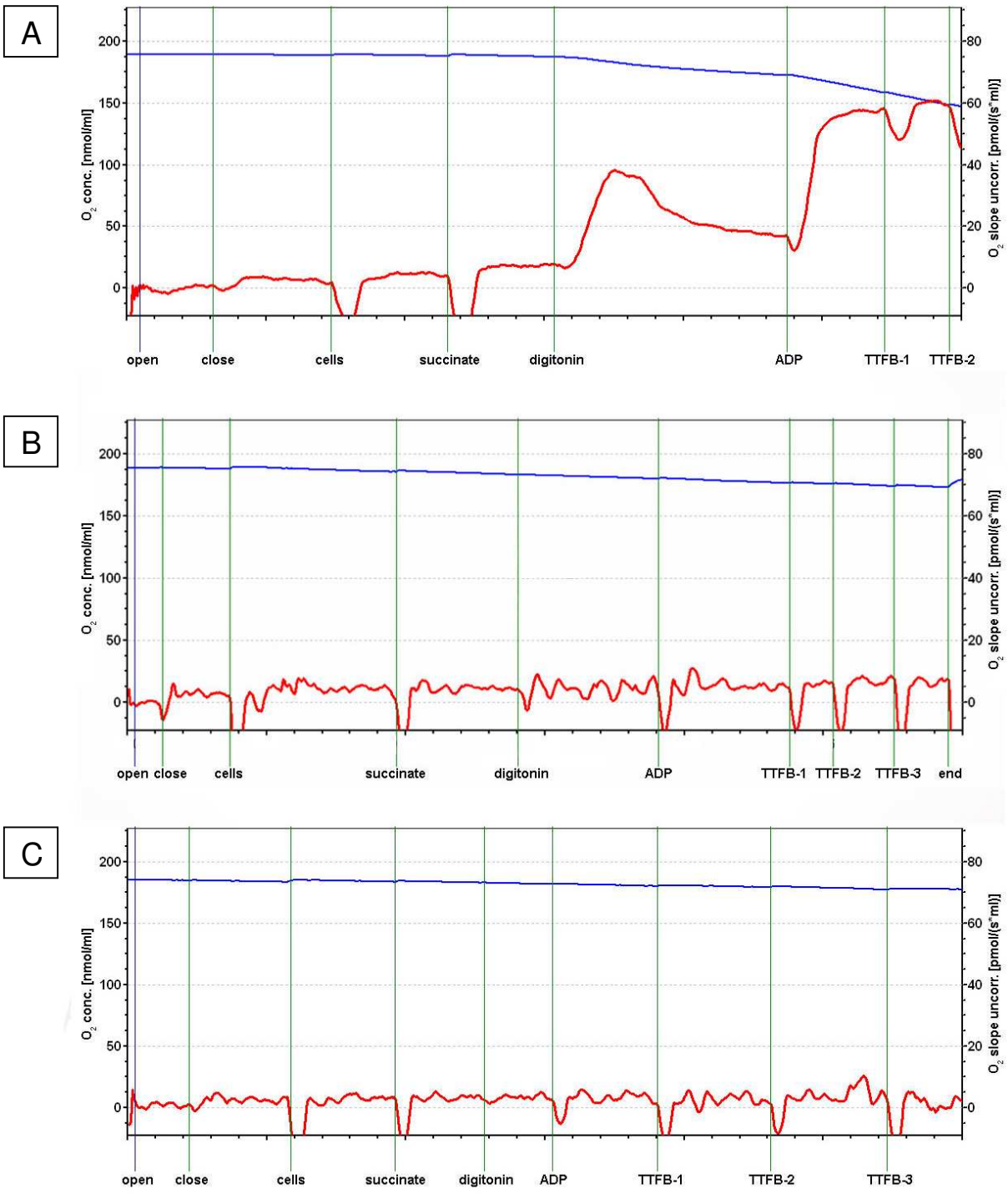

Figure 21. Complex II-dependent respiration of fibroblasts. Blue – oxygen concentration [nmol/ml], red – first derivative [pmol/(s·ml)]. A – wildtype fibroblasts, B – 25 days treatment with 2', 3'-dideoxycytidine (ddC), C – 25 days treatment with ethidium bromide (EtBr). Cells – addition of fibroblasts to the chamber, succinate – substrate for complex II, digitonin – permeabilization with

digitonin, ADP – stimulation with ADP, TTFB-1 up to TTFB-3 – stepwise addition of the toxic uncoupler TTFB for stimulation of the respiratory chain.

The respiratory activity of the fibroblasts was measured at specific time points of the depletion treatment. During these respiratory measurements, the basic respiration of the cells, the ADP-stimulated respiration as well as the TTFB-uncoupled respiration were recorded (figure 22-25). Both in ddC- and EtBr-treated fibroblasts, the complex I- and complex II-dependent respiratory activity itself (figure 22A-25A) as well as the ability of the cells to be stimulated by ADP (figure 22B-25B) and TTFB (figure 22C-25C) decreased. This decrease was proved to be significant in an ANOVA for all treatments.

The respiratory activity depending on complex I was determined by a measurement using pyruvate and malate as substrates (figure 20). Furthermore, glutamate, a further complex I-dependent substrate, was added to exclude a direct influence of pyruvate dehydrogenase on the respiration (paragraph 4.5.3). However, bypassing pyruvate dehydrogenase with glutamate resulted in no significant changes.
Initially, the ddC-treated fibroblasts showed a milder decrease of the respiratory activity compared to the EtBr-treated fibroblasts (figure 22; figure 23; table 23; table 24). This milder course of the decrease can be exemplified at day ten. At this point of time, the respiratory activity had fallen stronger in EtBr- than in ddC-treated cells.
Likewise, the significance of this reduction appeared earlier in EtBr- than in ddC-treated cells. In ddC-treated cells, a significance starting at day ten for ADP-stimulated respiration and at day 15 for basic and TTFB-uncoupled respiration was found in an ANOVA with adjacent Dunnett test. However, in EtBr-treated cells a statistical difference appeared earlier at day four for ADP-stimulated, at day five for TTFB-uncoupled and at day six for basic respiration. The statistical difference strengthened both for ddC- and EtBr-treated cells over the further course of the experiment (table 23; table 24).
The treatment was extended in order to examine, to which extent the respiratory activity could be minimized in living fibroblasts. During the ongoing treatment, the basic, the ADP-stimulated and the TTFB-uncoupled respiration were almost equal, which is illustrated by the very similar course of the respiration curves (figure 20; figure 21). At day 25 of the treatment, the fibroblasts showed a similar basic

respiratory activity in ddC- and EtBr-treated cells of 12 % and 5 % compared to the controls, respectively (table 23; table 24).

Table 23. Measurement of the respiratory activity depending on complex I of ddC-treated fibroblasts. Values are represented with arithmetic mean (number of experiments - n = 3) and standard deviation, * $p < 0.05$, *** $p < 0.001$.

		Wildtype	**10 d ddC**	**25 d ddC**
Basic respiration	[nmol O_2/(min·mg prot)]	7.91 ± 1.59	5.25 ± 0.88	0.93 ± 0.72***
	[%]	100	66	12
ADP-stimulated respiration	[nmol O_2/(min·mg prot)]	10.92 ± 1.85	4.90 ± 1.15*	0.53 ± 0.56***
	[%]	100	45	5
TTFB-uncoupled respiration	[nmol O_2/(min·mg prot)]	14.63 ± 3.84	6.93 ± 1.90	1.02 ± 0.51***
	[%]	100	47	7

Table 24. Measurement of the respiratory activity depending on complex I of EtBr-treated fibroblasts. Values are represented with arithmetic mean (number of experiments - n = 3) and standard deviation, ** $p < 0.01$, *** $p < 0.001$.

		Wildtype	**10 d EtBr**	**25 d EtBr**
Basic respiration	[nmol O_2/(min·mg prot)]	7.91 ± 1.59	2.41 ± 0.44**	0.39 ± 0.03***
	[%]	100	30	5
ADP-stimulated respiration	[nmol O_2/(min·mg prot)]	10.92 ± 1.85	1.91 ± 0.41***	0.64 ± 0.08***
	[%]	100	17	6
TTFB-uncoupled respiration	[nmol O_2/(min·mg prot)]	14.63 ± 3.84	4.05 ± 1.36**	0.69 ± 0.50***
	[%]	100	28	5

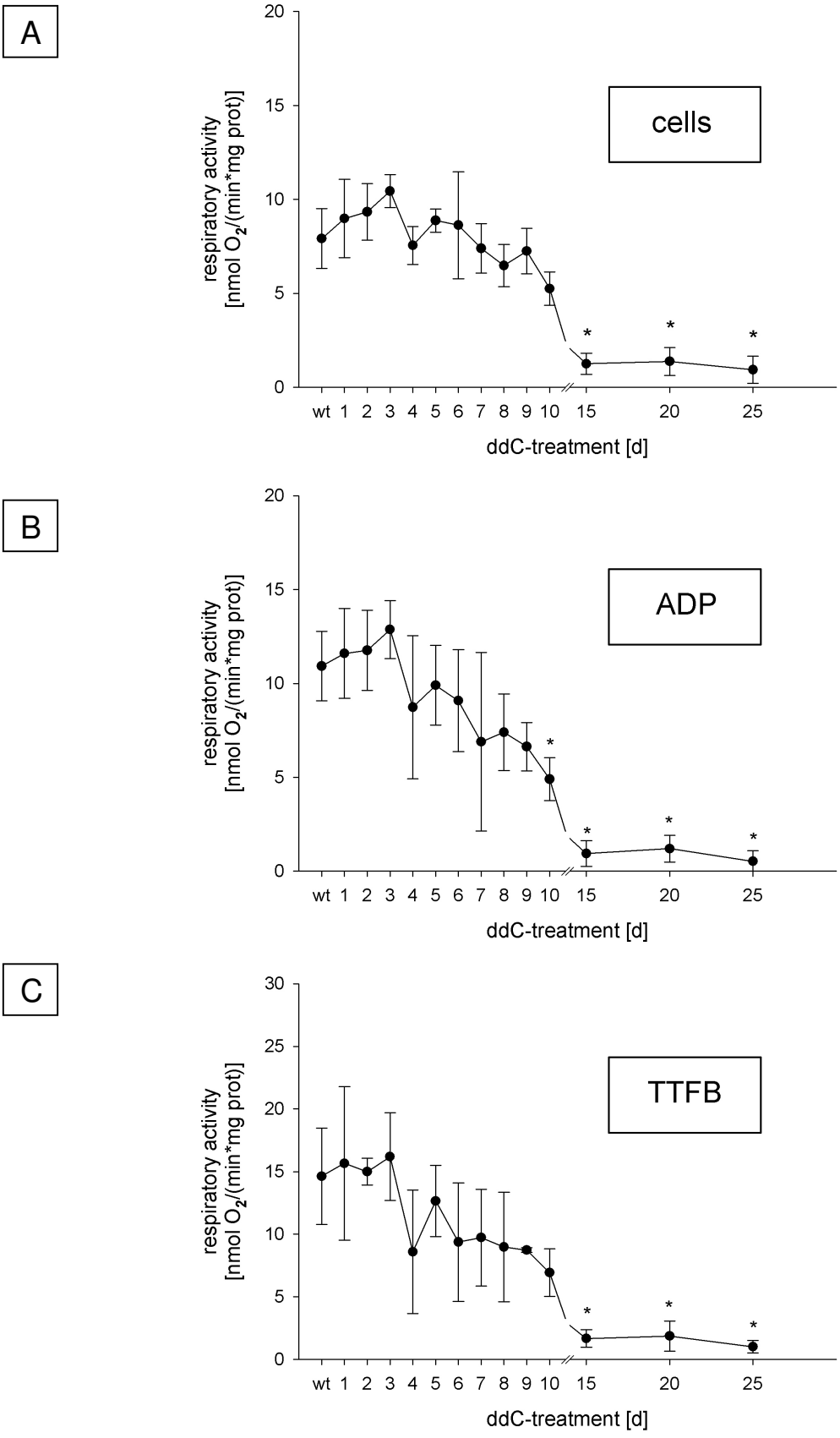

Figure 22. Complex I-dependent respiratory activity in ddC-treated fibroblasts. Basic respiratory activity (A), stimulation with ADP (B), uncoupling with TTFB (C). Values are represented with arithmetic mean (number of experiments - n = 3) and standard deviation, * $p < 0.05$.

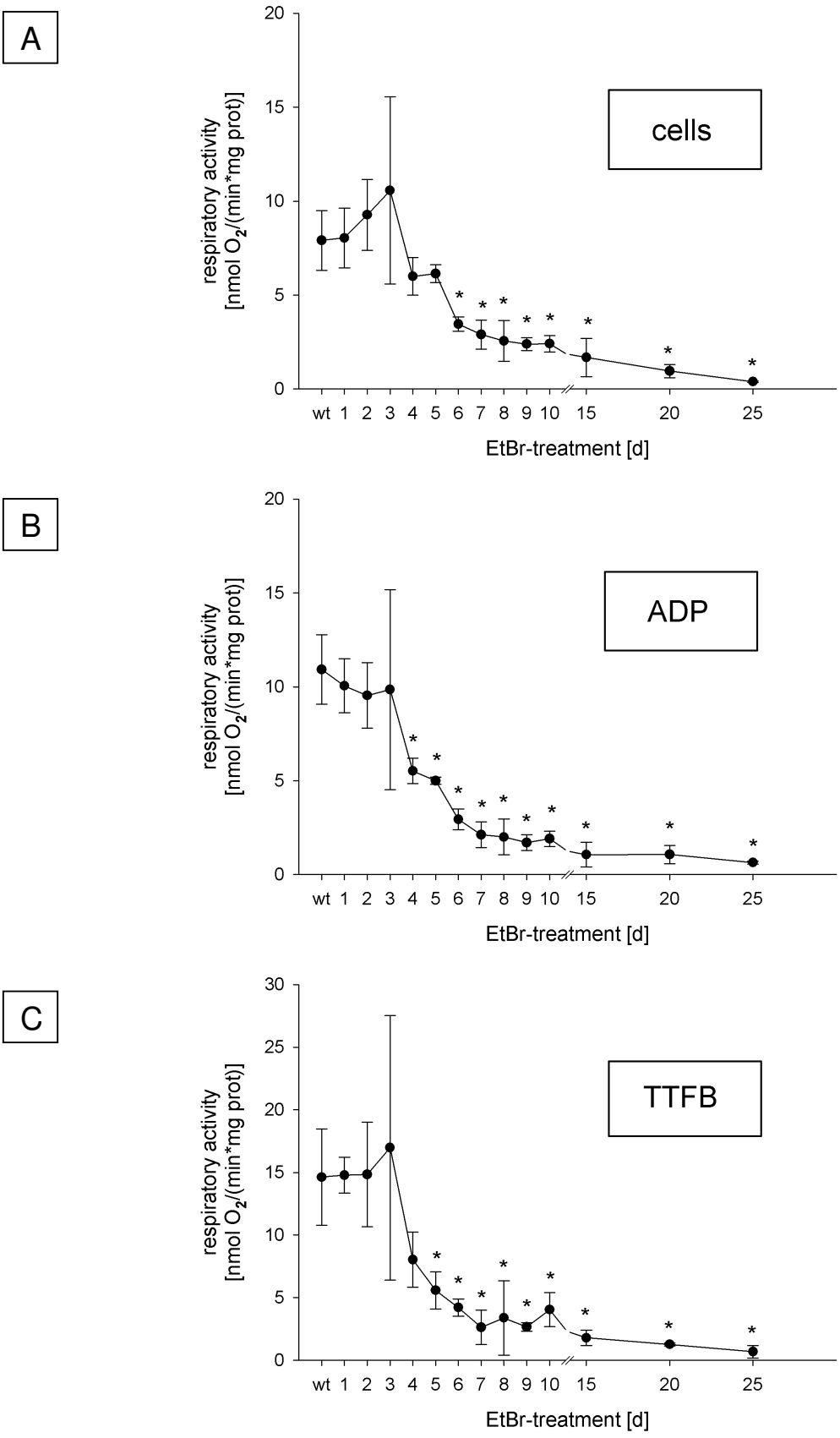

Figure 23. Complex I-dependent respiratory activity in EtBr-treated fibroblasts. Basic respiratory activity (A), stimulation with ADP (B), uncoupling with TTFB (C). Values are represented with arithmetic mean (number of experiments - n = 3) and standard deviation, * $p < 0.05$.

The complex II-dependent measurements were performed by application of succinate combined with rotenone addition causing complex I inhibition (figure 21). The depletion dependent respiratory inhibition shown in former experiments was reflected in a milder way also in the complex II-dependent respiration (figure 24; figure 25; table 25; table 26). This milder inhibition could be a result from the lower amounts of mtDNA encoded proteins involved in this reaction.

Like for complex I-dependent respiration, the reduction of the respiratory activity proceeded faster in EtBr-treated cells. The respiratory activity at day ten can be presented as an example. At that point of time, the respiratory activity of ddC-treated cells had fallen to 89 % of the control value (table 25). However, EtBr-treated cells exhibited an impairment of their activity to 65 % (table 26).

Also the significance of this reduction increased earlier in EtBr-treated cells. In ddC-treated cells, a significant difference from the control value was detectable starting from day 15 of the treatment persisting over the further progression of the experiment (figure 24). However, in EtBr-treated cells, a significant reduction was detected starting from day four for ADP-stimulated, day seven for TTFB-uncoupled and day 20 for basic respiration, remaining during the further progress of the experiment (figure 25).

The treatment was extended in order to examine, to which value the respiratory activity of living fibroblasts could be minimized under this conditions. The complex II-dependent respiratory activity decreased in ddC- and EtBr-treated cells down to 28 % and 25 % of the control value, respectively (table 25; table 26). Likewise to the measurement regarding complex I-dependent respiratory activity, the course of the graphic respiration curves reached a relatively stable level in the final phase of the experiment (figure 24; figure 25).

One can conclude that, although the complex I- and the complex II-dependent respiratory activity decreased strongly both in ddC- and EtBr-treated cells (figure 22-25; table 23-26), this respiratory inhibition became manifest faster in EtBr-treated cells (figure 23; figure 25; table 24; table 26). The respiratory activity indicates the bioenergetic state of the fibroblasts. A possible reason for the faster impairment of the respiration during EtBr-induced depletion could lie in the toxic side effects of EtBr like an impairment of transcription and translation (Hayashi et al., 1990; Maniura-Weber et al., 2004; Tønnesen and Friesen, 1973; Zylber et al., 1969).

Table 25. Measurement of the respiratory activity depending on complex II of ddC-treated fibroblasts. Values are represented with arithmetic mean (number of experiments - n = 3) and standard deviation, ** $p < 0.01$, *** $p < 0.001$.

		Wildtype	**10 d ddC**	**25 d ddC**
Basic respiration	[nmol O_2/(min·mg prot)]	3.44 ± 0.76	3.07 ± 0.80	0.97 ± 0.65**
	[%]	100	89	28
ADP-stimulated respiration	[nmol O_2/(min·mg prot)]	12.25 ± 2.15	8.45 ± 2.63	1.06 ± 0.68***
	[%]	100	69	9
TTFB-uncoupled respiration	[nmol O_2/(min·mg prot)]	12.46 ± 2.67	10.57 ± 1.93	2.12 ± 1.38***
	[%]	100	85	17

Table 26. Measurement of the respiratory activity depending on complex II of EtBr-treated fibroblasts. Values are represented with arithmetic mean (number of experiments - n = 3) and standard deviation, * $p < 0.05$, *** $p < 0.001$.

		Wildtype	**10 d EtBr**	**25 d EtBr**
Basic respiration	[nmol O_2/(min·mg prot)]	3.44 ± 0.76	2.22 ± 0.39	0.87 ± 0.07*
	[%]	100	65	25
ADP-stimulated respiration	[nmol O_2/(min·mg prot)]	12.25 ± 2.15	2.47 ± 0.52***	0.77 ± 0.15***
	[%]	100	20	6
TTFB-uncoupled respiration	[nmol O_2/(min·mg prot)]	12.46 ± 2.67	5.50 ± 1.58*	0.87 ± 0.41***
	[%]	100	44	7

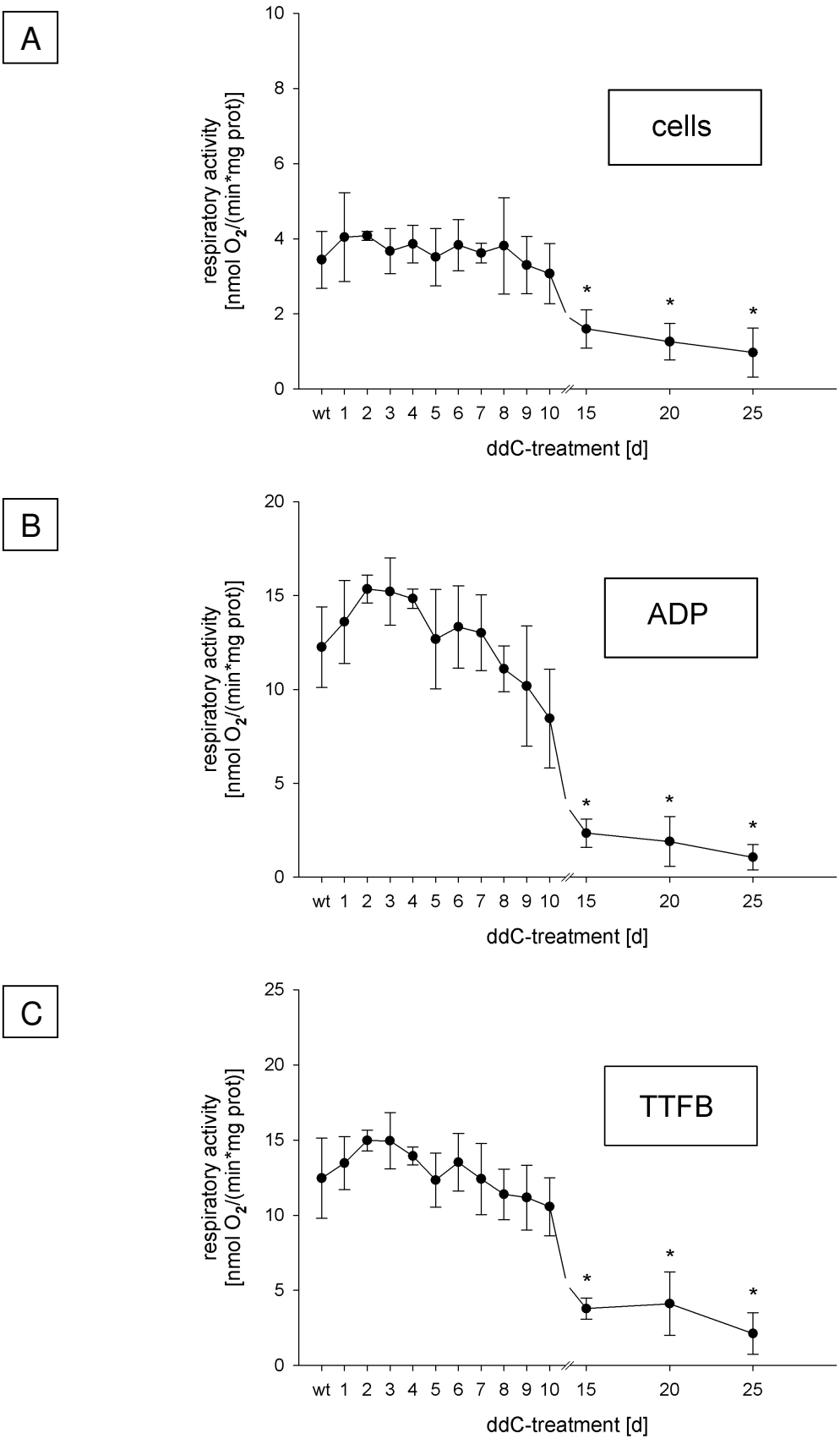

Figure 24. Complex II-dependent respiratory activity in ddC-treated fibroblasts. Basic respiratory activity (A), stimulation with ADP (B), uncoupling with TTFB (C). Values are indicated with arithmetic mean and standard deviation, * $p < 0.05$.

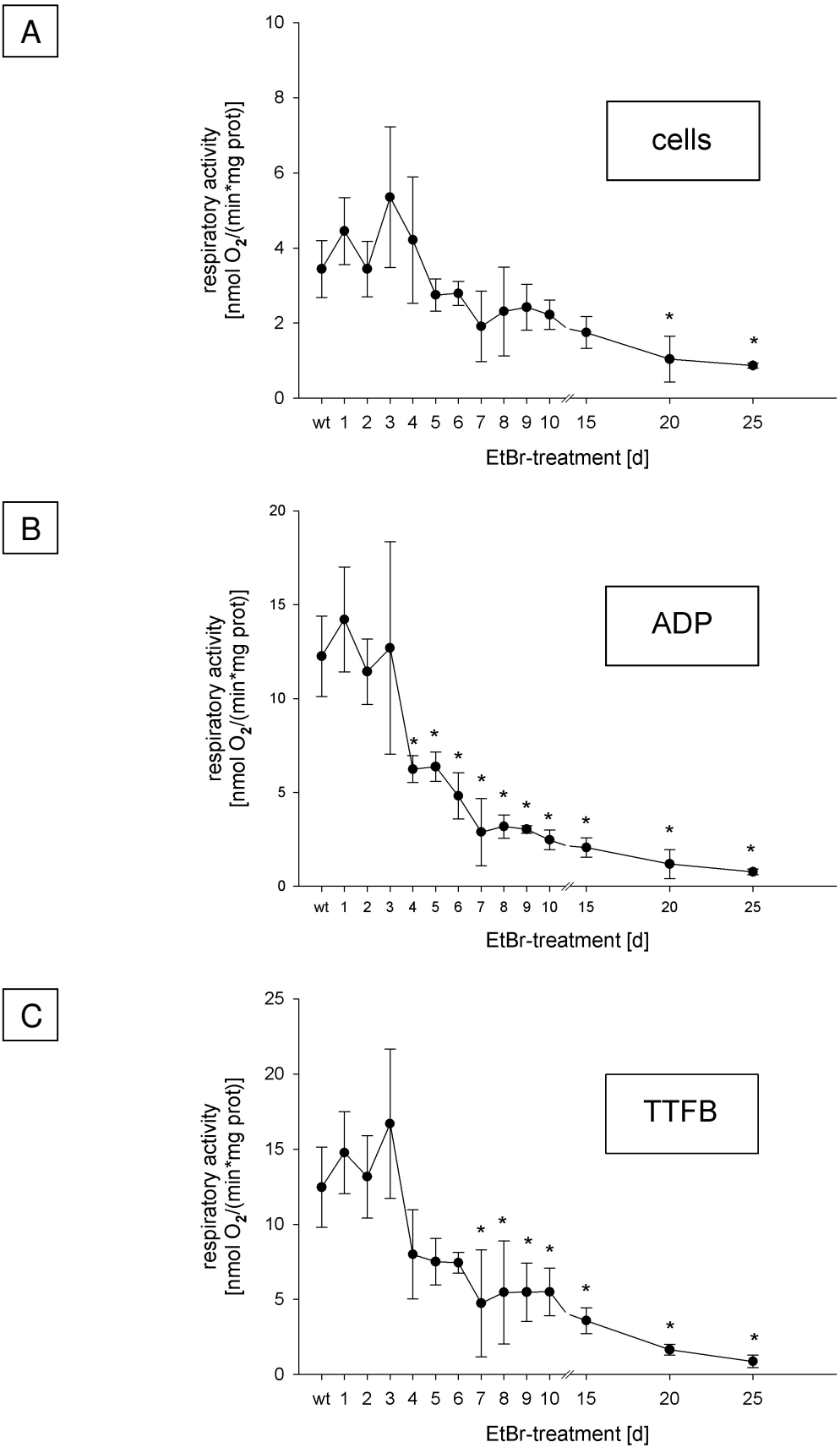

Figure 25. Complex II-dependent respiratory activity in EtBr-treated fibroblasts. Basic respiratory activity (A), stimulation with ADP (B), uncoupling with TTFB (C). Values are indicated with arithmetic mean and standard deviation, * $p < 0.05$.

The depletion of the mtDNA is the direct cause for the respiratory impairment of the cells. However, the depletion and the respective respiratory impairment could have either a linear or a logarithmic relationship to each other. A linear correlation hints to a proportional decrease, whereas a logarithmic correlation is a sign of a threshold. The respiratory activity would then be relatively stable above this threshold point, but would show a sharp decline below.
The maximal respiratory activity resulting from TTFB-uncoupling was plotted against the mtDNA copy number (figure 26; figure 27). The correlation of respiration and mtDNA copy number measured during the ddC-treatment shows the logarithmic relationship both for complex I- and complex II-dependent respiratory activity (figure 26). This indicates a threshold for the relation between respiration and mtDNA content.
The threshold was calculated as a halfmaximal value of the mtDNA copy number out of a logarithmic regression provided by SigmaPlot 2001 (table 9) with the following cubic function:

$$y = y_0 + a \cdot \ln x + b(\ln x)^2 + c \cdot (\ln x)^3$$

The four parameters y_0, a, b and c are scalars describing the shape of the curve.
The possible solutions for x were calculated by Cardano's method. The half maximal y value was used to calculate the according x value for the mtDNA threshold referring to increasing bioenergetic consequences.

A half maximal value ($x_{max}/2$) of 23.90 mtDNA copies is achieved with the correlation with the complex I-dependent respiratory activity (figure 26A). The correlation with the complex II-dependent respiratory activity leads to $x_{max}/2$ of 7.06 mtDNA copies (figure 26B). According to these results, a mtDNA copy number of approximately 24 and seven copies per nucleus would be necessary for a stable complex I- and II-dependent respiration, respectively. The existence of the threshold could possibly originate from a superabundance of mtDNA copies in intact cells.

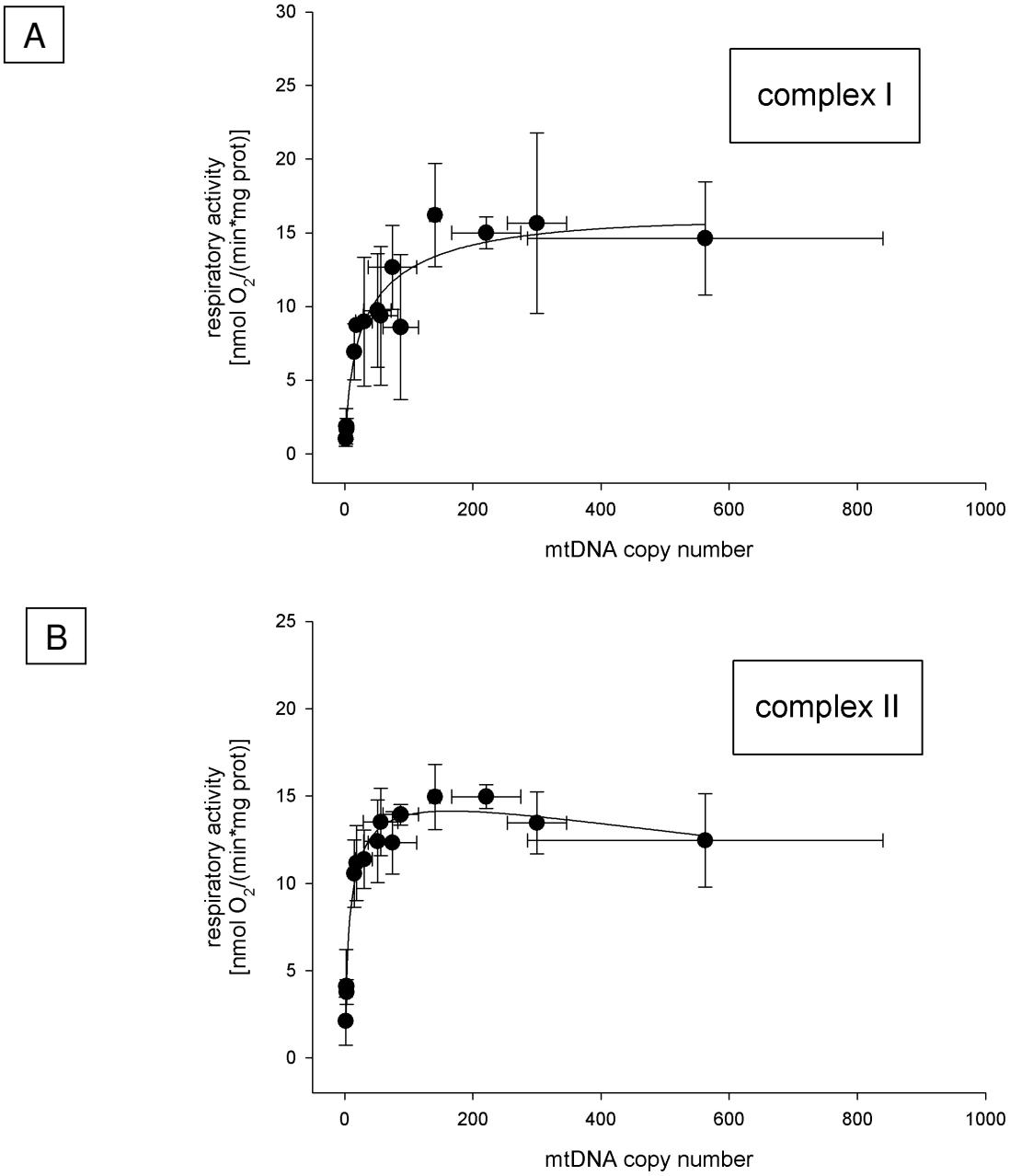

Figure 26. Correlation of mtDNA copy number and respiratory activity for ddC-treated fibroblasts. The mtDNA copy number is correlated with the maximal complex I- (A) respectively complex II- (B) dependent respiratory activity after TTFB-uncoupling. Values are represented with arithmetic mean and standard deviation.

A plotting of the respiratory activity after TTFB-uncoupling against the mtDNA copy number was performed likewise for EtBr-treated cells (figure 27). However, the complex I- and II-dependent respiratory activity values taken during the EtBr-treatment showed a linear relationship. This linear relationship could be based on the toxic side effects of EtBr like an impairment of transcription and translation (Hayashi

et al., 1990; Maniura-Weber et al., 2004; Tønnesen and Friesen, 1973; Zylber et al., 1969) leading to a faster reduction of the respiratory activity of the fibroblasts.

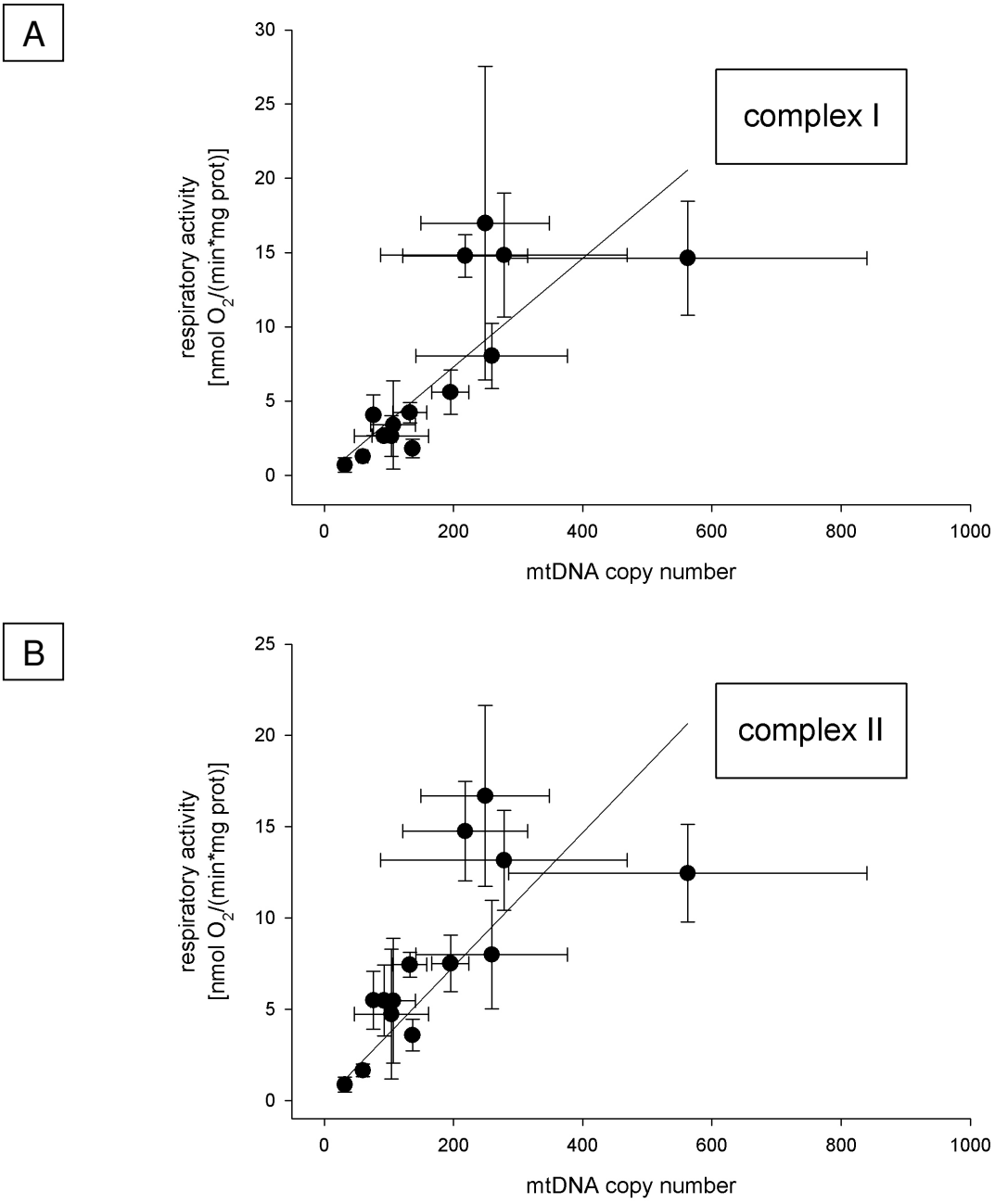

Figure 27. Correlation of mtDNA copy number and respiratory activity for EtBr-treated fibroblasts. The mtDNA copy number is correlated with the maximal complex I- (A) respectively complex II- (B) dependent respiratory activity after TTFB-uncoupling. Values are indicated with arithmetic mean and standard deviation.

6. Discussion

6.1 Effect of mtDNA depletion on the bioenergetic status of the cell

Mitochondria contain their own DNA (mtDNA) that encodes for 13 protein subunits of the oxidative phosphorylation system (OXPHOS). A reduction of the mtDNA content, i.e. mtDNA depletion, can lead to a decreased energy production and consequently to bioenergetic problems within the cell.

In literature reports, an artificial reduction of the mtDNA copy number has been already described, but the effect on the bioenergetic status has not been studied in great detail. MtDNA depletion was generated using ethidium bromide (EtBr) in the majority of studies (Diaz et al., 2002; King and Attardi, 1989; Maniura-Weber et al., 2004; Miller et al., 1996; Piechota et al., 2006a; Trounce et al., 1994). A prominent example for a cell line successfully depleted with EtBr are the so called ρ^0 cells, which completely lack mtDNA (King and Attardi, 1989). EtBr intercalates between the bases of the DNA and hence inhibits the replication leading to depletion of the nuclear and mitochondrial DNA. However, it is well-known that EtBr shows several undesirable side effects like the inhibition of transcription and translation as well as the generation of mutations (Hayashi et al., 1990; Maniura-Weber et al., 2004; Tønnesen and Friesen, 1973; Zylber et al., 1969). EtBr is assumed to selectively inhibit the transcription of the circular mtDNA by altering the tertiary structure, e.g. by introducing twists (Zylber et al., 1969). The effect of EtBr on the protein synthesis results both indirectly from a decay of the mRNA pool and directly from a decay of the protein synthesizing capacity (Tønnesen and Friesen, 1973).

Another possibility to decrease the mtDNA copy number is using 2', 3'-dideoxycytidine (ddC). This substance is a prominent antiviral analog of deoxycytidine, lacking the 3'-oxygen additionally to the 2'-oxygen of the ribose moiety and serving as a substitute substrate for the virally encoded reverse transcriptase (Brown and Clayton, 2002; Chen and Cheng, 1989; Martin et al., 1994; Pan-Zhou et al., 2000; Piechota et al., 2006a; Reardon, 1992; Waqar et al., 1984; Zimmermann et al., 1980). It competes with the natural substrate deoxycytidin for incorporation into the DNA (Waqar et al., 1984). The replication is terminated due to the missing 3'-oxygen of ddC leading to cessation of strand elongation (Mitsuya et al., 1987;

Starnes and Cheng, 1987). The substance ddC has been shown to possess a negligible low cytotoxicity (Mitsuya et al., 1987; Starnes and Cheng, 1987; Waqar et al., 1984). This low cytotoxicity can be explained by the high resistance of polymerase α, the major enzyme involved in nuclear DNA replication, which is presumably related to its high substrate specifity (van der Vliet and Kwant, 1981), whereas polymerase γ (POLG) can use ddC as substrate (Lee et al., 2009; Waqar et al., 1984). This indicates that the mitochondrially located POLG is a likely target for inhibition of replication by ddC (Lee et al., 2009). In contrast to EtBr with its manifold effects, the substance ddC is assumed to preferably inhibit the DNA replication within the mitochondria with minimal other cytotoxic side effects.

To test the effects of mtDNA depletion on the bioenergetic activity of the cells, an *in vitro* system with fibroblasts was utilized, since the availability of different human tissues was limited. Firstly, we depleted the mtDNA using EtBr or ddC. To minimize the risk of artifacts, which could be generated by toxic side effects, we compared the effects of the two substances, which act by different mechanisms.
The concentration of 20 µM ddC was chosen according to Brown and Clayton (2002) and Piechota et al. (2006a), which successfully depleted murine LA9 and HeLa cells down to 20 % and 4 % mtDNA, respectively. The concentration of 0.13 µM EtBr was likewise based on literature reports (Diaz et al., 2002; Piechota et al., 2006a; Trounce et al., 1994). We observed in our experiments with fibroblasts treated for 25 days with ddC or EtBr *in vitro* a strong decrease in their mtDNA copy number down to 0.31 % or 5.65 %, respectively (figure 18A; figure 18B). The efficiency of the mtDNA depletion is certainly dependent on the used cell type and the applied concentration of the depletive reagent. In one study, where the hepatic tumor cell line HepG2 was exposed to a concentration of 0.5 µM ddC for five days, a reduction of the mtDNA content to about 8 % of untreated cells was observed, and moreover a concentration of 5 µM ddC even led to cell death (Martin et al., 1994). On the other hand, a 20 µM ddC concentration applied on mouse fibroblast LA9 cells for five days resulted in a weaker depletion to about 20 % of control cells (Brown and Clayton, 2002). This difference is possibly due to different cell lines.

The citrate synthase (CS) activity was measured additionally in order to discriminate the effects of mtDNA depletion from potential changes in the amount of mitochondria

(figure 19). The CS activity is generally used as indicator for the mitochondrial amount (Figueiredo et al., 2008; Sarnat and Marín-García, 2005). The CS activity did not significantly change during the depletion treatment. This stability in the time course of depletion treatment is consistent with the data reported by Pan-Zhou et al. (2000).
Based on the stability of the CS activity, it can be concluded that the mitochondrial mass stayed relatively stable within the cells, so that only the number of mtDNA molecules per mitochondrion decreased. One can suggest that defects detected during the depletion experiment are related to mtDNA depletion, whereas an influence of mitochondrial mass changes can be excluded.

To assess the bioenergetic activity of the cells, a measurement of respiration rates using complex I- and complex II-dependent substrates was performed.
The complex I-dependent respiratory activity was determined by application of the substrates pyruvate and malate. Glutamate, a further complex I-dependent substrate, was added to exclude a direct influence of pyruvate dehydrogenase on the respiratory activity. In case of a potential pyruvate dehydrogenase (PDH) complex defect, a ‘short variant’ of citric acid cycle can take place, since glutamate is imported into the mitochondrial matrix by the glutamate/aspartate exchanger. In this ‘short variant’ of citric acid cycle, malate is metabolized until oxaloacetate is generated. Then the glutamate oxaloacetate transaminase converts glutamate and oxaloacetate to aspartate and α-ketoglutarate. Bypassing PDH with glutamate resulted in no significant changes in our experiments.
The complex II-dependent respiratory activity was measured by application of the substrate succinate and the complex I inhibitor rotenone.

The mtDNA depletion caused by ddC- and EtBr-treatment led to a strong decrease of the respiratory activity of the cells. It can consequently be argued that the mtDNA content influences the bioenergetic state of the cell.
The inhibition of the respiratory activity was stronger visible in the measurements of the complex I-dependent than of the complex II-dependent respiration. This can be explained by the additional involvement of complex II, who contains seven mitochondrially encoded subunits.

The reduction of the respiratory activity proceeded initially faster in EtBr-treated cells possibly due to toxic side effects of EtBr. During the later course of the experiment, the impairment of the respiration reached similar values in EtBr- and ddC-treated cells. The reduction impaired not only the basic cell respiration, but to a large extend respiration under stimulated conditions e.g. after ADP-addition or TTFB-uncoupling. This means that the depletion has, beside effects on the basic metabolism of cells, additionally strong consequences on the handling of metabolic short-term loads. Patients affected by mitochondrial disorders often suffer from a severe impairment of muscle and brain activity. These tissues are strongly dependent on a short-term energy supply. Therefore, an energy deficit due to depletion would have a high impact preferably on tissues with an elevated energy demand.

The reduction of the mtDNA copy number and the decrease of the respiratory activity in EtBr-treated fibroblasts were found to be correlated in a linear way (figure 27). By contrast, the relationship between mtDNA copy number and respiration in ddC-treated fibroblasts possesses a logarithmic dynamics with a potential threshold (figure 26). Various factors could cause the difference between the experimental results of ddC- and EtBr-depleted cells. The linear correlation in EtBr-treated cells could result from toxic side effects of EtBr like an impairment of transcription and translation (Hayashi et al., 1990; Maniura-Weber et al., 2004; Tønnesen and Friesen, 1973; Zylber et al., 1969). The amount of required mitochondrial proteins involved in the respiratory chain would not only be reduced by a lower mtDNA copy number, but also by a diminished synthesis of mitochondrial encoded mRNAs and proteins. The decreased amount of mitochondrial encoded subunits of the respiratory chain would impair the ability of the cells to maintain their bioenergetic properties even at higher mtDNA copy numbers.

The mtDNA content and the respiratory activity in ddC-treated cells are correlated by a threshold-like dependency. Before reaching a certain limit, the mtDNA copy number has no strong influence on the respiratory activity and the cell possesses a relatively normal metabolism. However, as soon as the mtDNA content falls under this limit, the bioenergetic activity decreases rapidly. This suggests that the mtDNA content potentially features a certain threshold, which could represent the limit for the

ability of the cells to maintain with the residual mtDNA amount an almost constant, regular bioenergetic status.

It can be assumed that the mtDNA molecules could possibly exist in a surplus within the cell. This surplus of mtDNA molecules could have a protective effect against deleterious mutations. A certain reserve amount of wildtype mtDNA molecules in heteroplasmic cells ensures the energy production within the cell. Strictly speaking, the cell could than tolerate a certain loss of wildtype mtDNA without major problems.

The threshold was calculated as the mtDNA content at half maximal respiratory activity. For the complex I- and the complex II-dependent respiration, a threshold of about 24 (4 %) and seven (1 %) mtDNA copies per nucleus was determined, respectively (figure 26), which indicates a considerable excess of mtDNA in human fibroblasts.
An amount between two and ten mtDNA molecules per mitochondrion is quoted in several literature reports (Graziewicz et al., 2006; Shuster et al., 1988; Wiesner et al., 1992). According to this generally accepted ratio between mtDNA copies and mitochondria within cells, the mtDNA content of 563 mtDNA molecules detected in the applied fibroblast cell line would correspond theoretically to 56-282 mitochondria per cell.

The calculated mtDNA copy number threshold lies with 24 (4 %) and seven (1 %) mtDNA copies per nucleus somewhat below the minimal amount of one mtDNA molecule per mitochondrion. Considering that the mtDNA molecules are clustered in protein-DNA-structures called nucleoids (Chen and Butow, 2005, Wang and Bogenhagen, 2006), it is most likely that the calculated threshold value is consequently also below the minimal amount of one mtDNA molecule per nucleoid.
However, since we correlated the respiratory activity of cells to a permanently decreasing mtDNA copy number, a delayed impairment of the respiration due to a residual activity of proteins with a long half-life cannot be excluded. For this reason, it is conceivable that the bioenergetic activity could be lower in cells *in vivo* with a stably depleted mtDNA content.
This potential discrepancy could be explained by intermitochondrial exchange processes, which would attenuate the bioenergetic problems. Since it is assumed

that mitochondria exist in a dynamic network within the cell (Frazier et al., 2006; Rizzuto et al., 1998), an exchange of mRNA, tRNAs or even missing subunits of the OXPHOS within the mitochondria could alleviate the effects of depletion.

Addressing the aspect, whether accumulating mutant mtDNA molecules or missing wildtype mtDNA molecules are more relevant for the phenotype of mitochondrial disorders, we provided evidence that a small amount of wildtype mtDNA molecules in the cell could sustain the biochemical functionality of the cell. It is controversially discussed if the onset and severity of mitochondrial disorders with mtDNA heteroplasmy, i.e. a mixture of wildtype and mutated mtDNA molecules within the cells, results from the presence of mutated molecules (Shoubridge et al., 1990), from the absence of wildtype molecules (Attardi et al., 1995) or from a mixture of both (Attardi et al., 1995; Bentlage and Attardi, 1996). A couple of mitochondrial disorders exist, where identical mutations with a different level of mutated mtDNA molecules lead to different symptoms. Prominent examples are the disorders maternally-inherited Leigh syndrome (MILS) and neuropathy, ataxia and retinitis pigmentosa (NARP) (Alexeyev et al., 2008; Mäkelä-Bengs et al., 1995) The mtDNA mutation T8993G is present at a level of 60-90 % and at a level of more than 90 % in patients affected by NARP and MILS, respectively (Alexeyev et al., 2008; Mäkelä-Bengs et al., 1995).

A sharp threshold was similarly observed in one study, where heteroplasmic mixtures of mtDNA wildtype and mutant molecules were generated in an *in vitro* system (Chomyn et al., 1992). The mutant molecules carried the A8344G mutation, which is associated with the disorder myoclonic epilepsy and ragged red fibers (MERRF) (Chomyn et al., 1992). A correlation between the oxygen consumption and the mutation load of the transformants revealed a threshold at a wildtype mtDNA content of approximately 6 % (Chomyn et al., 1992). They concluded that a small minority of wildtype molecules could protect the transformants against the defect caused by the mutation (Chomyn et al., 1992). One interpretation of these findings was that the products of the wildtype and the mutant mtDNA molecules could interact leading to a complementation of the defect caused by the mutation (Attardi et al., 1995).
However, our experiment, which was performed without potentially interfering mutant mtDNA molecules, supports the interpretation that the wildtype molecules are

themselves sufficient to provide the cells with normal respiratory activity (Attardi et al., 1995). This finding extends the knowledge on the relationship between the mtDNA content and bioenergetic problems, which improves the assessment of the phenotype of several diseases.

However, several factors could lead to an underestimation of the mtDNA threshold detected for ddC-treated cells. The decrease of the respiratory activity could be delayed due to a relatively long half-life of residual RNA and proteins.
A time-shift of the respiration decrease due to transcript stability is negligible since mitochondrial transcripts in HeLa cells are assumed to generally possess a relatively short half-life between one and seven hours (Piechota et al., 2006b). However, a delayed decrease of the respiration due to residual proteins cannot be excluded. It has been reported that the turnover rate of mitochondrial proteins from rat liver lasts several days (Swick et al., 1968). A delayed decrease of the protein content could influence the kinetics during the experiment. This could potentially alter the relationship between the mtDNA content and the bioenergetic status of the cell, leading to the detected “too low” threshold.

The processes, which influence the size of this potential threshold, remain to be elucidated. Very likely, the critical amount of mtDNA copies is influenced by the content and distribution of the mitochondria within the cells.

6.2 Importance of the mtDNA content on neurodegeneration

It was intended to take a closer look at the importance of the mtDNA maintenance on the mitochondrial functionality with a possible view on the clinical phenotype of patients with a mitochondrial disease. For this reason, the mtDNA content should be correlated to the clinical phenotype found in patients with Ammon’s horn sclerosis (AHS), a prominent pathological finding of temporal lobe epilepsy (TLE) (Liu et al., 1995; Sommer, 1880).

In TLE with AHS, neurodegenerative mechanisms are associated with extensive seizures, which take place in the hippocampal region (Chang and Lowenstein, 2003). It has been reported that seizures can lead to necrotic and apoptotic cell death processes in neurons (Bengzon et al., 1997). However, the cause and effect

relationship between seizures and the apoptosis of specific cell types still remains to be elucidated (Chang and Lowenstein, 2003; Kunz, 2002). It is controversially discussed, whether the hippocampal sclerosis in TLE with AHS is a consequence of prolonged seizures, or whether it contributes to the development of the epileptic focus (Berkovic and Jackson, 2000; Jefferys, 1999). Studies revealed that an experimental focal status epilepticus resulted in histological changes resembling human hippocampal sclerosis (Sloviter, 1994). On the contrary, seizures with only a low incidence of neuronal cell loss or hippocampal sclerosis are likewise reported (Jefferys et al., 1992). It has been hypothesized that even if hippocampal sclerosis may not be essential for epilepsy, it could still promote its development (Jefferys, 1999). This raises the question, how the decreased mitochondrial activity is correlated with the pathogenic changes in neuronal cells within specific brain regions.

To address the issue of mtDNA copy number changes during neurodegenerative processes within the brain, a comparison of the hippocampal regions of TLE patients with AHS and control patients was performed. The control patients were only affected by lesional damage of the brain tissue close to the hippocampus (e.g. parahippocampal tumor), which is not related to the sclerotic processes observed in AHS patients. Since the loss of pyramidal neurons in the areas cornu ammonis 1 (CA1) and cornu ammonis 3 (CA3) in the hippocampus is a histopathological hallmark of AHS (Baron et al., 2007; Ben-Ari et al., 1980; Kunz et al., 2000; Liu et al., 1994; Liu et al., 1995; Nadler, 1981), these areas were of special interest.

The mtDNA copy number was found to be significantly decreased in AHS patients in the hippocampal regions CA1 to 47 % and CA3 to 56 % compared to the respective regions from lesion patients, whereas no significant mtDNA depletion was detected in the neighboring tissue regions area dentata (AD) and parahippocampus (PH) (figure 17; table 22; paragraph 5.6; Baron et al., 2007). A depletion of mtDNA in the regions CA1 and CA3 was also detected in the hippocampus of pilocarpin-treated epileptic rats underlining the observed phenomenon (Kudin et al., 2002). Furthermore, both a mitochondrial dysfunction, marked by an impairment of the respiratory chain complexes (Kudin et al., 2002; Kunz et al., 2000), and a decrease of the mitochondrial density, indicated by a decrease of the CS activity (Baron et al., 2007), have been reported for the affected areas CA1 and CA3.

The decrease of mtDNA copy number, mitochondrial content and mitochondrial functionality in specific neuronal areas hints to cell-type specific changes in these areas. The detected mtDNA depletion in the hippocampal regions CA1 and CA3 in TLE patients with AHS can be an indication of a loss of pyramidal neurons induced by epileptic seizures. Since the mtDNA depletion was specifically reduced in the hippocampal regions CA1 and CA3, which are associated with a decreased mitochondrial number and function as well as the loss of pyramidal neurons, one can assume an intimate relationship between a decrease in the mtDNA copy number and neuronal damages that characterize AHS.

In this selective neurodegenerative process in the hippocampus, which finally leads to sclerosis of brain tissue, mitochondria are both targets of oxidative damage and sources of reactive oxygen species (ROS). A dysfunction of mitochondrial electron transport proteins leads to the production of ROS (Han et al., 2001; Kudin et al., 2004). In addition to the formation of 8-hydroxyguanosine (8-OHG) (Halliwell and Aruoma, 1991; Richter et al., 1988), the hydroxyl radical •OH can react with deoxyribose, which leads to sugar radicals. ROS can induce single and double strand breaks in the mtDNA, which can induce active degradation of the mtDNA (Lee and Wei, 2005; Richter et al., 1988; Shibutani et al., 1991; Shokolenko et al., 2009). For this reason, a causative relationship between an increased ROS production and a decreased mtDNA copy number is plausible.

Since the mitochondrial content of cell types varies regionally within the brain, the regional selectivity of neurodegenerative processes can be explained. Certain brain areas seem to be preferentially affected by mtDNA changes. The reasons for this selectivity have not been elucidated yet. Different neuronal cell types might be dependent to a different degree on the energy supply by mitochondria. Their functionality can be impaired due to mtDNA depletion, deletion or point mutations. Thus critical factors, which could determine the survival of the particular neuronal cells are the degree of mtDNA damage as well as their intrinsic threshold (Baron et al., 2007). These factors influence different neuronal cells to a different degree according to their mitochondrial content. This might explain at least in part the cell type specifity of this process.

6.3 Influence of the nuclear gene *POLG* on the mtDNA copy number

There are several primary *POLG* mutations known to cause secondary defects in the mtDNA, for example point mutations or deletions, which can lead to various mitochondrial diseases like progressive external ophthalmoplegia (PEO) or Alpers-Huttenlocher syndrome (Chan and Copeland, 2009). The relationship between the location of mutated amino acids encoded by *POLG* and their specific functional consequences remains to be elucidated.

It is assumed that a defect in the proof reading ability of polymerase γ leads to the accumulation of mutations within the mtDNA, whereas an inhibited polymerase activity causes a reduction of the mtDNA copy number (Spelbrink et al., 2000). The most frequent pathogenic *POLG* mutations are located in the so-called linker region (Chan and Copeland, 2009; Kaguni, 2004; Luoma et al., 2005; Van Goethem et al., 2001). This region is proposed to fulfil multiple functions, whereby mutations located in this region lead to various biochemical effects (Lee et al., 2009). The correlation between pathogenic mutations in the linker region and the occurrence of the disease phenotype could thus be based on an impaired enzyme catalysis, a decreased DNA binding affinity, or a reduced interaction of the catalytic and the accessory polymerase γ subunits (Lee et al., 2009).

Since the mutation A467T probably occurs in 36 % of all alleles in *POLG* disease populations, it is regarded as the most widespread pathogenic mutation in *POLG* (Chan and Copeland, 2009). It has been reported that a recombinant polymerase γ catalytic subunit, containing the A467T mutation in the linker region, exhibits both a lowered binding capability to the accessory subunit and a severe DNA binding defect (Chan et al., 2005). These observations were accompanied by a lowered polymerase and exonuclease activity (Chan et al., 2005). The mutation W748S and the polymorphism E1143G are often found together in *cis* on the same allele (Chan et al., 2006; Hakonen et al., 2005; Nguyen et al., 2005; Nguyen et al., 2006; Tzoulis et al., 2006; Van Goethem et al., 2004). A recombinant polymerase γ catalytic subunit with the W748S mutation possessed low DNA polymerase activity, low processivity and a reduced DNA binding capability (Chan et al., 2006).

The Alpers-Huttenlocher syndrome is a mitochondrial disease, which is associated with mutations in *POLG*. It is known as a typical mtDNA depletion disorder (Naviaux et al., 1999), whereas only few reports on mtDNA point mutations (Zsurka et al., 2008) or deletions (Ashley et al., 2008; Zsurka et al., 2008) exist. For this reason, the tissues of Alpers-Huttenlocher patients were examined for mutations in the *POLG* gene. In five pediatric patients, a total of four pathogenic mutations A467T, W748S, F749S and L752P in the linker region as well as the mutation G848S and the polymorphism E1143G in the polymerase domain were identified (paragraph 5.5; Zsurka et al., 2008). The mutations A467T, W748S, F749S and G848S are well-known deleterious *POLG* mutations associated with mitochondrial disease (Chan et al., 2005; Davidzon et al., 2005; Hakonen et al., 2005; Nguyen et al., 2006; Van Goethem et al., 2004; Zsurka et al., 2008). The newly identified mutation L752P occurred in one patient in compound heterozygous way (Zsurka et al., 2008).

In all examined tissues of the patients with Alpers-Huttenlocher syndrome, a mtDNA depletion was detected (table 20). The severity of this depletion ranged from a mild decrease to 75 % mtDNA to a severe reduction to 11 % mtDNA of the control values in hippocampal brain and liver, respectively. The determined mtDNA depletion values are supported by literature data, where a reduction to 25 % mtDNA (Naviaux et al., 1999) and 13 % mtDNA (Ashley et al., 2008) of control specimen in liver has been detected. In muscle specimen, a comparable reduction to 30 % mtDNA (Naviaux et al., 1999) and 55 % mtDNA (Ashley et al., 2008) has been reported.
In contrast, an analysis for mtDNA deletion revealed only a very small amount of deleted mtDNA molecules of less than 1 % in each tissue (Zsurka et al., 2008). If one compares the strength of the effect of the mtDNA deletion and the mtDNA reduction, the crucial factor related to bioenergetic problems in patients suffering from Alpers-Huttenlocher syndrome seems to be the mtDNA depletion. The detected depletion indicates a correlation of specific *POLG* mutations and the mtDNA copy number phenotype.

We assumed a relation between the valproate-induced liver failure and the severe mtDNA depletion in liver tissue of patient one (p1) (table 19; table 20; Zsurka et al., 2008). Histochemically, liver regions with different cytochrome *c* oxidase (COX) activity were observed (figure 15; Zsurka et al., 2008) indicating regions with intact

and defect mitochondria. A variation of the mitochondria content and morphology in neighboring hepatocytes from patients with Alpers-Huttenlocher syndrome has already been reported (Naviaux et al., 1999). The mitochondrial morphology ranges from mitochondria with tightly packed cristae or concentric cristae to normal appearing mitochondria (Naviaux et al., 1999).

We correlated the histochemical findings, showing defects of the OXPHOS, with the mtDNA copy number. Liver regions with different COX staining were microdissected to determine the OXPHOS activity and the mtDNA content. The COX-negative areas contained indeed about fourfold less mtDNA (6 % from control) than the COX-positive areas (26 % from control) (figure 16; table 21). These findings hint to a correlation between the mitochondrial functionality and the mtDNA copy number. They are in accordance with Ashley et al. (2008), who observed a corresponding pattern of depletion and COX deficiency in cultured fibroblast cells of Alpers-Huttenlocher patients.

In contrast to the strong depletion, only a very low amount of 0.02 % deleted mtDNA molecules was detected in liver (Zsurka et al., 2008). The negligible small amount of deleted molecules suggests an only marginal contribution of the deletion to the disease phenotype although a specific impairment of single cells with an impact on larger tissue areas cannot be excluded.

Additionally to the patients with the severe Alpers-Huttenlocher syndrome, a mild phenotype of PEO with epilepsy/ataxia was surprisingly detected in a family carrying the *POLG* mutations A467T and W748S (figure 12; paragraph 5.4; Paus et al, 2008). The family members carrying either heterozygously the mutation W748S or A467T showed no disease phenotype. However, the two daughters with both compound heterozygous mutations were affected by a number of neurological symptoms like epilepsy, ataxia, neuropathy and a mild phenotype of PEO. Additionally, they exhibited a significantly reduced mtDNA copy number in blood samples (figure 13; table 18).

It is therefore most likely that the combination of the pathogenic *POLG* mutations W748S and A467T could have an influence on the mtDNA copy number as well as on the pathogenic phenotype of the disease. In addition, a DNA mutation analysis was performed. Indeed, also multiple deletions were detected in muscle tissue specimen of both affected daughters (Paus et al., 2008). Therefore, an additional

influence of the deleted molecules found in the patients with the PEO phenotype cannot be excluded.

Disregarding the relevance of deletions, one can assume that the pathogenic factor in patients with the investigated pathogenic *POLG* mutations causing a mitochondrial disease phenotype, is mtDNA depletion. The impaired polymerase activity caused by primary *POLG* mutations can cause the reduction of the mtDNA copy number. Additionally, secondary mtDNA point mutations and deletions can be generated either by lowered rate of mutation repair or higher rate of mutagenesis of single stranded replication intermediates resulting from abnormal replication stalling (Wanrooij et al., 2007). The accumulation of these mutated molecules can moreover be enhanced by a decreased total amount of mtDNA molecules since the segregation speed is higher when less segregating units are present (Coller et al., 2002; Preiss et al., 1995). This would consequently lead to a stronger segregational drift to mutated mtDNA molecules.

6.4 Tissue-specifity of the mtDNA content

A mitochondrial dysfunction mainly occurs in tissues, which are highly dependent on energy supply and consequently on their mitochondria. The functionality of the OXPHOS depends, amongst others, on a correct transcription and translation of the mtDNA.
Since literature data on the tissue-specifity of the mtDNA content are ambiguous, we focused our interest on the mtDNA copy number in several tissues and cell types. We were also interested in the correlation between the mtDNA copy number and the mitochondria content in various tissues.

Firstly, we determined the mtDNA content in several tissues and cell types of human controls (figure 11; table 16; paragraph 5.2). The samples were taken from skeletal muscle, brain specimen, liver, buccal mucosa, fibroblasts and blood. The highest mtDNA copy number values were detected in tissue specimen of skeletal muscle and brain with 16,864 ± 8,843 and 7,145 ± 4,086 mtDNA copies, respectively. A high mtDNA copy number is in line with a high energy requirement since the energy support via mitochondria is especially needed in brain and muscle tissue. The brain

is metabolically a very active organ with a high constant demand for oxygen, i.e. 20 % of the resting total body consumption (Clarke and Sokoloff, 1999). Muscle fibers generally perform a large scale of mechanical work and require energy dependent on their physiological activity.

Other tissues and cell types with a lower energy demand possessed a lower mtDNA copy number with the lowest value of 283 ± 99 mtDNA copies detected in our blood DNA isolates. This value is in accordance with literature data like 240-420 mtDNA copies in lymphocytes (Szuhai et al., 2001) and ~ 250-500 mtDNA copies in leukocytes (Pyle et al., 2007). These data for lymphocytes and leukocytes were likewise quantified with quantitative PCR (qPCR) (Pyle et al., 2007; Szuhai et al., 2001). In one literature study, a value of ~ 800 mtDNA copies in lung fibroblasts has been quantified with Southern blot (Robin and Wong, 1988). This value is comparable with our data of 961 ± 242 mtDNA copies in cultured fibroblasts, even though different techniques for mtDNA quantification were applied.

In addition to normal human tissues and cell types, we investigated the epithelial cancer HeLa cell line. In comparison to epithelia with low energy demand like fibroblasts, the HeLa cells showed a relatively high value of 1,161 ± 228 mtDNA copies. This value is similar to the mtDNA copy number determined by others. The reported data for the mtDNA content in HeLa cells are in a range between 1000 (Takamatsu et al., 2002) and 9100 mtDNA copies (King and Attardi, 1989). A high mtDNA content in cervical HeLa cells is in accordance with the upregulation of the mtDNA content reported for a number of human malignancies (Jones et al., 2001; Simonnet et al., 2002; Wang et al., 2006; Wong et al., 2004). Possible reasons for the mtDNA copy number increase in cancer cells could be either directed metabolic adaptions or undirected defective regulations. However, the issue of mtDNA copy number variations in tumorous cells is very complex. For instance, also contradictory reports pointing to a downregulation of the mtDNA copy number in tumorous cells exist (Lee et al., 2004; Wong et al., 2004).

Several mtDNA copy number data for some species and different tissues are available in the recent literature. However, mainly data of singular tissues or cell types exist, but systematic studies on mtDNA copy number values in several human

tissues are still missing. Our determined values, which are in agreement with literature data, suggest a tissue dependent variation of the mtDNA copy number.

The current opinions in the literature state a proportion of two to ten mtDNA molecules per mitochondrion (Graziewicz et al., 2006; Shuster et al., 1988; Wiesner et al., 1992). The mitochondria content varies strongly in a tissue- and celltype-specific range of about 100,000 mitochondria per oocyte (Ankel-Simons and Cummins, 1996; Chen et al., 1995) to four mitochondria per platelet (Shuster et al., 1988). We intended to examine in depth the general assumption of a stable ratio of the mtDNA copy number among mitochondria. In this context, we decided to determine the mitochondria content on the basis of the CS activity and to correlate these CS activity values to the mtDNA copy number afterwards (table 17; paragraph 5.3). Here, the CS activity presumably indicates the mitochondrial mass (Figueiredo et al., 2008; Sarnat and Marín-García, 2005).

In hippocampal brain and skeletal muscle, the determined CS activity exhibited high values of 195 ± 30 µmol/(g·min) and 166 ± 36 µmol/(g·min), respectively. The high CS activity values are an indicator for a high mitochondria content. This is in accordance with the high energy demand of these tissues. Several similar data can be found in literature with values for muscle between 113 and 232 µmol/(g·min) (Barthélémy et al., 2001; Gellerich et al., 2002; Sarnat and Marín-García, 2005; Van den Bogert et al., 1993). In brain specimen, CS activity values between 89 and 375 µmol/(g·min) have been mentioned (Bowling et al., 1993; Van den Bogert et al., 1993). Cell types with a lower energy demand contained a lower CS activity. For instance, a low CS activity of 68 ± 7 µmol/(g·min) in fibroblasts and 32 ± 10 µmol/(g·min) in buccal mucosa was detected. Similar data for fibroblasts with 62 µmol/(g·min) and HeLa cells with 136 µmol/(g·min) can be found in literature (Van den Bogert et al., 1993). The lower CS activity indicates a smaller total volume of mitochondria in the cells, which can be due both to a smaller volume of individual mitochondria or a smaller total number of mitochondria in the cells. It can be concluded that the mitochondrial mass corresponds to the energy demand of the respective tissue.

The CS activity of the tumorous HeLa wildtype cell line is in the range of the other measured values. Surprisingly, Hela ρ^0 cells containing mitochondria depleted of their mtDNA exhibited a CS activity, which was raised about 44 % compared to HeLa wildtype cells. It could be possible that the HeLa ρ^0 cells increase their mitochondrial mass as an attempt to compensate the missing mtDNA.

Furthermore, the mtDNA copy number was correlated to the CS activity, which resulted in a ratio between 14 and 35 in the majority of examined cell types. One value, which differed from the other measured data was the ratio of 109 related to skeletal muscle specimen. The origin of this unexpected value is not clear, but could originate from different causes.
Firstly, it could be possible that the unexpected high ratio between mtDNA copy number and mitochondria content in muscle fibers might result from a high mtDNA accumulation. This could be correlated to tissue specific tasks of these organelles in skeletal muscle fibers. Each of the skeletal muscle fibers is a syncytium containing several nuclei in a combined cytoplasma, which is generated by the fusion of myoblasts during muscle development (Horsley and Pavlath, 2004; Jansen and Pavlath, 2008).
Secondly, a tissue specific variation of the CS expression cannot be excluded. CS is an accepted marker for the mitochondrial volume (Figueiredo et al., 2008; Sarnat and Marín-García, 2005), although a variation of the CS activity in several tissues has been reported (Kirby et al., 2007). However, in comparison to other metabolic enzymes like the respiratory chain complexes, the changes of the CS activity are lower, justifying the usage of the CS activity as an indicator for the abundance of mitochondria (Kirby et al., 2007).

From our experiments, we concluded that the mitochondria content is generally proportionate to the mtDNA content in most healthy human tissues. This confirms earlier reports of the proportionality of the mtDNA content and the mitochondrial volume (Moyes et al., 1997; Puntschart et al., 1995). However, muscle seems to be an exception possibly due to its special requirements for mitochondrial tasks.
Even though the ratio between mtDNA copy number and mitochondria content in muscle seems to be exceptionally high, it has been reported that the principle of a stable relation between mtDNA content and oxidative capacity maintained within this

tissue (Wang et al., 1999; Williams, 1986). More precisely, a relation of mtDNA content and oxidative capacity was not only reported in differing types of muscle fibers, but it also persisted during metabolic alterations due to exercise and chronic stimulation of skeletal muscle (Wang et al., 1999; Williams, 1986).

7. Summary

The aim of this thesis was to investigate the relevance of the mitochondrial DNA (mtDNA) depletion, i.e. copy number reduction, as potential cause of mitochondrial disorders. The combined occurrence of mtDNA depletion and several clinical syndromes of mitochondrial diseases has been reported in the literature (Clay Montier et al., 2009; Durham et al., 2005). However, the causative relationship between mtDNA copy number and the clinical phenotype is not elucidated yet. The analysis of the mtDNA depletion was performed with quantitative PCR (qPCR) on tissue specimen of patients affected by a mild phenotype of progressive external ophthalmoplegia (PEO) with epilepsy/ataxia, Alpers-Huttenlocher syndrome, and temporal lobe epilepsy (TLE) with Ammon's horn sclerosis (AHS).

A reduction of the mtDNA copy number was likewise determined in several tissues and cell types of Alpers-Huttenlocher patients with *POLG* (polymerase γ) mutations. Only a small amount of deleted mtDNA molecules was present in tissues of Alpers-Huttenlocher patients, which suggests a negligible impact of deleted molecules to the disease phenotype, whereas the mtDNA copy number reduction strongly correlates with the biochemical phenotype. However, an influence of deleted molecules detected in patients affected by a mild phenotype of PEO with epilepsy/ataxia cannot fully be excluded.

A pattern of liver areas with decreased cytochrome *c* oxidase (COX) activity and a corresponding pattern of mtDNA copy number reduction were observed in one Alpers-Huttenlocher patient. Since these patterns overlap, it can be suggested that a reduction of the mtDNA content potentially limits the metabolic activity of cells. The comparison of muscle specimen from an Alpers-Huttenlocher patient at an early and a later biopsy time point revealed that the mtDNA copy number was more severely reduced in the sample biopsied at a later life-time. This finding hints to a progressive decline of the mtDNA copy number in the affected tissues.

A relation of mtDNA depletion to the energy requirement of cell types and tissues could be confirmed. A high mtDNA copy number was measured in tissues with a high energy demand like muscle or brain, whereas accordingly a low mtDNA copy number

was detected in low energy demand tissues and cell types like blood. This tissue specific mtDNA content further correlated with the mitochondrial mass.

In different hippocampal regions of patients affected by AHS, a depletion of the mtDNA was detected. These specific hippocampal regions cornu ammonis 1 (CA1) and cornu ammonis 3 (CA3) with mtDNA depletion are additionally affected by a decreased mitochondrial mass (Baron et al., 2007) and mitochondrial functionality (Kudin et al., 2002; Kunz et al., 2000) as well as a neuronal cell loss. Since an increased level of reactive oxygen species (ROS) was reported for several neurodegenerative diseases as a hallmark of mitochondrial impairment, it can be suggested that a ROS induced mtDNA depletion might result in a decreased expression of mtDNA encoded enzymes of respiratory chain complexes and consequently to an energy deficit in the cell and finally to cell death. A correlation between the mtDNA copy number reduction and the neuronal impairment can be assumed.

Using an *in vitro* assay, it was determined that a mtDNA copy number reduction can lead to an impaired respiratory metabolism in artificially depleted fibroblasts. The biochemical phenotype in cells treated by 2',3'-dideoxycytidine (ddC) seems to occur at a certain threshold level. This threshold indicates that the respiratory activity remains stable above a certain mtDNA content, but decreases rapidly below this value. The threshold possibly originates from a surplus of mtDNA copies within the cell buffering mtDNA mutations or deletions up to a certain level.

One can conclude that a decrease of the mtDNA content affects the expression of the mitochondrially encoded enzymes of the oxidative phosphorylation system (OXPHOS). A dysfunction of the OXPHOS can result in an energy deficit of the cell. The lacking energy can lead to general metabolic problems and even to cell death as molecular cause of the clinical phenotype in mitochondrial diseases.

8. Appendices

8.1 List of references

1. Alexeyev M. F., Venediktova N., Pastukh V., Shokolenko I., Bonilla G., and Wilson G. L. (2008) Selective elimination of mutant mitochondrial genomes as therapeutic strategy for the treatment of NARP and MILS syndromes. *Gene Ther.* 15, 516–523.

2. Alpers B. J. (1931) Diffuse progressive degeneration of the gray matter of the cerebrum. *Arch. Neurol. Psychiatry* 25, 469–505.

3. Amaral D. G. and Lavenex P. (2007) Hippocampal Neuroanatomy. In *The hippocampus book* (eds. Andersen P., Morris R., Amaral D.G., Bliss T., and O'Keefe J.). Oxford University Press, New York, pp. 37–114.

4. Andersen P., Bliss T. V., and Skrede K. K. (1971) Lamellar organization of hippocampal excitatory pathways. *Exp. Brain Res.* 13, 222–238.

5. Anderson S., Bankier A. T., Barrell B. G., de Bruijn M. H., Coulson A. R., Drouin J., Eperon I. C., Nierlich D. P., Roe B. A., Sanger F., Schreier P. H., Smith A. J., Staden R., and Young I. G. (1981) Sequence and organization of the human mitochondrial genome. *Nature* 290, 457–465.

6. Ankel-Simons F. and Cummins J. M. (1996) Misconceptions about mitochondria and mammalian fertilization: implications for theories on human evolution. *Proc. Natl. Acad. Sci. U.S.A*. 93, 13859–13863.

7. Ashley N., O'Rourke A., Smith C., Adams S., Gowda V., Zeviani M., Brown G. K., Fratter C., and Poulton J. (2008) Depletion of mitochondrial DNA in fibroblast cultures from patients with *POLG1* mutations is a consequence of catalytic mutations. *Hum. Mol. Genet.* 17, 2496–2506.

8. Attardi G. and Schatz G. (1988) Biogenesis of mitochondria. *Annu. Rev. Cell Biol.* 4, 289–333.

9. Attardi G., Yoneda M., and Chomyn A. (1995) Complementation and segregation behavior of disease-causing mitochondrial DNA mutations in cellular model systems. *Biochim. Biophys. Acta* 1271, 241–248.

10. Baron M., Kudin A. P., and Kunz W. S. (2007) Mitochondrial dysfunction in neurodegenerative disorders. *Biochem. Soc. Trans*. 35, 1228–1231.

11. Barthélémy C., Ogier de Baulny H., Diaz J., Cheval M. A., Frachon P., Romero N., Goutieres F., Fardeau M., and Lombès A. (2001) Late-onset mitochondrial DNA depletion: DNA copy number, multiple deletions, and compensation. *Ann. Neurol.* 49, 607–617.

12. Battersby B. J. and Moyes C. D. (1998) Are there distinct subcellular populations of mitochondria in rainbow trout red muscle? *J. Exp. Biol.* 201, 2455–2460.

13. Ben-Ari Y., Tremblay E., Ottersen O. P., and Meldrum B. S. (1980) The role of epileptic activity in hippocampal and "remote" cerebral lesions induced by kainic acid. *Brain Res.* 191, 79–97.

14. Bender A., Krishnan K. J., Morris C. M., Taylor G. A., Reeve A. K., Perry R. H., Jaros E., Hersheson J. S., Betts J., Klopstock T., Taylor R. W., and Turnbull D. M. (2006) High levels of mitochondrial DNA deletions in substantia nigra neurons in aging and Parkinson disease. *Nat. Genet.* 38, 515–517.

15. Bengzon J., Kokaia Z., Elmér E., Nanobashvili A., Kokaia M., and Lindvall O. (1997) Apoptosis and proliferation of dentate gyrus neurons after single and intermittent limbic seizures. *Proc. Natl. Acad. Sci. U.S.A.* 94, 10432–10437.

16. Bensadoun A. and Weinstein D. (1976) Assay of proteins in the presence of interfering materials. *Anal. Biochem.* 70, 241–250.

17. Bentlage H. A. and Attardi G. (1996) Relationship of genotype to phenotype in fibroblast-derived transmitochondrial cell lines carrying the 3243 mutation associated with the MELAS encephalomyopathy: shift towards mutant genotype and role of mtDNA copy number. *Hum. Mol. Genet.* 5, 197–205.

18. Bereiter-Hahn J. (1990) Behavior of mitochondria in the living cell. *Int. Rev. Cytol.* 122, 1–63.

19. Bergmeyer H. U. (1970) *Methoden der enzymatischen Analyse*. Akademie Verlag. Berlin.

20. Berkovic S. F. and Jackson G. D. (2000) The hippocampal sclerosis whodunit: enter the genes. *Ann. Neurol.* 47, 557–558.

21. Blass J. P. and Gibson G. E. (1991) The role of oxidative abnormalities in the pathophysiology of Alzheimer's disease. *Rev. Neurol. (Paris)* 147, 513–525.

22. Blok R. B., Thorburn D. R., Thompson G. N., and Dahl H. H. (1995) A topoisomerase II cleavage site is associated with a novel mitochondrial DNA deletion. *Hum. Genet.* 95, 75–81.

23. Bohlega S., Tanji K., Santorelli F. M., Hirano M., al-Jishi A., and DiMauro S. (1996) Multiple mitochondrial DNA deletions associated with autosomal recessive ophthalmoplegia and severe cardiomyopathy. *Neurology* 46, 1329–1334.

24. Bolden A., Noy G. P., and Weissbach A. (1977) DNA polymerase of mitochondria is a γ-polymerase. *J. Biol. Chem.* 252, 3351–3356.

25. Bowling A. C., Schulz J. B., Brown R. H., Jr., and Beal M. F. (1993) Superoxide dismutase activity, oxidative damage, and mitochondrial energy metabolism in familial and sporadic amyotrophic lateral sclerosis. *J. Neurochem.* 61, 2322–2325.

26. Bowmaker M., Yao Yang M., Yasukawa T., Reyes A., Jacobs H. T., Huberman J. A., and Holt I. J. (2003) Mammalian mitochondrial DNA replicates bidirectionally from an initiation zone. *J. Biol. Chem.* 278, 50961–50969.

27. Brown T. A. and Clayton D. A. (2002) Release of replication termination controls mitochondrial DNA copy number after depletion with 2',3'-dideoxycytidine. *Nucleic Acids Res.* 30, 2004–2010.

28. Calvo S., Jain M., Xie X., Sheth S. A., Chang B., Goldberger O. A., Spinazzola A., Zeviani M., Carr S. A., and Mootha V. K. (2006) Systematic identification of human mitochondrial disease genes through integrative genomics. *Nat. Genet.* 38, 576–582.

29. Camello-Almaraz C., Gomez-Pinilla P. J., Pozo M. J., and Camello P. J. (2006) Mitochondrial reactive oxygen species and Ca^{2+} signaling. *Am. J. Physiol. Cell Physiol.* 291, C1082–C1088.

30. Cardaioli E., Da Pozzo P., Gallus G. N., Malandrini A., Gambelli S., Gaudiano C., Malfatti E., Viscomi C., Zicari E., Berti G., Serni G., Dotti M. T., and Federico A. (2007) A novel heteroplasmic $tRNA^{Ser(UCN)}$ mtDNA point mutation associated with progressive external ophthalmoplegia and hearing loss. *Neuromuscul. Disord.* 17, 681–683.

31. Carrodeguas J. A., Theis K., Bogenhagen D. F., and Kisker C. (2001) Crystal structure and deletion analysis show that the accessory subunit of mammalian DNA polymerase γ, Polγ B, functions as a homodimer. *Mol. Cell* 7, 43–54.

32. Chan S. S. and Copeland W. C. (2009) DNA polymerase γ and mitochondrial disease: Understanding the consequence of *POLG* mutations. *Biochim. Biophys. Acta* 1787, 312–319.

33. Chan S. S., Longley M. J., and Copeland W. C. (2005) The common A467T mutation in the human mitochondrial DNA polymerase *(POLG)* compromises catalytic efficiency and interaction with the accessory subunit. *J. Biol. Chem.* 280, 31341-31346.

34. Chan S. S., Longley M. J., and Copeland W. C. (2006) Modulation of the W748S mutation in DNA polymerase γ by the E1143G polymorphismin mitochondrial disorders. *Hum. Mol. Genet.* 15, 3473–3483.

35. Chang B. S. and Lowenstein D. H. (2003) Mechanisms of disease. Epilepsy. *N. Engl. J. Med.* 349, 1257–1266.

36. Chen C. H. and Cheng Y. C. (1989) Delayed cytotoxicity and selective loss of mitochondrial DNA in cells treated with the anti-human immunodeficiency virus compound 2',3'-dideoxycytidine. *J. Biol. Chem.* 264, 11934-11937.

37. Chen X., Prosser R., Simonetti S., Sadlock J., Jagiello G., and Schon E. A. (1995) Rearranged mitochondrial genomes are present in human oocytes. *Am. J. Hum. Genet.* 57, 239–247.

38. Chen X. J. and Butow R. A. (2005) The organization and inheritance of the mitochondrial genome. *Nat. Rev. Genet.* 6, 815–825.

39. Chinnery P. F. and Schon E. A. (2003) Mitochondria. *J. Neurol. Neurosurg. Psychiatr.* 74, 1188–1199.

40. Chinnery P. F., Thorburn D. R., Samuels D. C., White S. L., Dahl H. M., Turnbull D. M., Lightowlers R. N., and Howell N. (2000) The inheritance of mitochondrial DNA heteroplasmy: random drift, selection or both? *Trends Genet.* 16, 500–505.

41. Chinnery P. F., Zwijnenburg P. J., Walker M., Howell N., Taylor R. W., Lightowlers R. N., Bindoff L., and Turnbull D. M. (1999) Nonrandom tissue distribution of mutant mtDNA. *Am. J. Med. Genet.* 85, 498–501.

42. Chomyn A., Martinuzzi A., Yoneda M., Daga A., Hurko O., Johns D., Lai S. T., Nonaka I., Angelini C., and Attardi G. (1992) MELAS mutation in mtDNA binding site for transcription termination factor causes defects in protein synthesis and in respiration but no change in levels of upstream and downstream mature transcripts. *Proc. Natl. Acad. Sci. U.S.A.* 89, 4221–4225.

43. Clarke D. D. and Sokoloff S. (1999) Circulation and Energy Metabolism of the Brain. In *Basic Neurochemistry: Molecular, Cellular and Medical Aspects* (eds. G. J. Siegel, B. W. Agranoff, R.

W. Albers, S. K. Fisher, and M. D. Uhler). Lippincott - Raven, Philadelphia - New York, pp. 637–669.

44. Clay Montier L. L., Deng J. J., and Bai Y. (2009) Number matters: control of mammalian mitochondrial DNA copy number. *J. Genet. Genomics* 36, 125–131.

45. Clayton D. A. (1982) Replication of animal mitochondrial DNA. *Cell* 28, 693–705.

46. Coller H. A., Bodyak N. D., and Khrapko K. (2002) Frequent intracellular clonal expansions of somatic mtDNA mutations: significance and mechanisms. *Ann. N. Y. Acad. Sci.* 959, 434–447.

47. Coller H. A., Khrapko K., Bodyak N. D., Nekhaeva E., Herrero-Jimenez P., and Thilly W. G. (2001) High frequency of homoplasmic mitochondrial DNA mutations in human tumors can be explained without selection. *Nat. Genet.* 28, 147–150.

48. Collins T. J., Berridge M. J., Lipp P., and Bootman M. D. (2002) Mitochondria are morphologically and functionally heterogeneous within cells. *EMBO J.* 21, 1616–1627.

49. Copeland W. C. (2008) Inherited mitochondrial diseases of DNA replication. *Annu. Rev. Med.* 59, 131–146.

50. Davidzon G., Mancuso M., Ferraris S., Quinzii C., Hirano M., Peters H. L., Kirby D., Thorburn D. R., and DiMauro S. (2005) *POLG* mutations and Alpers syndrome. *Ann. Neurol*. 57, 921–923.

51. Diaz F., Bayona-Bafaluy M. P., Rana M., Mora M., Hao H., and Moraes C. T. (2002) Human mitochondrial DNA with large deletions repopulates organelles faster than full-length genomes under relaxed copy number control. *Nucleic Acids Res.* 30, 4626–4633.

52. Dubowitz V. (1985) *Muscle biopsy, a practical approach*. Ballière Tindall. London.

53. Dunnett C. W. (1955) A multiple comparison procedure for comparing several treatments with a control. *J. Am. Stat. Assoc.* 50, 1096–1121.

54. Dunnett C. W. (1964) New tables for multiple comparisons with a control. *Biometrics* 20, 482–491.

55. Durham S. E., Bonilla E., Samuels D. C., DiMauro S., and Chinnery P. F. (2005) Mitochondrial DNA copy number threshold in mtDNA depletion myopathy. *Neurology* 65, 453–455.

56. Figueiredo P. A., Ferreira R. M., Appell H. J., and Duarte J. A. (2008) Age-induced morphological, biochemical, and functional alterations in isolated mitochondria from murine skeletal muscle. *J. Gerontol. A Biol. Sci. Med. Sci.* 63, 350–359.

57. Förster T. (1946) Energiewanderung und Fluoreszenz. *Naturwissenschaften* 33, 166–175.

58. Frazier A. E., Kiu C., Stojanovski D., Hoogenraad N. J., and Ryan M. T. (2006) Mitochondrial morphology and distribution in mammalian cells. *Biol. Chem.* 387, 1551–1558.

59. Freeman W. M., Walker S. J., and Vrana K. E. (1999) Quantitative RT-PCR: pitfalls and potential. *BioTechniques* 26, 112–115.

60. Fridlender B., Fry M., Bolden A., and Weissbach A. (1972) A new synthetic RNA-dependent DNA polymerase from human tissue culture cells (HeLa-fibroblast-synthetic oligonucleotides-template-purified enzymes). *Proc. Natl. Acad. Sci. U.S.A.* 69, 452–455.

61. Gauthier G. F. and Padykula H. A. (1966) Cytological studies of fiber types in skeletal muscle. A comparative study of the mammalian diaphragm. *J. Cell Biol.* 28, 333-354.

62. Gauthier-Villars M., Landrieu P., Cormier-Daire V., Jacquemin E., Chrétien D., Rötig A., Rustin P., Munnich A., and de Lonlay P. (2001) Respiratory chain deficiency in Alpers syndrome. *Neuropediatrics* 32, 150–152.

63. Gellerich F. N., Deschauer M., Chen Y., Müller T., Neudecker S., and Zierz S. (2002) Mitochondrial respiratory rates and activities of respiratory chain complexes correlate linearly with heteroplasmy of deleted mtDNA without threshold and independently of deletion size. *Biochim. Biophys. Acta* 1556, 41–52.

64. Graziewicz M. A., Longley M. J., and Copeland W. C. (2006) DNA polymerase γ in mitochondrial DNA replication and repair. *Chem. Rev.* 106, 383–405.

65. Hakonen A. H., Heiskanen S., Juvonen V., Lappalainen I., Luoma P. T., Rantamäki M., Van Goethem G. , Löfgren A., Hackman P., Paetau A., Kaakkola S., Majamaa K., Varilo T., Udd B., Kääriäinen H., Bindoff L. A., and Suomalainen A. (2005) Mitochondrial DNA polymerase W748S mutation: a common cause of autosomal recessive ataxia with ancient European origin. *Am. J. Hum. Genet.* 77, 430–441.

66. Halliwell B. and Aruoma O. I. (1991) DNA damage by oxygen-derived species. Its mechanism and measurement in mammalian systems. *FEBS Lett.* 281, 9–19.

67. Han D., Williams E., and Cadenas E. (2001) Mitochondrial respiratory chain-dependent generation of superoxide anion and its release into the intermembrane space. *Biochem. J.* 353, 411-416.

68. Harding A. E. and Hammans S. R. (1992) Deletions of the mitochondrial genome. *J. Inherit. Metab Dis.* 15, 480–486.

69. Harding B. N., Alsanjari N., Smith S. J., Wiles C. M., Thrush D., Miller D. H., Scaravilli F., and Harding A. E. (1995) Progressive neuronal degeneration of childhood with liver disease (Alpers' disease) presenting in young adults. *J. Neurol. Neurosurg. Psychiatr.* 58, 320–325.

70. Hatefi Y. (1985) The mitochondrial electron transport and oxidative phosphorylation system. *Annu. Rev. Biochem.* 54, 1015–1069.

71. Hayashi J., Ohta S., Kagawa Y., Takai D., Miyabayashi S., Tada K., Fukushima H., Inui K., Okada S., Goto Y., and Nonaka I. (1994) Functional and morphological abnormalities of mitochondria in human cells containing mitochondrial DNA with pathogenic point mutations in tRNA genes. *J. Biol. Chem.* 269, 19060–19066.

72. Hayashi J., Ohta S., Kikuchi A., Takemitsu M., Goto Y., and Nonaka I. (1991) Introduction of disease-related mitochondrial DNA deletions into HeLa cells lacking mitochondrial DNA results in mitochondrial dysfunction. *Proc. Natl. Acad. Sci. U.S.A.* 88, 10614–10618.

73. Hayashi J., Tanaka M., Sato W., Ozawa T., Yonekawa H., Kagawa Y., and Ohta S. (1990) Effects of ethidium bromide treatment of mouse cells on expression and assembly of nuclear-

coded subunits of complexes involved in the oxidative phosphorylation. *Biochem. Biophys. Res. Commun.* 167, 216–221.

74. Hengartner M. O. (2000) The biochemistry of apoptosis. *Nature* 407, 770–776.

75. Henze K. and Martin W. (2003) Evolutionary biology: essence of mitochondria. *Nature* 426, 127–128.

76. Hirai K., Aliev G., Nunomura A., Fujioka H., Russell R. L., Atwood C. S., Johnson A. B., Kress Y., Vinters H. V., Tabaton M., Shimohama S., Cash A. D., Siedlak S. L., Harris P. L., Jones P. K., Petersen R. B., Perry G., and Smith M. A. (2001) Mitochondrial abnormalities in Alzheimer's disease. *J. Neurosci*. 21, 3017–3023.

77. Hollenbeck P. J. and Saxton W. M. (2005) The axonal transport of mitochondria. *J. Cell Sci*. 118, 5411–5419.

78. Holt I. J., Harding A. E., Cooper J. M., Schapira A. H., Toscano A., Clark J. B., and Morgan-Hughes J. A. (1989a) Mitochondrial myopathies: clinical and biochemical features of 30 patients with major deletions of muscle mitochondrial DNA. *Ann. Neurol*. 26, 699–708.

79. Holt I. J., Harding A. E., and Morgan-Hughes J. A. (1988) Deletions of muscle mitochondrial DNA in patients with mitochondrial myopathies. *Nature* 331, 717–719.

80. Holt I. J., Harding A. E., and Morgan-Hughes J. A. (1989b) Deletions of muscle mitochondrial DNA in mitochondrial myopathies: sequence analysis and possible mechanisms. *Nucleic Acids Res.* 17, 4465–4469.

81. Holt I. J., Lorimer H. E., and Jacobs H. T. (2000) Coupled leading- and lagging-strand synthesis of mammalian mitochondrial DNA. *Cell* 100, 515–524.

82. Horsley V. and Pavlath G. K. (2004) Forming a multinucleated cell: molecules that regulate myoblast fusion. *Cells Tissues Organs* 176, 67-78.

83. Huang X. P., O'Brien P. J., and Templeton D. M. (2006) Mitochondrial involvement in genetically determined transition metal toxicity I. Iron toxicity. *Chem. Biol. Interact.* 163, 68–76.

84. Huttenlocher P. R., Solitare G. B., and Adams G. (1976) Infantile diffuse cerebral degeneration with hepatic cirrhosis. *Arch. Neurol.* 33, 186–192.

85. Jansen K. M. and Pavlath G. K. (2008) Molecular control of mammalian myoblast fusion. *Methods Mol. Biol.* 475, 115-133.

86. Jefferys J. G. (1999) Hippocampal sclerosis and temporal lobe epilepsy: cause or consequence? *Brain* 122, 1007–1008.

87. Jefferys J. G., Evans B. J., Hughes S. A., and Williams S. F. (1992) Neuropathology of the chronic epileptic syndrome induced by intrahippocampal tetanus toxin in rat: preservation of pyramidal cells and incidence of dark cells. *Neuropathol. Appl. Neurobiol*. 18, 53–70.

88. Jenner P. (2003) Oxidative stress in Parkinson's disease. *Ann. Neurol*. 53, S26–S36.

89. Johnson A. A., Tsai Y., Graves S. W., and Johnson K. A. (2000) Human mitochondrial DNA polymerase holoenzyme: reconstitution and characterization. *Biochemistry* 39, 1702–1708.

90. Johnson M. A., Turnbull D. M., Dick D. J., and Sherratt H. S. (1983) A partial deficiency of cytochrome *c* oxidase in chronic progressive external ophthalmoplegia. *J. Neurol. Sci*. 60, 31–53.

91. Jones D. P. and Aw T. Y. (1988) Mitochondrial distribution and O_2 gradients in mammalian cells. In *Microcompartimentation* (ed. Jones D.P.). CRC Press, Boca Raton, Florida, pp. 37–54.

92. Jones J. B., Song J. J., Hempen P. M., Parmigiani G., Hruban R. H., and Kern S. E. (2001) Detection of mitochondrial DNA mutations in pancreatic cancer offers a "mass"-ive advantage over detection of nuclear DNA mutations. *Cancer Res*. 61, 1299–1304.

93. Kaguni L. S. (2004) DNA polymerase γ, the mitochondrial replicase. *Annu. Rev. Biochem.* 73, 293-320.

94. Kayar S. R., Hoppeler H., Mermod L., and Weibel E. R. (1988) Mitochondrial size and shape in equine skeletal muscle: a three-dimensional reconstruction study. *Anat. Rec*. 222, 333–339.

95. Kelley D. E., He J., Menshikova E. V., and Ritov V. B. (2002) Dysfunction of mitochondria in human skeletal muscle in type 2 diabetes. *Diabetes* 51, 2944–2950.

96. King M. P. and Attardi G. (1989) Human cells lacking mtDNA: repopulation with exogenous mitochondria by complementation. *Science* 246, 500–503.

97. Kirby D. M., Thorburn D. R., Turnbull D. M., and Taylor R. W. (2007) Biochemical assays of respiratory chain complex activity. *Methods Cell Biol.* 80, 93-119.

98. Kovacs R., Schuchmann S., Gabriel S., Kardos J., and Heinemann U. (2001) Ca^{2+} signalling and changes of mitochondrial function during low-Mg^{2+}-induced epileptiform activity in organotypic hippocampal slice cultures. *Eur. J. Neurosci*. 13, 1311–1319.

99. Krebs H. A. (1970) The history of the tricarboxylic acid cycle. *Perspect. Biol. Med*. 14, 154–170.

100. Krishnan K. J., Reeve A. K., Samuels D. C., Chinnery P. F., Blackwood J. K., Taylor R. W., Wanrooij S., Spelbrink J. N., Lightowlers R. N., and Turnbull D. M. (2008) What causes mitochondrial DNA deletions in human cells? *Nat. Genet*. 40, 275–279.

101. Kudin A. P., Bimpong-Buta N. Y., Vielhaber S., Elger C. E., and Kunz W. S. (2004) Characterization of superoxide-producing sites in isolated brain mitochondria. *J. Biol. Chem*. 279, 4127–4135.

102. Kudin A. P., Debska-Vielhaber G., and Kunz W. S. (2005) Characterization of superoxide production sites in isolated rat brain and skeletal muscle mitochondria. *Biomed. Pharmacother*. 59, 163–168.

103. Kudin A. P., Kudina T. A., Seyfried J., Vielhaber S., Beck H., Elger C. E., and Kunz W. S. (2002) Seizure-dependent modulation of mitochondrial oxidative phosphorylation in rat hippocampus. *Eur. J. Neurosci*. 15, 1105–1114.

104. Kudin A. P., Zsurka G., Elger C. E., and Kunz W. S. (2009) Mitochondrial involvement in temporal lobe epilepsy. *Exp. Neurol*. 218, 326–332.

105. Kunz W. S. (2002) The role of mitochondria in epileptogenesis. *Curr. Opin. Neurol*. 15, 179–184.

106. Kunz W. S., Kudin A. P., Vielhaber S., Blümcke I., Zuschratter W., Schramm J., Beck H., and Elger C. E. (2000) Mitochondrial complex I deficiency in the epileptic focus of patients with temporal lobe epilepsy. *Ann. Neurol*. 48, 766–773.

107. Lee H. C., Li S. H., Lin J. C., Wu C. C., Yeh D. C., and Wei Y. H. (2004) Somatic mutations in the D-loop and decrease in the copy number of mitochondrial DNA in human hepatocellular carcinoma. *Mutat. Res*. 547, 71–78.

108. Lee H. C. and Wei Y. H. (2005) Mitochondrial biogenesis and mitochondrial DNA maintenance of mammalian cells under oxidative stress. *Int. J. Biochem. Cell Biol*. 37, 822–834.

109. Lee Y. S., Kennedy W. D., and Yin Y. W. (2009) Structural insight into processive human mitochondrial DNA synthesis and disease-related polymerase mutations. *Cell* 139, 312–324.

110. Liang L. P., Ho Y. S., and Patel M. (2000) Mitochondrial superoxide production in kainate-induced hippocampal damage. *Neuroscience* 101, 563–570.

111. Lill R., Diekert K., Kaut A., Lange H., Pelzer W., Prohl C., and Kispal G. (1999) The essential role of mitochondria in the biogenesis of cellular iron-sulfur proteins. *Biol. Chem*. 380, 1157–1166.

112. Lim S. E., Longley M. J., and Copeland W. C. (1999) The mitochondrial p55 accessory subunit of human DNA polymerase γ enhances DNA binding, promotes processive DNA synthesis, and confers *N*-ethylmaleimide resistance. *J. Biol. Chem*. 274, 38197–38203.

113. Liu W. and Saint D. A. (2002) Validation of a quantitative method for real time PCR kinetics. *Biochem. Biophys. Res. Commun*. 294, 347–353.

114. Liu Z., Mikati M., and Holmes G. L. (1995) Mesial temporal sclerosis: pathogenesis and significance. *Pediatr. Neurol*. 12, 5–16.

115. Liu Z., Nagao T., Desjardins G. C., Gloor P., and Avoli M. (1994) Quantitative evaluation of neuronal loss in the dorsal hippocampus in rats with long-term pilocarpine seizures. *Epilepsy Res*. 17, 237–247.

116. Lombardi A., Damon M., Vincent A., Goglia F., and Herpin P. (2000) Characterisation of oxidative phosphorylation in skeletal muscle mitochondria subpopulations in pig: a study using top-down elasticity analysis. *FEBS Lett*. 475, 84–88.

117. Longley M. J., Clark S., Yu Wai M. C., Hudson G., Durham S. E., Taylor R. W., Nightingale S., Turnbull D. M., Copeland W. C., and Chinnery P. F. (2006) Mutant *POLG2* disrupts DNA polymerase γ subunits and causes progressive external ophthalmoplegia. *Am. J. Hum. Genet.* 78, 1026-1034.

118. Longley M. J., Prasad R., Srivastava D. K., Wilson S. H., and Copeland W. C. (1998a) Identification of 5'-deoxyribose phosphate lyase activity in human DNA polymerase γ and its role in mitochondrial base excision repair *in vitro*. *Proc. Natl. Acad. Sci. U.S.A.* 95, 12244–12248.

119. Longley M. J., Ropp P. A., Lim S. E., and Copeland W. C. (1998b) Characterization of the native and recombinant catalytic subunit of human DNA polymerase γ: identification of residues critical for exonuclease activity and dideoxynucleotide sensitivity. *Biochemistry* 37, 10529–10539.

120. Lopes da Silva F. H. and Arnolds D. E. (1978) Physiology of the hippocampus and related structures. *Annu. Rev. Physiol*. 40, 185–216.

121. Lopez M. F., Kristal B. S., Chernokalskaya E., Lazarev A., Shestopalov A. I., Bogdanova A., and Robinson M. (2000) High-throughput profiling of the mitochondrial proteome using affinity fractionation and automation. *Electrophoresis* 21, 3427–3440.

122. Lowry O. H., Rosebrough N. J., Farr A. L., and Randall R. J. (1951) Protein measurement with the Folin phenol reagent. *J. Biol. Chem*. 193, 265–275.

123. Luoma P. T., Luo N., Löscher W. N., Farr C. L., Horvath R., Wanschitz J., Kiechl S., Kaguni L. S., and Suomalainen A. (2005) Functional defects due to spacer-region mutations of human mitochondrial DNA polymerase in a family with an ataxia-myopathy syndrome. *Hum. Mol. Genet.* 14, 1907-1920.

124. Maia A. L., Kim B. W., Huang S. A., Harney J. W., and Larsen P. R. (2005) Type 2 iodothyronine deiodinase is the major source of plasma T_3 in euthyroid humans. *J. Clin. Invest.* 115, 2524–2533.

125. Mäkelä-Bengs P., Suomalainen A., Majander A., Rapola J., Kalimo H., Nuutila A., and Pihko H. (1995) Correlation between the clinical symptoms and the proportion of mitochondrial DNA carrying the 8993 point mutation in the NARP syndrome. *Pediatr. Res*. 37, 634–639.

126. Maniura-Weber K., Goffart S., Garstka H. L., Montoya J., and Wiesner R. J. (2004) Transient overexpression of mitochondrial transcription factor A (TFAM) is sufficient to stimulate mitochondrial DNA transcription, but not sufficient to increase mtDNA copy number in cultured cells. *Nucleic Acids Res*. 32, 6015–6027.

127. Margulis L. (1981) The Endosymbiotic Theory. In *Symbiosis in Cell Evolution - life and its environment on the early earth* W. H. Freeman and Company, San Francisco, pp. 1–14.

128. Martin J. L., Brown C. E., Matthews-Davis N., and Reardon J. E. (1994) Effects of antiviral nucleoside analogs on human DNA polymerases and mitochondrial DNA synthesis. *Antimicrob. Agents Chemother*. 38, 2743–2749.

129. Maurer I., Zierz S., and Möller H. J. (2000) A selective defect of cytochrome *c* oxidase is present in brain of Alzheimer disease patients. *Neurobiol. Aging* 21, 455–462.

130. McFarland R., Hudson G., Taylor R. W., Green S. H., Hodges S., McKiernan P. J., Chinnery P. F., and Ramesh V. (2008) Reversible valproate hepatotoxicity due to mutations in mitochondrial DNA polymerase γ (*POLG1*). *Arch. Dis. Child.* 93, 151–153.

131. Meeusen S. and Nunnari J. (2003) Evidence for a two membrane-spanning autonomous mitochondrial DNA replisome. *J. Cell Biol*. 163, 503–510.

132. Mendel G. (1866) Versuche über Pflanzenhybriden. *Verhandlungen des Naturforschenden Vereins zu Brünn* 4, 3–47.

133. Miller S. W., Trimmer P. A., Parker W. D., Jr., and Davis R. E. (1996) Creation and characterization of mitochondrial DNA-depleted cell lines with "neuronal-like" properties. *J. Neurochem*. 67, 1897–1907.

134. Minin A. A., Kulik A. V., Gyoeva F. K., Li Y., Goshima G., and Gelfand V. I. (2006) Regulation of mitochondria distribution by RhoA and formins. *J. Cell Sci*. 119, 659–670.

135. Mita S., Rizzuto R., Moraes C. T., Shanske S., Arnaudo E., Fabrizi G. M., Koga Y., DiMauro S., and Schon E. A. (1990) Recombination via flanking direct repeats is a major cause of large-scale deletions of human mitochondrial DNA. *Nucleic Acids Res*. 18, 561–567.

136. Mitchell P. (1961) Coupling of phosphorylation to electron and hydrogen transfer by a chemi-osmotic type of mechanism. *Nature* 191, 144–148.

137. Mitsuya H., Jarrett R. F., Matsukura M., Di Marzo Veronese, F., DeVico A. L., Sarngadharan M. G., Johns D. G., Reitz M. S., and Broder S. (1987) Long-term inhibition of human T-lymphotropic virus type III/lymphadenopathy-associated virus (human immunodeficiency virus) DNA synthesis and RNA expression in T cells protected by 2',3'-dideoxynucleosides *in vitro*. *Proc. Natl. Acad. Sci. U.S.A.* 84, 2033–2037.

138. Moore D. J., West A. B., Dawson V. L., and Dawson T. M. (2005) Molecular pathophysiology of Parkinson's disease. *Annu. Rev. Neurosci*. 28, 57–87.

139. Moraes C. T., Shanske S., Tritschler H. J., Aprille J. R., Andreetta F., Bonilla E., Schon E. A., and DiMauro S. (1991) mtDNA depletion with variable tissue expression: a novel genetic abnormality in mitochondrial diseases. *Am. J. Hum. Genet*. 48, 492–501.

140. Moyes C. D., Mathieu-Costello O. A., Tsuchiya N., Filburn C., and Hansford R. G. (1997) Mitochondrial biogenesis during cellular differentiation. *Am. J. Physiol.* 272, C1345–C1351.

141. Mullis K. B. and Faloona F. A. (1987) Specific synthesis of DNA *in vitro* via a polymerase-catalyzed chain reaction. *Meth. Enzymol.* 155, 335-350.

142. Munnich A. (2008) Casting an eye on the Krebs cycle. *Nat. Genet*. 40, 1148–1149.

143. Murphy M. P. (2009) How mitochondria produce reactive oxygen species. *Biochem. J*. 417, 1–13.

144. Nadler J. V. (1981) Minireview. Kainic acid as a tool for the study of temporal lobe epilepsy. *Life Sci*. 29, 2031–2042.

145. Naviaux R. K., Nyhan W. L., Barshop B. A., Poulton J., Markusic D., Karpinski N. C., and Haas R. H. (1999) Mitochondrial DNA polymerase γ deficiency and mtDNA depletion in a child with Alpers' syndrome. *Ann. Neurol*. 45, 54–58.

146. Nekhaeva E., Bodyak N. D., Kraytsberg Y., McGrath S. B., Van Orsouw N. J., Pluzhnikov A., Wei J. Y., Vijg J., and Khrapko K. (2002) Clonally expanded mtDNA point mutations are abundant in individual cells of human tissues. *Proc. Natl. Acad. Sci. U.S.A.* 99, 5521–5526.

147. Nelson I., d'Auriol L., Galibert F., Ponsot G., and Lestienne P. (1989) Identification nucléotidique et modèle cinétique d'une deletion hétéroplasmique de 4666 paires de bases de l'ADN mitochondrial dans le syndrome de Kearns-Sayre. *C. R. Acad. Sci. III, Sci. Vie* 309, 403–407.

148. Nguyen K. V., Østergaard E., Ravn S. H., Balslev T., Rubæk Danielsen E., Vardag A., McKiernan P. J., Gray G., and Naviaux R. K. (2005) *POLG* mutations in Alpers syndrome. *Neurology* 65, 1493–1495.

149. Nguyen K. V., Sharief F. S., Chan S. S., Copeland W. C., and Naviaux R. K. (2006) Molecular diagnosis of Alpers syndrome. *J. Hepatol*. 45, 108–116.

150. Nicholls D. G., Vesce S., Kirk L., and Chalmers S. (2003) Interactions between mitochondrial bioenergetics and cytoplasmic calcium in cultured cerebellar granule cells. *Cell Calcium* 34, 407–424.

151. Nishino I., Spinazzola A., and Hirano M. (1999) Thymidine phosphorylase gene mutations in MNGIE, a human mitochondrial disorder. *Science* 283, 689–692.

152. Ogata T. and Yamasaki Y. (1997) Ultra-high-resolution scanning electron microscopy of mitochondria and sarcoplasmic reticulum arrangement in human red, white, and intermediate muscle fibers. *Anat. Rec*. 248, 214–223.

153. Pan-Zhou X. R., Cui L., Zhou X. J., Sommadossi J. P., and Darley-Usmar V. M. (2000) Differential effects of antiretroviral nucleoside analogs on mitochondrial function in HepG2 cells. *Antimicrob. Agents Chemother*. 44, 496–503.

154. Papadimitriou A., Comi G. P., Hadjigeorgiou G. M., Bordoni A., Sciacco M., Napoli L., Prelle A., Moggio M., Fagiolari G., Bresolin N., Salani S., Anastasopoulos I., Giassakis G., Divari R., and Scarlato G. (1998) Partial depletion and multiple deletions of muscle mtDNA in familial MNGIE syndrome. *Neurology* 51, 1086–1092.

155. Paus S., Zsurka G., Baron M., Deschauer M., Bamberg C., Klockgether T., Kunz W. S., and Kornblum C. (2008) Apraxia of lid opening mimicking ptosis in compound heterozygosity for A467T and W748S *POLG1* mutations. *Mov. Disord.* 23, 1286-1288.

156. Peterson G. L. (1977) A simplification of the protein assay method of Lowry et al. which is more generally applicable. *Anal. Biochem*. 83, 346–356.

157. Pfaffl M. W. (2001) A new mathematical model for relative quantification in real-time RT-PCR. *Nucleic Acids Res*. 29, e45.

158. Piechota J., Szczęsny R., Wolanin K., Chlebowski A., and Bartnik E. (2006a) Nuclear and mitochondrial genome responses in HeLa cells treated with inhibitors of mitochondrial DNA expression. *Acta Biochim. Pol*. 53, 485–495.

159. Piechota J., Tomecki R., Gewartowski K., Szczęsny R., Dmochowska A., Kudła M., Dybczyńska L., Stepien P. P., and Bartnik E. (2006b) Differential stability of mitochondrial mRNA in HeLa cells. *Acta Biochim. Pol*. 53, 157–168.

160. Porteous W. K., James A. M., Sheard P. W., Porteous C. M., Packer M. A., Hyslop S. J., Melton J. V., Pang C. Y., Wei Y. H., and Murphy M. P. (1998) Bioenergetic consequences of accumulating the common 4977-bp mitochondrial DNA deletion. *Eur. J. Biochem*. 257, 192–201.

161. Preiss T., Lowerson S. A., Weber K., and Lightowlers R. N. (1995) Human mitochondria: distinct organelles or dynamic network? *Trends Genet*. 11, 211–212.

162. Puntschart A., Claassen H., Jostarndt K., Hoppeler H., and Billeter R. (1995) mRNAs of enzymes involved in energy metabolism and mtDNA are increased in endurance-trained athletes. *Am. J. Physiol.* 269, C619–C625.

163. Pyle A., Taylor R. W., Durham S. E., Deschauer M., Schaefer A. M., Samuels D. C., and Chinnery P. F. (2007) Depletion of mitochondrial DNA in leucocytes harbouring the 3243A→G mtDNA mutation. *J. Med. Genet*. 44, 69–74.

164. Reardon J. E. (1992) Human immunodeficiency virus reverse transcriptase: steady-state and pre-steady-state kinetics of nucleotide incorporation. *Biochemistry* 31, 4473–4479.

165. Richter C., Park J. W., and Ames B. N. (1988) Normal oxidative damage to mitochondrial and nuclear DNA is extensive. *Proc. Natl. Acad. Sci. U.S.A.* 85, 6465–6467.

166. Rizzuto R., Pinton P., Carrington W., Fay F. S., Fogarty K. E., Lifshitz L. M., Tuft R. A., and Pozzan T. (1998) Close contacts with the endoplasmic reticulum as determinants of mitochondrial Ca^{2+} responses. *Science* 280, 1763-1766.

167. Robin E. D. and Wong R. (1988) Mitochondrial DNA molecules and virtual number of mitochondria per cell in mammalian cells. *J. Cell Physiol.* 136, 507–513.

168. Ropp P. A. and Copeland W. C. (1996) Cloning and characterization of the human mitochondrial DNA polymerase, DNA polymerase γ. *Genomics* 36, 449–458.

169. Rossignol R., Faustin B., Rocher C., Malgat M., Mazat J. P., and Letellier T. (2003) Mitochondrial threshold effects. *Biochem. J.* 370, 751–762.

170. Rutledge R. G. (2004) Sigmoidal curve-fitting redefines quantitative real-time PCR with the prospective of developing automated high-throughput applications. *Nucleic Acids Res*. 32, e178.

171. Sandbank U. and Lerman P. (1972) Progressive cerebral poliodystrophy - Alpers' disease. Disorganized giant neuronal mitochondria on electron microscopy. *J. Neurol. Neurosurg. Psychiatr.* 35, 749–755.

172. Saraste M. (1999) Oxidative phosphorylation at the fin de siècle. *Science* 283, 1488–1493.

173. Sarnat H. B. and Marín-García J. (2005) Pathology of mitochondrial encephalomyopathies. *Can. J. Neurol. Sci*. 32, 152–166.

174. Sasaki S. and Iwata M. (1996) Ultrastructural study of synapses in the anterior horn neurons of patients with amyotrophic lateral sclerosis. *Neurosci. Lett*. 204, 53–56.

175. Satoh M. and Kuroiwa T. (1991) Organization of multiple nucleoids and DNA molecules in mitochondria of a human cell. *Exp. Cell Res*. 196, 137–140.

176. Schapira A. H. and Cock H. R. (1999) Mitochondrial myopathies and encephalomyopathies. *Eur. J. Clin. Invest.* 29, 886–898.

177. Schimper A. F. (1883) Über die Entwicklung der Chlorophyllkörner und Farbkörper. *Bot. Ztg.* 41, 105–120.

178. Schmitt M. E. and Clayton D. A. (1993) Conserved features of yeast and mammalian mitochondrial DNA replication. *Curr. Opin. Genet. Dev*. 3, 769–774.

179. Schon E. A., Rizzuto R., Moraes C. T., Nakase H., Zeviani M., and DiMauro S. (1989) A direct repeat is a hotspot for large-scale deletion of human mitochondrial DNA. *Science* 244, 346–349.

180. Schwabe M. J., Dobyns W. B., Burke B., and Armstrong D. L. (1997) Valproate-induced liver failure in one of two siblings with Alpers disease. *Pediatr. Neurol*. 16, 337–343.

181. Sciacco M., Bonilla E., Schon E. A., DiMauro S., and Moraes C. T. (1994) Distribution of wild-type and common deletion forms of mtDNA in normal and respiration-deficient muscle fibers from patients with mitochondrial myopathy. *Hum. Mol. Genet*. 3, 13–19.

182. Seligman A. M., Karnovsky M. J., Wasserkrug H. L., and Hanker J. S. (1968) Nondroplet ultrastructural demonstration of cytochrome oxidase activity with a polymerizing osmiophilic reagent, diaminobenzidine (DAB). *J. Cell Biol*. 38, 1–14.

183. Shadel G. S. and Clayton D. A. (1997) Mitochondrial DNA maintenance in vertebrates. *Annu. Rev. Biochem*. 66, 409–435.

184. Shibutani S., Takeshita M., and Grollman A. P. (1991) Insertion of specific bases during DNA synthesis past the oxidation-damaged base 8-oxodG. *Nature* 349, 431–434.

185. Shoffner J. M., Lott M. T., Voljavec A. S., Soueidan S. A., Costigan D. A., and Wallace D. C. (1989) Spontaneous Kearns-Sayre/chronic external ophthalmoplegia plus syndrome associated with a mitochondrial DNA deletion: a slip-replication model and metabolic therapy. *Proc. Natl. Acad. Sci. U.S.A.* 86, 7952–7956.

186. Shokolenko I., Venediktova N., Bochkareva A., Wilson G. L., and Alexeyev M. F. (2009) Oxidative stress induces degradation of mitochondrial DNA. *Nucleic Acids Res*. 37, 2539–2548.

187. Shoubridge E. A., Karpati G., and Hastings K. E. (1990) Deletion mutants are functionally dominant over wild-type mitochondrial genomes in skeletal muscle fiber segments in mitochondrial disease. *Cell* 62, 43–49.

188. Shuster R. C., Rubenstein A. J., and Wallace D. C. (1988) Mitochondrial DNA in anucleate human blood cells. *Biochem. Biophys. Res. Commun*. 155, 1360–1365.

189. Simonnet H., Alazard N., Pfeiffer K., Gallou C., Béroud C., Demont J., Bouvier R., Schägger H., and Godinot C. (2002) Low mitochondrial respiratory chain content correlates with tumor aggressiveness in renal cell carcinoma. *Carcinogenesis* 23, 759–768.

190. Sloviter R. S. (1994) The functional organization of the hippocampal dentate gyrus and its relevance to the pathogenesis of temporal lobe epilepsy. *Ann. Neurol*. 35, 640–654.

191. Sloviter R. S. (2005) The neurobiology of temporal lobe epilepsy: too much information, not enough knowledge. *C. R. Biol*. 328, 143–153.

192. Smeitink J., van den Heuvel L., and DiMauro S. (2001) The genetics and pathology of oxidative phosphorylation. *Nat. Rev. Genet*. 2, 342–352.

193. Sommer W. (1880) Erkrankung des Ammonshorns als aetiologisches Moment der Epilepsie. *Arch. Psychiatr. Nervenkr.* 10, 631–675.

194. Spelbrink J. N., Toivonen J. M., Hakkaart G. A., Kurkela J. M., Cooper H. M., Lehtinen S. K., Lecrenier N., Back J. W., Speijer D., Foury F., and Jacobs H. T. (2000) *In vivo* functional analysis of the human mitochondrial DNA polymerase *POLG* expressed in cultured human cells. *J. Biol. Chem*. 275, 24818–24828.

195. Spinazzola A. and Zeviani M. (2005) Disorders of nuclear-mitochondrial intergenomic signaling. *Gene* 354, 162–168.

196. Starnes M. C. and Cheng Y. C. (1987) Cellular metabolism of 2',3'-dideoxycytidine, a compound active against human immunodeficiency virus *in vitro*. *J. Biol. Chem*. 262, 988–991.

197. Swerdlow R. H., Parks J. K., Cassarino D. S., Maguire D. J., Maguire R. S., Bennett J. P., Jr., Davis R. E., and Parker W. D., Jr. (1997) Cybrids in Alzheimer's disease: a cellular model of the disease? *Neurology* 49, 918–925.

198. Swick R. W., Rexroth A. K., and Stange J. L. (1968) The metabolism of mitochondrial proteins. III. The dynamic state of rat liver mitochondria. *J. Biol. Chem*. 243, 3581–3587.

199. Szuhai K., Ouweland J., Dirks R., Lemaître M., Truffert J., Janssen G., Tanke H., Holme E., Maassen J., and Raap A. (2001) Simultaneous A8344G heteroplasmy and mitochondrial DNA copy number quantification in myoclonus epilepsy and ragged-red fibers (MERRF) syndrome by a multiplex molecular beacon based real-time fluorescence PCR. *Nucleic Acids Res*. 29, e13.

200. Takamatsu C., Umeda S., Ohsato T., Ohno T., Abe Y., Fukuoh A., Shinagawa H., Hamasaki N., and Kang D. (2002) Regulation of mitochondrial D-loops by transcription factor A and single-stranded DNA-binding protein. *EMBO Rep*. 3, 451–456.

201. Taylor R. W. and Turnbull D. M. (2005) Mitochondrial DNA mutations in human disease. *Nat. Rev. Genet*. 6, 389–402.

202. Thorsness P. E. (1992) Structural dynamics of the mitochondrial compartment. *Mutat. Res*. 275, 237–241.

203. Thorsness P. E. and Weber E. R. (1996) Escape and migration of nucleic acids between chloroplasts, mitochondria, and the nucleus. *Int. Rev. Cytol*. 165, 207–234.

204. Tichopad A., Dzidic A., and Pfaffl M. W. (2002) Improving quantitative real-time RT-PCR reproducibility by boosting primer-linked amplification efficiency. *Biotechnol. Lett*. 24, 2053–2056.

205. Tønnesen T. and Friesen J. D. (1973) The effects of daunomycin and ethidium bromide on *Escherichia coli*. *Mol. Gen. Genet*. 124, 177–186.

206. Treem W. R. and Sokol R. J. (1998) Disorders of the mitochondria. *Semin. Liver Dis*. 18, 237–253.

207. Trounce I., Neill S., and Wallace D. C. (1994) Cytoplasmic transfer of the mtDNA nt 8993 T→G (*ATP6*) point mutation associated with Leigh syndrome into mtDNA-less cells demonstrates cosegregation with a decrease in state III respiration and ADP/O ratio. *Proc. Natl. Acad. Sci. U.S.A*. 91, 8334–8338.

208. Tzoulis C., Engelsen B. A., Telstad W., Aasly J., Zeviani M., Winterthun S., Ferrari G., Aarseth J. H., and Bindoff L. A. (2006) The spectrum of clinical disease caused by the A467T and W748S *POLG* mutations: a study of 26 cases. *Brain* 129, 1685–1692.

209. Van den Bogert C., De Vries H., Holtrop M., Muus P., Dekker H. L., Van Galen M. J., Bolhuis P. A., and Taanman J. W. (1993) Regulation of the expression of mitochondrial proteins: relationship between mtDNA copy number and cytochrome-*c* oxidase activity in human cells and tissues. *Biochim. Biophys. Acta* 1144, 177–183.

210. van der Vliet P. C. and Kwant M. M. (1981) Role of DNA polymerase γ in adenovirus DNA replication. Mechanism of inhibition by 2',3'-dideoxynucleoside 5'-triphosphates. *Biochemistry* 20, 2628-2632.

211. Van Goethem G., Dermaut B., Löfgren A., Martin J. J., and Van Broeckhoven C. (2001) Mutation of *POLG* is associated with progressive external ophthalmoplegia characterized by mtDNA deletions. *Nat. Genet*. 28, 211–212.

212. Van Goethem G., Luoma P., Rantamäki M., Al Memar A., Kaakkola S., Hackman P., Krahe R., Löfgren A., Martin J. J., De Jonghe P., Suomalainen A., Udd B., and Van Broeckhoven C. (2004) *POLG* mutations in neurodegenerative disorders with ataxia but no muscle involvement. *Neurology* 63, 1251–1257.

213. Vasington F. D. and Murphy J. V. (1962) Ca^{2+} ion uptake by rat kidney mitochondria and its dependence on respiration and phosphorylation. *J. Biol. Chem*. 237, 2670–2677.

214. von Kleist-Retzow J. C., Schauseil-Zipf U., Michalk D. V., and Kunz W. S. (2003) Mitochondrial diseases – an expanding spectrum of disorders and affected genes. *Exp. Physiol.* 88, 155–166.

215. Wallace D. C. (1992) Diseases of the mitochondrial DNA. *Annu. Rev. Biochem*. 61, 1175–1212.

216. Wallace D. C., Singh G., Lott M. T., Hodge J. A., Schurr T. G., Lezza A. M., Elsas L. J., II, and Nikoskelainen E. K. (1988) Mitochondrial DNA mutation associated with Leber's hereditary optic neuropathy. *Science* 242, 1427–1430.

217. Wang H., Hiatt W. R., Barstow T. J., and Brass E. P. (1999) Relationships between muscle mitochondrial DNA content, mitochondrial enzyme activity and oxidative capacity in man: alterations with disease. *Eur. J. Appl. Physiol. Occup. Physiol*. 80, 22–27.

218. Wang Y. and Bogenhagen D. F. (2006) Human mitochondrial DNA nucleoids are linked to protein folding machinery and metabolic enzymes at the mitochondrial inner membrane. *J. Biol. Chem.* 281, 25791–25802.

219. Wang Y., Liu V. W., Xue W. C., Cheung A. N., and Ngan H. Y. (2006) Association of decreased mitochondrial DNA content with ovarian cancer progression. *Br. J. Cancer* 95, 1087–1091.

220. Wanrooij S., Goffart S., Pohjoismäki J. L., Yasukawa T., and Spelbrink J. N. (2007) Expression of catalytic mutants of the mtDNA helicase Twinkle and polymerase POLG causes distinct replication stalling phenotypes. *Nucleic Acids Res.* 35, 3238-3251.

221. Waqar M. A., Evans M. J., Manly K. F., Hughes R. G., and Huberman J. A. (1984) Effects of 2',3'-dideoxynucleosides on mammalian cells and viruses. *J. Cell Physiol.* 121, 402–408.

222. Wiesner R. J., Rüegg J. C., and Morano I. (1992) Counting target molecules by exponential polymerase chain reaction: copy number of mitochondrial DNA in rat tissues. *Biochem. Biophys. Res. Commun.* 183, 553–559.

223. Williams R. S. (1986) Mitochondrial gene expression in mammalian striated muscle. Evidence that variation in gene dosage is the major regulatory event. *J. Biol. Chem*. 261, 12390–12394.

224. Wittwer C. T., Herrmann M. G., Moss A. A., and Rasmussen R. P. (1997) Continuous fluorescence monitoring of rapid cycle DNA amplification. *BioTechniques* 22, 130–138.

225. Wittwer C. T. and Kusukawa N. (2004) Real-time PCR. In *Molecular Microbiology: Diagnostic Principles and Practice* (ed. T. F. Persing DH). ASM Press, Washington, DC, pp. 71–84.

226. Wong L. J., Tan D. J., Bai R. K., Yeh K. T., and Chang J. (2004) Molecular alterations in mitochondrial DNA of hepatocellular carcinomas: is there a correlation with clinicopathological profile? *J. Med. Genet*. 41, e65.

227. Wong P. C., Pardo C. A., Borchelt D. R., Lee M. K., Copeland N. G., Jenkins N. A., Sisodia S. S., Cleveland D. W., and Price D. L. (1995) An adverse property of a familial ALS-linked *SOD1* mutation causes motor neuron disease characterized by vacuolar degeneration of mitochondria. *Neuron* 14, 1105–1116.

228. Yaffe M. P. (1999) The machinery of mitochondrial inheritance and behavior. *Science* 283, 1493–1497.

229. Yao Yang M., Bowmaker M., Reyes A., Vergani L., Angeli P., Gringeri E., Jacobs H. T., and Holt I. J. (2002) Biased incorporation of ribonucleotides on the mitochondrial L-strand accounts for apparent strand-asymmetric DNA replication. *Cell* 111, 495–505.

230. Zeviani M., Servidei S., Gellera C., Bertini E., DiMauro S., and DiDonato S. (1989) An autosomal dominant disorder with multiple deletions of mitochondrial DNA starting at the D-loop region. *Nature* 339, 309–311.

231. Zhao S. and Fernald R. D. (2005) Comprehensive algorithm for quantitative real-time polymerase chain reaction. *J. Comput. Biol*. 12, 1047–1064.

232. Zimmermann W., Chen S. M., Bolden A., and Weissbach A. (1980) Mitochondrial DNA replication does not involve DNA polymerase α. *J. Biol. Chem.* 255, 11847-11852.

233. Zsurka G., Baron M., Stewart J. D., Kornblum C., Bös M., Sassen R., Taylor R. W., Elger C. E., Chinnery P. F., and Kunz W. S. (2008) Clonally expanded mitochondrial DNA mutations in epileptic individuals with mutated DNA polymerase γ. *J. Neuropathol. Exp. Neurol*. 67, 857–866.

234. Zsurka G., Kraytsberg Y., Kudina T., Kornblum C., Elger C. E., Khrapko K., and Kunz W. S. (2005) Recombination of mitochondrial DNA in skeletal muscle of individuals with multiple mitochondrial DNA heteroplasmy. *Nat. Genet*. 37, 873–877.

235. Zsurka G., Schröder R., Kornblum C., Rudolph J., Wiesner R. J., Elger C. E., and Kunz W. S. (2004) Tissue dependent co-segregation of the novel pathogenic G12276A mitochondrial $tRNA^{Leu(CUN)}$ mutation with the A185G D-loop polymorphism. *J. Med. Genet*. 41, e124.

236. Zylber E., Vesco C., and Penman S. (1969) Selective inhibition of the synthesis of mitochondria-associated RNA by ethidium bromide. *J. Mol. Biol*. 44, 195–204.

8.2 List of abbreviations

acetyl CoA	acetyl coenzyme A
AD	area dentata
ADP	Adenosine diphosphate
adPEO	autosomal dominant PEO
AHS	Ammon's horn sclerosis
ALS	amyotrophic lateral sclerosis
ANOVA	univariate variance analysis
ANT1	*adenine nucleotide translocator 1*
arPEO	autosomal recessive PEO
ATP	adenosine-5'-triphosphate
BLAST	basic local alignment search tool
Bromophenol blue	3', 3" ,5' ,5"-tetrabromophenolsulfonphthalein
BS	brain stem
C	complex
CA	cornu ammonis
CA1	cornu ammonis 1
CA3	cornu ammonis 3
CB	cerebellum
DNA	deoxyribonucleic acid
CoA-SH	coenzyme A
COX	cytochrome *c* oxidase
DAB	3, 3'-diaminobenzidine tetrahydrochloride
DAPI	4',6-diamidino-2-phenylindole
ddC	2',3'-dideoxycytidine
dil	dilution factor
DMEM	Dulbecco's modified eagle medium
DMSO	dimethyl sulfoxide
dNTP	deoxyribonucleotide
dRP	5'-deoxyribose phosphate
DTNB	5, 5'-dithiobis-(2-nitrobenzoic acid)
EDTA	diaminoethanetetraacetic acid
EtBr	3, 8-diamino-5-ethyl-6-phenylphenanthridinium bromide (Ethidiumbromide)
Exo	3'-5'-exonuclease
$FADH_2$	flavin adenine dinucleotide
FAM	6-carboxyfluorescein
FBS	fetal bovine serum
FL	frontal lobe
FRDA	Friedreich's ataxia

GDP	guanosine diphosphate
GTP	guanosine-5'-triphosphate
H	hippocampus
HeLa	Henrietta Lacks
IMM	inner mitochondrial membrane
IMS	intermembrane space
KSS	Kearns-Sayre syndrome
L	length
LHON	Leber's hereditary optic neuropathy
MELAS	mitochondrial encephalomyopathy, lactic acidosis and stroke-like episodes
MERRF	myoclonic epilepsy and ragged red fibers
MILS	maternally-inherited Leigh syndrome
MNGIE	mitochondrial neurogastrointestinal encephalomyopathy
MP	morbus Parkinson
mtDNA	mitochondrial DNA
MTS	mitochondrial targeting sequence
NAD^+/NADH	nicotinamide adenine dinucleotide
$NADP^+$/NADPH	nicotinamide adenine dinucleotide phosphate
NARP	neuropathy, ataxia and retinitis pigmentosa
NBT	Nitro blue tetrazolium chloride
NCBI	National Center for Biotechnology Information
O_2^-•	superoxide anion
OD	optical density
•OH	hydroxyl radical
8-OHG	8-hydroxyguanosine
OL	occipital lobe
OMM	outer mitochondrial membrane
oxalacetic acid	oxobutanedioic acid
OXPHOS	oxidative phosphorylation system
p55	55 kDa protein
PDH	pyruvate dehydrogenase
PEO	progressive external ophthalmopegia
PBS	phosphate buffered saline
PCR	polymerase chain reaction
PH	parahippocampus
PL	parietal lobe
Pol	DNA-polymerase
POLG	mtDNA polymerase γ
RFLP	restriction fragment length polymorphism
ROS	reactive oxygen species

RNA	ribonucleic acid
rRNA	ribosomal RNA
RT	room temperature
qPCR	quantitative real time PCR
SDH	succinate dehydrogenase
SDS	sodium dodecyl sulfate
SE	salt EDTA
succinyl –CoA	succinyl coenzyme A
TAE	tris acetate EDTA
TAMRA	*N, N, N', N'*-6-tetramethyl-6-carboxyrhodamine
Taq	*Thermus aquaticus*
TBE	tris borate EDTA
TE	Tris EDTA
TFAM	mitochondrial transcription factor A
TL	temporal lobe
TLE	temporal lobe epilepsy
TNB	5-thio-2-nitrobenzoic acid
Triethanolamine	Tris(2-hydroxyethyl)amine
Tris	2-Amino-2-hydroxymethyl-propane-1,3-diol
Triton X-100	Octoxinol-9
tRNA	transfer RNA
TTFB	4, 5, 6, 7-Tetrachloro-2-trifluoromethylbenzimidazole
Tween 20	Polyoxyethylene (20) sorbitan monolaurate
V	volume

Table 27. Standard amino acid abbreviations

A	Alanine	G	Glycine	M	Methionine	S	Serine
C	Cysteine	H	Histidine	N	Asparagine	T	Threonine
D	Aspartic acid	I	Isoleucine	P	Proline	V	Valine
E	Glutamic acid	K	Lysine	Q	Glutamine	W	Tryptophan
F	Phenylalanine	L	Leucine	R	Arginine	Y	Tyrosine

8.3 List of figures

8.4 List of tables

List of publications

1. **Baron M.**, Kudin A. P., and Kunz W. S. (2007) Mitochondrial dysfunction in neurodegenerative disorders. *Biochem. Soc. Trans.* 35, 1228-1231.

2. Boes M., Bauer J., Urbach H., Elger C. E., Frank S., **Baron M.**, Zsurka G., Kunz W. S., and Kornblum C. (2009) Proof of progression over time: finally fulminant brain, muscle, and liver affection in Alpers syndrome associated with the A467T *POLG1* mutation. *Seizure*. 18, 232-234.

3. Paus S., Zsurka G., **Baron M.**, Deschauer M., Bamberg C., Klockgether T., Kunz W. S., and Kornblum C. (2008) Apraxia of lid opening mimicking ptosis in compound heterozygosity for A467T and W748S *POLG1* mutations. *Mov Disord*. 23, 1286-1288.

4. Phillips J. R. *, Fischer E. *, **Baron M.**, van den Dries N., Facchinelli F., Kutzer M., Rahmanzadeh R., Remus D., and Bartels D. (2008) *Lindernia brevidens*: a novel desiccation-tolerant vascular plant, endemic to ancient tropical rainforests. *Plant J.* 54, 938-948.

5. Zsurka G.*, **Baron M. ***, Stewart J. D., Kornblum C., Bös M., Sassen R., Taylor R. W., Elger C. E., Chinnery P. F., and Kunz W. S. (2008) Clonally expanded mitochondrial DNA mutations in epileptic individuals with mutated DNA polymerase γ. *J. Neuropathol. Exp. Neurol.* 67, 857-866.

*These authors contributed equally.